

Eirik Jelstad

Study of different promoters in the thermotolerant methylotrophic bacterium *Bacillus methanolicus*

Master's thesis in Chemical Engineering and Biotechnology

Supervisor: Sigrid Hakvåg

June 2019

Eirik Jelstad

**Study of different promoters in the
thermotolerant methylotrophic
bacterium *Bacillus methanolicus***

Master's thesis in Chemical Engineering and Biotechnology
Supervisor: Sigrid Hakvåg
June 2019

Norwegian University of Science and Technology
Faculty of Natural Sciences
Department of Biotechnology and Food Science

Abstract

Bacillus methanolicus is a thermotolerant, methylotrophic, Gram-positive bacteria that have been shown to produce high yields of amino acids by the over-expression of genes. The methylotrophy and tolerance towards high cultivation temperature make *B. methanolicus* highly relevant in future biotechnological applications by allowing large scale cultivations to be cost-effective and environmentally friendly. However, the poorly developed genetic toolbox is a limiting factor in further utilization of *B. methanolicus* in science, or as an industrially applicable microorganism.

In this report, a set of putative promoter sequences discovered by RNA-sequencing of *Bacillus methanolicus* MGA3 has been studied. The putative promoter strengths were characterized either with the use of a thermostable, super folded green fluorescence protein (sfGFP) or riboflavin producing operon as reporter genes. The expression from eleven putative promoter sequences was estimated and compared to the constitutive, and widely used methanol dehydrogenase promoter (P_{mdh}) in microplate cultivations under multiple conditions.

Putative glutamate synthase promoter (P_{gltAB}) was shown to be constitutive, and over twice as strong as P_{mdh} . Further, putative hexulose 6-phosphate synthase promoter (P_{hps}) depicted a 15-fold increase in riboflavin production compared to the putative P_{gltAB} in microbioreactor cultivations using pBV2 as shuttle vector and riboflavin operon as reporter genes. Interestingly, fluorescent protein expression was found to be higher in the pBV2 plasmid rather than the pTH1 plasmid, conflicting previous transcriptome data.

The discovery of multiple putative promoters in *B. methanolicus* with varying strengths serves as a much-needed expansion to the genetic toolbox as it increases the options researchers have in studying synthesis pathways, and facilitates the development of *Bacillus methanolicus* as a biocatalyst in industrial production.

Sammendrag

Bacillus methanolicus er en termotolerant, metyloτροφ, Gram-positiv bakterie som har vist seg å gi høyt utbytte av aminosyrene glutamat og lysin ved overuttrykkelse av gener. Metylotrofi og toleranse mot høy dyrkningstemperatur gjør *Bacillus methanolicus* høyt ettertraktet i fremtidig bioteknologiske bruksområder ved å gjøre stor-skala kultivering økonomisk og miljøvennlig. Imidlertid er den dårlig utviklede genetiske verktøykassen en begrensende faktor for videre bruk av *B. methanolicus* i vitenskap, eller som en industrielt anvendelig mikroorganisme.

I denne rapporten har et sett av mulige promotorsekvenser, oppdaget ved RNA-sekvensering av *Bacillus methanolicus* MGA3, blitt studert. Promotorstyrken ble karakterisert enten ved bruk av et termostabilt, overfoldet grønt fluorescensprotein (sfGFP) eller et riboflavin-produserende operon som rapporteringsgener. Uttrykket fra elleve promotorsekvenser ble estimert og sammenlignet med den konstitutive og ofte brukte metanol dehydrogenasepromotoren (P_{mdh}) i brønn-platekulturer under flere kultiveringsbetingelser.

Den antatte glutamat syntase promotoren (P_{gltAB}) ble vist til å være konstitutiv og over dobbelt så sterk som P_{mdh} . Videre viste hexulose 6-fosfat syntase promotoren (P_{hps}) en 15-ganger økning i riboflavinproduksjonen sammenlignet med P_{gltAB} i mikrobioreaktorkulturer ved bruk av pBV2 som vektor og riboflavin operonet som rapporteringsgener. I tillegg ble fluorescerende proteinuttrykk funnet å være høyere i pBV2-plasmidet sammenlignet med pTH1-plasmidet, noe som motstrider tidligere transkriptomdata.

Oppdagelsen av flere mulige promotorer i *B. methanolicus* med varierende styrke fungerer som en etterlengtet utvidelse av genomverktøyet, da det gir forskere flere muligheter i forskning på synteseveier, og letter videre utvikling av *B. methanolicus* som en biokatalysator i industriell produksjon.

Acknowledgement

This masters thesis was carried out at the Norwegian University of Science and Technology (NTNU), Faculty of Natural Sciences, Departments of Biotechnology and Food Science.

Firstly, I would like to thank my supervisor, postdoctoral researcher Sigrid Hakvåg, for always being available, her extensive support throughout my project and for supplying me with all the help I needed in the laboratory work, as well as with writing the thesis. Her guidance and support has been beyond expectations.

Additionally, I would like to thank postdoc Marta Irla and PhD-candidate Eivind B. Drejer for sharing their invaluable knowledge of *B. methanolicus*, and for helping me with various issues during my project last semester, and the thesis this semester. Their guidance has made working on the thesis both inspiring and enjoyable.

Lastly, I would like to extend my gratitude towards the rest of the Cell Factory research group, postdoc Luciana Fernandes de Brito and PhD candidate Agnieszka Gawin for including me as a part of the group, and for patiently helping me with my never-ending questions.

Eirik Jelstad, June 9, 2019, Trondheim

Table of Contents

Abstract	i
Abstract	ii
Preface	iii
Table of Contents	vii
List of Tables	ix
List of Figures	xiii
1 Introduction	1
1.1 General aims of the project	2
1.2 Background	3
1.2.1 <i>Bacillus methanolicus</i> as an exiting candidate for future applica- tions in industrial production	4
1.2.2 Genetic advancements in molecular tool development for <i>Bacillus</i> <i>methanolicus</i>	4
2 Materials and Method	7
2.1 Media and cultivation conditions	7
2.1.1 PCR-conditions	8
2.2 Constructing recombinant plasmid	9
2.2.1 PCR amplification of putative promoters and vectors	9
2.2.2 Assembly of backbone and inserts	12
2.3 Cloning, sequencing of recombinant plasmids	13
2.3.1 Transforming <i>B. methanolicus</i> with recombinant plasmids	13
2.4 Detection of fluorescent intensity with Tecan Infinite plate reader	14
2.5 Cultivation in BioLector Pro and riboflavin quantification with HPLC	14

3	Results	16
3.1	Amplification, optimizing PCR-conditions and the sequencing of transformed plasmids from <i>E. coli</i>	17
3.1.1	Transformation of plasmids to <i>E. coli</i> and <i>B. methanolicus</i>	18
3.2	Growth characteristics in different carbon sources and cultivation conditions	19
3.3	Relating fluorescence to OD and calibrating riboflavin signal to concentration	19
3.4	Estimating promoter strength based on detected fluorescence intensity	20
3.4.1	Comparing protein expression from cells cultivated in flasks and deep well plates	20
3.4.2	Comparing promoter strengths in different cultivation conditions	21
3.4.3	Difference in expression rates for pTH1 plasmids and pBV2 plasmids	24
3.5	Predicting promoter strength of putative promoter 1 based on riboflavin production	25
4	Discussion	26
4.1	Amplification, optimizing PCR-conditions and sequencing transformed plasmids from <i>E. coli</i>	26
4.1.1	Sequencing the promoter sequence and screening for mutations	27
4.2	Transformation of <i>Bacillus methanolicus</i> MGA3	27
4.3	Growth conditions and characteristics	29
4.4	Detection of fluorescence and riboflavin production	30
4.5	Estimating promoter strength based on detected fluorescence and riboflavin production	31
4.5.1	Putative promoter sequence 1 revealed 15 times higher production of riboflavin than glutamate synthase promoter (sp05) in micro-bioreactor cultivation	33
4.6	Future work	35
5	Conclusion	36
	Bibliography	37
	Appendix	43
A	Supplementary tables	43
A.1	Primer and promoter sequences	43
A.2	Plasmids used in this study	48
A.3	Fluorescence results data sheets	49
A.4	Riboflavin production	54
B	BioLector growth curves and riboflavin production	55
B.1	Biomass and riboflavin signal plotted against time for pBV2sp01-ribB1	55
B.2	Biomass and riboflavin signal plotted against time for pBV2sp05-ribB1	58

C	Electrophoresis results	60
C.1	Amplification of inserts	61
C.2	Colony-PCR product	63
D	Alignments of sequencing results	69
E	Calibration curves	71
F	Protocols	75
F.1	Takara Cloneamp HiFi polymerase	75
F.2	DNA gel electrophoresis	76
F.3	Gibson Assembly	77
F.4	Making chemically competent <i>Escherichia coli</i>	78
F.5	Making electrocompetent <i>Bacillus methanolicus</i>	79
F.6	Transformation of chemically competent <i>Escherichia coli</i>	80
F.7	Transformation of electrocompetent <i>Bacillus methanolicus</i>	81
G	Medium and buffer compositions	83
G.1	LB medium	83
G.2	SOC medium	83
G.3	SOBsuc medium	84
G.4	PSI medium	84
G.5	TfbI buffer	84
G.6	TfbII buffer	85
G.7	MVcM minimal media	85
G.8	MVcM high salt buffer 10X	86
G.9	MgSO ₄ stock solution	86
G.10	Trace metals solution	86
G.11	Vitamin stock solution	87
G.12	Electroporation buffer (EPB)	87

List of Tables

2.1	Bacterial strains used in this study	7
2.2	Table of concentrations used in the different cultivation conditions.	8
2.3	Primers and template used for the amplification of the vector backbones; pTH1-sfGFP, pBV2 and pBV2-ribB1, used in part 1, 2 and 3, respectively. The primer sequences along with overlapping region are added in appendix A.1	10
3.1	Putative promoters with associated downstream protein located in <i>Bacillus methanolicus</i> MGA3 (GenBank: CP007739.1)	16
3.1	Putative promoters with associated downstream protein located in <i>Bacillus methanolicus</i> MGA3 (GenBank: CP007739.1)	17
3.2	Table of the confirmed sequenced putative promoters inserted in pTH1-sfGFP, pBV2-sfGFP, and pBV2-ribB1 plasmids after transformation into <i>E. coli</i> DH5. X marks constructs that have been validated during this research whereas X* represent validated plasmids from preliminary studies made by Jelstad (not published). Mutated sequences are denoted as a hyphen. Plasmids that have not been transformed to <i>E. coli</i> are left blank	18
3.3	Table of the transformed putative promoters into <i>Bacillus methanolicus</i> MGA3 with the use of pTH1-sfGFP, pBV2-sfGFP, and pBV2-ribB1 as shuttle vectors. X marks constructs that have been transformed during this study, whereas X* represent transformed strains from previous work by Jelstad (not published). Failed transformations to <i>B. methanolicus</i> denoted as a hyphen. Plasmids that have not been validated by sequencing are left blank	19
A.1	Primer sequences used in this study. Bases in lower case denote overlapping regions.	43
A.1	Primer sequences used in this study. Bases in lower case denote overlapping regions.	44
A.1	Primer sequences used in this study. Bases in lower case denote overlapping regions.	45

A.2	Promoter sequences used in this study	46
A.2	Promoter sequences used in this study	47
A.3	Plasmids used and constructed in this study. Plasmids with sfGFP or riboflavin expression under control of the sequence promoters (spXX) or <i>mdh</i> -promoter. pTH1spXX-plasmids were further derived from pTH1mp-sfGFP, whereas pBV2-sfGFP plasmids were derived from pBV2mp-cadA	48
A.4	Settings for the fluorescent measurements in Tecan Infinite Plate Reader.	49
A.5	Cultivation datasheet for pTH1sp04-sfGFP in different cultivation conditions (see text).	50
A.6	Cultivation datasheet for pTH1sp05-sfGFP in different cultivation conditions (see text).	50
A.7	Cultivation datasheet for pTH1sp11-sfGFP in different cultivation conditions (see text).	50
A.8	Cultivation datasheet for pTH1sp12-sfGFP in different cultivation conditions (see text).	51
A.9	Cultivation datasheet for pTH1sp15-sfGFP in different cultivation conditions (see text).	51
A.10	Cultivation datasheet for pTH1sp17-sfGFP in different cultivation conditions (see text).	51
A.11	Cultivation datasheet for pTH1sp18-sfGFP in different cultivation conditions (see text).	52
A.12	Cultivation datasheet for pTH1sp19-sfGFP in different cultivation conditions (see text).	52
A.13	Cultivation datasheet for pTH1sp20-sfGFP in different cultivation conditions (see text).	52
A.14	Cultivation datasheet for pTH1mp-sfGFP in different cultivation conditions (see text).	53
A.15	Fluorescence from pBV2mp-sfGFP and pBV2sp03-sfGFP in different carbon sources. Mean values and standard deviation are presented.	53
A.16	Highest obtained riboflavin signal obtained from BioLector cultivation of strains with pBV2sp05-ribB1 and pBV2sp01-ribB1 cultivated in different carbon sources. Mean values and standard deviation are presented. Calculated highest riboflavin concentration for each of the conditions are also shown.	54
A.17	Calculated riboflavin concentration in supernatant from cultivations with pBV2xp-ribB1 and pBV2sp01-ribB1. Supernatant from strains cultivated in mannitol and induced osmotic stress (NaCl) was studied. The concentration was calculated based on the last obtained signal from the BioLector experiment and area under the curve of HPLC peak.	54
F.1	Master Mix as recommended by Clontech Laboratories	75
F.2	Thermocycler program as recommended by Clontech Laboratories	75
F.3	The recommended amount of fragments used for assembly	77

List of Figures

2.1	Example of the pTH1sp01-sfGFP plasmid with primers used for backbone and insert amplification. The primers used include p_pTH1mp-sfGFP_R and p_pTH1mp-sfGFP_F for amplification of the backbone, together with sfGFP01_F and sfGFP01_R for the amplification of the insert. The putative promoter 1 (sp01), <i>sfgfp</i> -gene and the gene encoding chloramphenicol resistance are annotated. Complete primer and promoter sequences are added in Appendix A.1	10
2.2	Example of the pBV2sp01-sfGFP plasmid with primers used for backbone and insert amplification. The primers used are p_pBV2_prom-sfGFP_F and p_pTH1mp-sfGFP_R for amplification of the backbone, and sfGFP01_F together with p_pBV2_prom-sfGFP_R for the amplification of the insert. The putative promoter 1 (sp01) and the <i>sfgfp</i> -gene are annotated. Complete primer and promoter sequences are added in Appendix A.1	11
2.3	Example of the pBV2sp01-ribB1 plasmid with primers used for backbone- and insert amplification. The primers used are p_pTH1mp-sfGFP_F and R125 for amplification of the backbone, and sfGFP01_R together with RF-F-1 for the amplification of the insert. The putative promoter 1 (sp01) and the riboflavin pathway operon (<i>ribDEAH</i> -genes) are annotated. Complete primer and promoter sequences are added in Appendix A.1	12
3.1	Electrophoresis results from PCR-amplified pBV2-sfGFP backbone by Q5 DNA polymerase kit with a temperature gradient in the annealing step of the PCR-program. Temperatures used are 58, 59, 60.8, 63.5, 66.7, 69.3, 71.2 and 72 °C, which is depicted above the gel image. Generuler 1 kb Plus C was used as the ladder, with 5000, 1500 and 500 base pairs (bp) being extra prominent.	17

3.2	Electrophoresis results from PCR-amplified pBV2-ribB1 backbone by Q5 DNA polymerase kit with a temperature gradient in the annealing step of the PCR-program. Temperatures used are 58, 59, 60.8, 63.5, 66.7, 69.3, 71,2 and 72 °C, which is depicted above the gel image. Generuler 1 kb Plus C was used as the ladder, with 5000, 1500 and 500 base pairs (bp) being extra prominent.	18
3.3	Comparison of relative fluorescence from strains cultivated in flask and 96-well plate with methanol as the carbon source. Presented strains contain pTH1-sfGFP vector with putative promoter 4, 5, 11, 15 17, 18, 19, 20, and mp inserted upstream a green fluorescent protein-encoding gene (<i>sfgfp</i>). Results from flask cultivations are collected from preliminary research, whereas plate cultivations were performed as a part of the presented research (see text).	21
3.4	Comparison of relative fluorescence from the different pTH1-sfGFP containing strains with mp, sp04, sp05, sp11, sp12, sp15, sp17, sp18, sp19, and sp20 as fluorescent reporter promoter. Cultures were grown in MVcM-media with methanol (MeOH), mannitol (Man) or glucose (Glu) as carbon source.	22
3.5	Comparison of relative fluorescence obtained from strains with sfGFP in control of <i>mdh</i> -promoter, putative promoter sequence 4, 5, 11, 12, 15, 17, 18, 19 or 20 in cultivation with induced osmotic stress. Osmotic stress was induced by addition of NaCl (160 mM) or sorbitol (Sorb, 300 mM) in MVcM-media with methanol as carbon source and pTH1 was used as the vector.	23
3.6	Relative fluorescence from putative promoter 4, 5, 11 and 15 inserted in pTH1-sfGFP and cultivated in different pH (pH=6, 6.5, 7.2 and 7.5) . . .	23
3.7	Fluorescent protein expression in pBV2 in control of sp03 and mp with methanol, mannitol and glucose as carbon source. pBV2mp-sfGFP are compared to pTH1mp-sfGFP	24
3.8	Maximum detected riboflavin signal from microbioreactor cultivations of pBV2sp01-ribB1 and pBV2sp05-ribB1 in MVcM minimal media containing methanol (MeOH), mannitol (Man) or glucose (Glu) as carbon source. Osmotic stress was induced by the addition of sodium chloride (160 mM) media with methanol as the carbon source.	25
B.1	Biomass and riboflavin signal plotted against time for pBV2sp01-ribB1 cultivated in methanol	55
B.2	Biomass and riboflavin signal plotted against time for pBV2sp01-ribB1 cultivated in mannitol	56
B.3	Biomass and riboflavin signal plotted against time for pBV2sp01-ribB1 cultivated in glucose	56
B.4	Biomass and riboflavin signal plotted against time for pBV2sp01-ribB1 cultivated in methanol with induced osmotic stress by added NaCl	57
B.5	Biomass and riboflavin signal plotted against time for pBV2sp05-ribB1 cultivated in methanol	58

B.6	Biomass and riboflavin signal plotted against time for pBV2sp05-ribB1 cultivated in mannitol	58
B.7	Biomass and riboflavin signal plotted against time for pBV2sp05-ribB1 cultivated in glucose	59
B.8	Biomass and riboflavin signal plotted against time for pBV2sp05-ribB1 cultivated in methanol with induced osmotic stress by added NaCl	59
C.1	Picture of electrophoresis bands with the use of GeneRuler 1kb plus DNA ladder. The fragment size ranges from 75 bp to 20 000 bp, with 500 bp, 1500 bp and 5000 bp giving the strongest bands.	60
C.2	Amplification of <i>mdh</i> -promoter with the <i>sfgfp</i> -gene (mp, 1798 bp) and putative promoter sequence 1, 2, 3, 11 and 18 with <i>sfgfp</i> (~ 900 bp) for insertion in pBV2 plasmid. GeneRuler 1kb Plus (Appendix C.1) was used as ladder.	61
C.3	Amplification of <i>mdh</i> -promoter (mp, 1079 bp) and putative promoter sequence 1, 2, 3, 11 and 18 (~ 150 bp) for insertion in pBV2-ribB1 plasmid. GeneRuler 1kb Plus (Appendix C.1) was used as ladder.	62
C.4	Amplification of putative promoter 4 (150 bp) for insertion in pBV2-ribB1 plasmid. GeneRuler 1kb Plus (Appendix C.1) was used as ladder.	62
C.5	Electrophoresis results after PCR-amplification of putative promoter 10 inserted upstream <i>sfgfp</i> gene in pTH1. Putative promoter 2, 6, 7, 8 and 16 are also attempted amplified, but without success. GeneRuler 1kb Plus (Appendix C.1) was used as ladder.	63
C.6	Electrophoresis results from colony PCR amplification of putative promoter sequences 2, 6, 7, 8, 9, 10, 12 and 16 together with upstream <i>sfgfp</i> gene inside a pTH1 plasmid. Colonies with putative promoter 02 (sp02) did not show a visible PCR-result. Weak bands are detected for sp12 and sp16. GeneRuler (Appendix C.1) was used as ladder.	64
C.7	Electrophoresis results from colony PCR amplification of putative promoter sequences 2, 6 and 7 together with upstream <i>sfgfp</i> gene inside a pTH1 plasmid. Weak bands are detected for sp02, sp06 and sp07 which were further studied by sequencing. GeneRuler 1kb Plus (Appendix C.1) was used as ladder.	64
C.8	Electrophoresis results from PCR-amplified putative promoter 1 and <i>mdh</i> promoter inserted in pBV2-ribB1 plasmid from <i>E. coli</i> DH5 α colonies. GeneRuler 1kb Plus (Appendix C.1) was used as ladder.	65
C.9	Electrophoresis results from colony PCR amplification of <i>mdh</i> promoter and putative promoter sequences 1, 3, 4 and 5 together with upstream <i>sfgfp</i> gene from a pBV2-sfGFP plasmid. Promoter sequences from pBV2-ribB1 with riboflavin in control by <i>mdh</i> promoter or putative promoter 1, 2, 3, 4, 11 or 18 were also amplified. Visible bands were not detected for mp and sp01 from the pBV2-ribB1 plasmid. GeneRuler 1kb Plus (Appendix C.1) was used as ladder	66
C.10	Electrophoresis results from PCR-amplified putative promoter 1 inserted in pBV2-ribB1 plasmid from <i>E. coli</i> DH5 α colonies. GeneRuler 1kb Plus (Appendix C.1) was used as ladder	67

C.11	Electrophoresis results from PCR-amplified putative promoter 3 (lane 1, 2, 3), 4 (lane 5, 6, 7), 11 (lane 8, 9, 10) and 18 (lane 12, 13, 14) inserted in pBV2-ribBI plasmid from <i>E. coli</i> DH5 α colonies. GeneRuler 1kb Plus (Appendix C.1) was used as ladder	68
D.1	Sequencing alignment from 6 colonies of <i>E. coli</i> with inserted pTH1sp09-sfGFP. The same deletion inside -10 element is present in sequencing attempt 1, 3 and 4. The sequenced promoters are aligned with putative promoter sequence, and primers (forward and reverse) for sp09. Mis-matches are marked in red, and gaps are filled with hyphen (-).	69
D.2	Example of correctly aligned putative promoter sequence to sequencing query. pBV2sp01-ribBI collected from <i>E. coli</i> was sequenced with primers flanking the putative promoter sequence. Mis-matches are marked in red, and gaps are filled with hyphen (-).	70
E.1	Calibration measurements of the relation of optical density with the wavelength of 600 nm of sample measured in cuvette, black Falcon 96-well plate and transparent Nunclon 96-well plate. A volume of 200 μ L was used for the Falcon plate, whereas 100 μ L was used in the Nunclon plate. The linear regression function with R^2 -value is presented inside orange and blue box for the Falcon and Nunclon plate respectively	72
E.2	Relation of fluorescence detected in Tecan infinite [®] plate reader and OD measured in cuvette spectrophotometer. The four lowest OD ₆₀₀ measurements are included in the linear regression, whereas the two highest OD ₆₀₀ measurements falls outside the linear region of detection.	73
E.3	Calibration curve for concentration and detected signal of riboflavin in the BioLector with gain=6. Regression function (inside box) was calculated in Excel using a polynomial function of 4 degrees.	73
E.4	Relation of area of riboflavin peak from HPLC and riboflavin concentration. Fluorescence detector (λ_{Ex} =370 nm, λ_{Em} =520 nm) detected riboflavin signal peak from HPLC with a C ₁₈ coloumn.	74

Introduction

Transcription regulation in bacteria

Bacteria are typically exposed to a dynamic environment with rapid fluctuations in nutrient availability. In order to cope with the changes in an energy efficient way, bacteria regulate their gene expression according to available carbon source or nutrient abundances [1]. The regulation is simplified by having genes that are a part of the same metabolic pathway or synthesis located in proximity, in either operons or gene clusters. Usually, the genes are found with 1 or 4 nucleotide (nt) overlap (frameshift) or with just a few nt separation [2]. The compact representation of genes hinder transcription termination, thus leaving the entire operon transcribed under the control of the same transcription initiation sequence. The allocation of similar genes enables the cells to swiftly turn on or off necessary gene expression with minimal effort and towards specific conditions [3].

The enzyme responsible for all transcription in bacteria is the multi-subunit DNA-dependent RNA polymerase, and is therefore the central component in transcriptional regulation [4]. RNA polymerase consists of a core enzyme ($\beta\beta'\alpha_2\omega$) and an interchangeable σ -factor which form the activated holoenzyme. The core enzyme includes the active site for DNA binding and RNA production (β and β') whereas the σ -factor facilitates recognition of promoter sequence, positioning of the holoenzyme and the unwinding of the duplex DNA [4]. In most bacteria, there are multiple different sigma-factors which recognize different promoter sequences, thus making modelling regulation of transcription initiation challenging [5, 4].

The interaction of promoter motifs and σ -factor binding affinity have been researched extensively for many bacteria [6, 7, 8] and four essential promoter sequence elements have been identified: the -10 hexamer, -35 hexamer, extended -10 element (TGn) and an UP element. The -10 and -35 elements are located 10 and 35 nucleotides upstream transcription start site (TSS), respectively, whereas the UP element is located upstream the -35 element. Consensus sequences for the -10 element and the -35 element have been established for several sigma-factors, and are used to screen for putative promoter sequences. The most active promoters are shown to inhere near consensus sequences with an effective UP element. However, no promoters have been found to naturally have perfect constructed

elements, as this would bind the RNA polymerase too tightly. All the elements initialize binding to the polymerase, but their relative contribution is promoter specific, making promoter design and prediction difficult.

The efficient regulation of gene expression is mainly due to the low abundances of RNA polymerase and σ -factors, making promoters compete for the RNA polymerase holoenzyme [9, 5]. However, the promoter elements alone are unable to modulate binding affinity towards RNA polymerase based on the environmental condition. In addition to promoter sequences and σ -factors, also small ligands, transcriptional factors, and folded bacterial chromosome ensure shrewd distribution of RNA polymerase to the competing promoters [4]. The variety of σ -factors that are accumulating in specific conditions allow different promoters to bind RNA polymerase in response to specific stresses. Following binding of RNA polymerase, the DNA needs to be untangled and opened to allow the chemistry of RNA synthesis to begin. The opening of the duplex DNA strands forms an open complex due to isomerization of DNA to domain two of the σ subunit, and are also prone to regulation [5]. Small ligands are used to modulate promoter strength based on the environment by e. g. destabilizing the open complex or activating/deactivating transcription factors [10, 4]. Transcription factors bind directly to the promoter sequence and either up-regulate (activators) or down-regulate (repressors) the expression of genes in response to environmental signals [11, 4].

Another regulatory factor is the compact supercoiling of bacterial chromosomes. The chromosomes interact with proteins (nucleotide proteins) and RNA to fold and lower RNA polymerase activity. The nucleotide proteins are abundant in the cells and are known to fluctuate depending on growth conditions. Most of the nucleotide proteins are found to have weak to non-specificity towards DNA, but the induced folding of the chromosome are presumed to affect the distribution and binding of available RNA polymerase to the promoters. However, no general rules have been established, and the effect of these proteins are studied on a case-by-case basis for the individual promoters [12, 13, 14].

The vast array of possible regulatory systems and the possibility of a complex interaction of multiple mechanisms makes regulation of gene expression challenging to predict. However, development of genomic technologies and increased understanding of physical biochemistry allow further insight into the rules of gene expression [5]. What is more, having tools that are able to fine-tune gene expression is essential for many applications in metabolic engineering, e. g. separation of pathway genes, or over-expression of homologous proteins.

1.1 General aims of the project

This project was to further establish novel promoters of different strength for *Bacillus methanolicus* MGA3 with the aim of giving researchers more options in specific gene regulation in various conditions and with the use of pTH1 and pBV2 as shuttle vectors. Practical examples of the utilization of the novel promoters are also set to be explored by the introduction of an operon containing genes of the riboflavin synthesis pathway (RBP).

1.2 Background

Bacteria are widely used as biocatalysts for organic compounds and protein production in science and industry. The large variety of bacterial strains permits selection based on features suitable for the desired production. Furthermore, available gene manipulation techniques for homologous protein over-expression or heterologous protein expression is a significant advantage for the use of bacteria in a sustainable way.

Bacteria are highly relevant for the production of amino acids used in food- and feed supplements, in polymeric materials, personal care, and pharmaceutical industries. Large-scale production of amino acids has long been researched, and biotechnological methods have been applied in order to supply the high global demand [15, 16, 17]. Utilization of microbial catalyst provides a cost-effective de-novo synthesis with possibilities of gene over-expression and gene regulation in order to develop bacterial strains with high production yield [18, 15]. However, improvements in molecular engineering are mostly limited by the available genetic toolbox and require a profound understanding of the metabolic pathways residing in the applied microorganism [19, 20].

The most widely used bacteria for expression of heterologous proteins are the Gram-negative bacteria *Escherichia coli*. Having a highly developed genetic toolbox, well-known genetics, and rapid growth rate make *E. coli* a sought after biocatalyst. However, *E. coli* expresses heterologous proteins intracellularly, which could lead to the formation of inclusion bodies and incorrect protein folding [21]. Alternatively, *Bacillus subtilis* is an extensively researched bacteria that have been found to secrete heterologous proteins into the cultivation media, making separation of product and biomass easier, thus reducing downstream costs [21].

The majority of bacterial strains used in industrial production uses sugars from agricultural crops as a carbon source. Significant interest in studying single carbon substrates such as methanol began in the late 1960s [16]. Methanol is a C₁ substrate that can easily be obtained from natural gas and serves as a desirable carbon source as it can not be consumed by animals nor humans [22, 8]. The price of methanol is similar to glucose [17], but the added environmental benefits of utilizing natural gas from the petroleum industry make methanol commercially and environmentally attractive [23]. Methanol is, however, more reduced than sugars due to missing C-C bonds, which leads to higher heat development during cultivation [22, 17]. Komieves et al. (2005) [23] found that cultivations of 200 m³ liquid volume, having cultures growing at 35 °C on glucose and cultures growing in 50 °C on methanol presented similar cooling requirements, thus, similar cooling costs. However, when increasing the reactor size, the cost savings on having methylotrophic cells growing in 50 °C became much more significant. Furthermore, the increased cultivation temperature, as well as the use of methanol in microbial cultivations limits the risk of contamination by unwanted microorganisms [8, 24].

Knowledge of methylotrophic bacteria has substantially increased as the genetic understanding is continuously evolving [16, 17, 21]. Furthermore, methylotrophic bacteria growing in elevated temperatures gave rise to application in chemical industry wastewater treatments [16]. Finding a thermotolerant bacteria that were capable of growing on C₁ carbon source as well as having similar traits as *B. subtilis* regarding protein secretion, made *Bacillus methanolicus* a sought after biocatalyst in future industrial application.

1.2.1 *Bacillus methanolicus* as an exiting candidate for future applications in industrial production

Bacillus methanolicus is a Gram-positive, thermotolerant, methylotroph bacteria with optimal cultivation pH at 6.8 [17]. Optimal cultivation temperature is between 50-53 °C, but viability has been reported between 30 °C to 60 °C [16, 17]. *B. methanolicus* is endospore-forming, though seldom in flask cultivations under normal growth conditions (50 °C), and auxotrophic for the vitamins biotin and B₁₂ [17, 8]. Model *B. methanolicus* MGA3 contains two plasmids, pBM69 and pBM19, where the latter is crucial for the cells methylotrophic traits [17, 8].

What is more, *B. methanolicus* has shown high production rates of glutamate (up to 60 g/L) in fed-batch cultivations with methanol as a carbon source [17]. Glutamate has been widely used as a flavor enhancer in the form of monosodium L-glutamate (MSG), that had a world demand valued at \$4.5 billion in 2014 [25]. The second largest amino acid on the market is the essential amino acid lysine with a global consumption exceeding 2.2 million metric tons. The Gram-positive *Corynebacterium glutanicum* mostly does both glutamate and lysine production with molasses and sugar canes as the carbon source [26]. The wild type *B. methanolicus* MGA3 only produces a small amount of lysine, but classical mutations has reported cells that are producing up to 47 g/L lysine [17], making *B. methanolicus* an interesting candidate for further research in both glutamate and lysine production.

1.2.2 Genetic advancements in molecular tool development for *Bacillus methanolicus*

The development of techniques for recombinant expression is mainly dependent on the available genetic tools and genetic delivery methods, e. g. regulatory systems, constitutive/inducible promoters, shuttle vectors, and reporter genes [27]. Considerable progress has been made in the last few years regarding enzymes involved in methanol utilization pathways and the limited alternative carbon sources for this facultative methylotroph [18, 8, 28, 29].

Utilization of the ribulose monophosphate (RuMP) pathway for methylotrophic growth in *B. methanolicus*

B. methanolicus has been shown to contain three types of NAD(P)-dependent cytoplasmic methanol dehydrogenase (MDH) for the oxidation of methanol to formaldehyde. Two chromosome-encoded, and one pBM18-encoded [18, 30, 31]. Formaldehyde is detoxified by assimilation in the ribulose 5-phosphate (RuMP)-pathway, or linearly oxidized by the tetrahydrofolate pathway to form CO₂, thus making *B. methanolicus* tolerant to high methanol concentrations in cultivation media. The enzymes responsible for the condensation of formaldehyde and ribulose 5-phosphate to fructose 6-phosphate, namely 3-hexulose-6-phosphate synthase (*hps*) and 6-phospho-hexulose-6-phosphate synthase (*phi*), are only encoded on the chromosome, whereas the five RuMP pathway genes (*pfk*, encoding 6-phosphofructo-kinase, *fba*, encoding fructose-bisphosphate aldolase, *tkt*, encoding transketolase, *glpX*, encoding fructose bisphosphatase, and *rpe*, encoding ribulose-5-phosphate

3-epimerase) are homologously represented in both the native pBM19 plasmid and the chromosome [18]. However, MGA3 strains lacking pBM19 shows a methylotrophy deficient phenotype. This because the five RuMP-cycle genes and the pBM19-encoded *mdh* gene are induced during growth on methanol [8, 18].

Furthermore, glucose and mannitol are two of the few multicarbon sources *B. methanolicus* can utilize. Both glucose and mannitol are converted to fructose 6-phosphate via glucose 6-phosphate and mannitol 1-phosphate, respectively. Fructose 6-phosphate is further metabolized via the Entner-Doudoroff pathway or oxidized via the PP pathway, thus sharing many of the same metabolites as methanol in the RuMP pathway [18].

The available promoters for recombinant gene expression in *B. methanolicus* are limited

The most frequently used inducible promoter for *B. methanolicus* is the tightly regulated and dose-dependent xylose inducible promoter derived from *Bacillus megaterium* [18, 32]. *B. methanolicus* does not possess any utilization pathways for xylose, making the inducible promoter a well functioning genetic regulator [19]. Alternatively, a mannitol inducible promoter has been applied in *B. methanolicus*. However, this promoter is not tightly regulated [19].

As for constitutive promoters, the methanol dehydrogenase (*mdh*) promoter is the most prominent and widely used for recombinant gene expression in *B. methanolicus* [33, 34, 35].

Studying and constructing low copy shuttle vectors with desirable reporter gene properties for thermotolerant cultivation

Previously, the main plasmid used in genetic engineering of *B. methanolicus* has been pNW33N and pHP13 [19]. Irla et al. (2016) [19] studied alternative plasmids, both rolling circle, and theta-replicating, to find four new plasmids that were able to replicate in *B. methanolicus*, i. e. pTH1mp, pUB110Smp, pNW33Nmp, and pBV2mp, where the latter is the only theta-replicating plasmid. The plasmids were studied with a fluorescence reporter gene controlled by a methanol dehydrogenase promoter P_{mdh} to compare copy number and expression of *gfpuv* in *B. methanolicus* MGA3. The study revealed copy numbers of 19 and 25 for pNW33N and pUB110S, respectively, and the copy number for pTH1 and pBV2 was found to be 5 and 3, respectively [19]. Further, pTH1mp-*gfpuv* suggested a higher GFPuv fluorescence than pBV2mp-*gfpuv* (0,9 and 0,2 respectively), indicating higher protein expression rates in the pTH1-plasmid [19].

Care must be taken when choosing the reporter gene for thermotolerant microorganisms. The first described and properly analyzed fluorescent protein (FP) is the green fluorescent protein isolated from the jellyfish *Aequorea victoria*. The fluorescent properties emanate from the distinct folding state of the protein and are therefore susceptible to media conditions. With this, a vast variety of FP variants are available as pH and redox sensors, photoswitchable and timer proteins with many more. Properly folded wild type green fluorescent protein (GFP) remain fluorescent to at least 65 °C [24]. However, the wild type protein only folds properly in low temperatures. Consequently, a robust GFP derivative that can fold correctly in harsh conditions has been developed and termed super folded

GFP (sfGFP). The sfGFP is thermostable and exhibit superior resistance to chemical denaturants in comparison to wild type GFP, thus providing a sustainable reporter gene for use in high-temperature cultivations [24, 21].

Transcriptome sequencing of *B. methanolicus* has facilitated further development in molecular biology tools

Transcriptome [8, 18] and proteomic [36] data has been used to study the expression of metabolically essential genes for *B. methanolicus* in both methylotrophic growth and with mannitol as the carbon source. What is more, a comprehensive transcriptome analysis of *B. methanolicus* MGA3 by Irla et al. (2015) [8] has led to the discovery of new putative transcription start sites (TSS) and putative promoter sequences. The transcriptome (mRNA) from cultures grown in different conditions, both in a bioreactor- and flask cultivations, were pooled and sequenced by either enrichment of 5' ends of primary transcript or by analysis of the entire transcript. The growth conditions varied in carbon source (methanol, glucose, and mannitol), dissolved oxygen, pH and osmotic stress (induced by NaCl or sorbitol) in order to induce transcript of various genes. The study searched for conserved promoter motifs within 70 bases upstream of each TSS and identified putative promoter sequences with conserved -10 elements (TATAaT) in 98.6 % of the upstream sequences and weakly conserved -35 hexamer sequence (ttgana) in 98.4 % of the upstream sequences. Further, the strength of the putative promoters was estimated based on the abundance of transcript facilitated by the putative promoters. The abundances of the transcript were normalized based on the logarithmic value of reads per kilobase of coding DNA sequence (CDS) per million mapped reads (log-RPKM) and categorized into four classes: low, middle, high and very high [8].

In this study, five of the putative promoter sequences of each class are studied with the goal of further augment the limited available promoters for *Bacillus methanolicus*. The presented study functions as a continuation of preliminary research performed by Jelstad (not published), where eight of the putative promoter sequences were studied in flask cultivation under methylotrophic growth.

Materials and Method

DNA sequences, plasmids, and primer data was handled in Benchling [37]. Putative promoter sequences were studied in NCBI's database using blastx in order to locate promoter position in *B. methanolicus* MGA3 genome (GenBank: CP007739.1) and relating putative promoters with associated gene. *E. coli* DH5 α was used as a general cloning host for the cloning of the recombinant plasmid before it was transformed into *Bacillus methanolicus* MGA3.

2.1 Media and cultivation conditions

Table 2.1 shows the bacterial strands used. Plasmids, as well as primer and promoter sequences, can be found in Appendix A

Table 2.1: Bacterial strains used in this study

Strain	Relevant characteristics	Reference
<i>Escherichia coli</i> DH5 α	General cloning host	Stratagene
<i>Bacillus methanolicus</i> MGA3	Wild type strain	ATCC 53907

Escherichia coli DH5 α was cultivated at 37 °C in Lysogeny Broth (LB) or on LB-agar plates supplemented with antibiotics (chloramphenicol 25 $\mu\text{g}/\text{mL}$ or kanamycin (50 $\mu\text{g}/\text{mL}$) when appropriate.

Bacillus methanolicus MGA3 was cultivated in MVcM minimal media (50 °C) supplemented with methanol (200 mM), mannitol (50 mM) or glucose (50mM) as carbon source. Either NaCl (160 mM) or sorbitol (300 mM) was added in order to induce osmotic stress when needed. Antibiotics (chloramphenicol 5 $\mu\text{g}/\text{mL}$ or kanamycin (50 $\mu\text{g}/\text{mL}$) were added in all cultivations containing recombinant MGA3 strains. SOBsuc was used when making electrocompetent *B. methanolicus* cells and for the transformation of competent *B. methanolicus* MGA3.

Freeze cultures of *E. coli* were made by mixing cell cultures in exponential growth-phase with glycerol (total glycerol concentration of 15 %) and storing in freezer (-80°C). Freeze cultures of *B. methanolicus* cultures harvested at OD₆₀₀=1.0 to 1.5 were made similarly, but with a higher concentration of glycerol (22%).

Pre-cultures were prepared either by transferring a small volume of the freeze culture to pre-warmed media, by thawing an ampule of the freeze culture and transferring 200 µL of cell culture into pre-warmed media or by transferring fresh cultures directly from agar-plate.

Production cultures of recombinant *B. methanolicus* were prepared by re-suspending pre-cultures in MVcM media with respective carbon source to an OD₆₀₀=2.0. The cell suspensions (70 µL) were then transferred to their respective well in pre-warmed media (630 µL) in the cultivation plate (96-well, 2 mL), and cultivated for approximately 6 hours. A heat-block (50 °C) was utilized to reduce heat loss during re-inoculation, and the outermost wells of the plates were filled with sterilized water to reduce evaporation. The MVcM-media differed in c-source and osmotic stress according to Table 2.2. Additionally, the MVcM media was adjusted to pH=6.0, pH=6.5 or pH=7.5 with the addition of HCl/NaOH before autoclaving.

Table 2.2: Table of concentrations used in the different cultivation conditions.

Condition	Compound	Concentration (mM)
C-source	Methanol	200
C-source	Mannitol	50
C-source	Glucose	50
Osmotic stress	NaCl	160
Osmotic stress	Sorbitol	300

All media and buffer compositions can be found in Appendix G

2.1.1 PCR-conditions

Three different polymerase-kits were used for the PCR reactions in this project, CloneAmp HiFi polymerase, standard taq-polymerase, and Q5 High-Fidelity polymerase. All thermocycler programs constituted of a lid temperature of 105 °C, a denaturation step, annealing step, and an extension step. The denaturation, annealing and extension steps were repeated 30 times before the temperature was decreased to 4 °C until the samples were collected and stored in the fridge (4 °C) or the freezer (-20 °C).

Amplification of the putative promoter sequences was performed using CloneAmp HiFi polymerase according to the protocol recommended by the supplier (Appendix F.1).

Q5 High-Fidelity polymerase was used for the amplification of the two pBV2 shuttle vectors. Initially, a gradient was used to find the optimal annealing temperature. The gradient contained temperatures of 72.0, 71.2, 69.3, 66.7, 63.5, 60.8, 59.0 and 58 °C. Equal volumes of the resulting PCR-product were separated with gel electrophoresis, and the lane with the strongest band representing the correct vector size depicted the optimal annealing temperature. Hence, trailing vector-amplifications of pBV2-ribBL and pBV2-sfGFP back-

bones using Q5 High-Fidelity polymerase were performed with annealing temperatures of 63.5 °C and 69.3 °C respectively. Further, the protocol containing step temperatures and -times was based on recommendations made by New England Biolabs Inc. (NEB) recommendations [38]. Denaturation time was set to 10 seconds, annealing time was extended to 40 seconds, and an extension time of 40 sec/kb was used. Additionally, a final extension period of 5 minutes at 72 °C was used.

Taq DNA polymerase was used for colony-PCR according to taq DNA polymerase protocol recommended by supplier [39] with the addition of an elongated initial denaturation step of 2 minutes at 98°C. The annealing temperature was calculated based on the primer melting temperatures according to NEBs T_m calculator ([40]).

2.2 Constructing recombinant plasmid

Putative promoter sequences were introduced into low copy plasmids pTH1 and pBV2. The project was divided into three parts based on the shuttle vector and the reporter gene. Part 1 comprised of pTH1 as the vector with *sfgfp* as the reporter gene. In part 2, the vector was exchanged to pBV2, still with *sfgfp* as the reporter gene. Part 3 includes pBV2 as vector and a riboflavin operon (*ribBl*) containing *ribD*, *ribE*, *ribA* and *ribH* as the reporter genes.

The amplification, assembly and constructing pTH1-sfGFP plasmids with fluorescent protein expression controlled by each of the 20 putative promoter sequences were completed as a part of previous work by Jelstad (not published). Twelve of these sequences have been transformed into *E. coli* and validated by sequencing (Table 3.2) as a part of the preliminary study. Further, eight of the validated recombinant plasmids were transferred into *B. methanolicus* MGA3, and the expression of sfGFP was studied in flask cultivations with MVcM media and methanol as sole carbon source, also in the previous work.

2.2.1 PCR amplification of putative promoters and vectors

Primer sequences for the different promoters and vectors can be seen in Appendix A.1. The promoter and vector primers were designed in order to be ligated into the vector by Gibson assembly, and with the putative promoters inserted upstream of identical ribosomal binding sites (RBS) and the corresponding reporter gene(s).

All of the primers were initially diluted (100 µg/ml) and aliquoted to sterile Eppendorf tubes (200 µL, 10 µg/L). Primers, along with the associated template for vector amplification, are presented in Table 2.3. Primers used for insert amplification are listed in Appendix A.1.

Table 2.3: Primers and template used for the amplification of the vector backbones; pTH1-sfGFP, pBV2 and pBV2-ribB1, used in part 1, 2 and 3, respectively. The primer sequences along with overlapping region are added in appendix A.1

Product vector	Template	Primer F	Primer R	Size (bp)
pTH1-sfGFP	pTH1mp-sfGFP	p_TH1_prom_sfGFP-F	p_TH1_prom_sfGFP-R	5592
pBV2	pBV2mp-CadA	p_BV2_prom_sfGFP-F	p_TH1_prom_sfGFP-R	6754
pBV2-ribB1	pBV2sp05-ribB1	p_TH1_prom_sfGFP-F	R125	10183

In part 1, genomic DNA from *B. methanolicus* MGA3 and purified pTH1mp-sfGFP was used as the template for the promoters and the vector, respectively. This resulted in promoter-sequences, ranging between 150-200 bp and a vector backbone (~6 kb) without novel methyl dehydrogenase promoter (P_{mdh}).

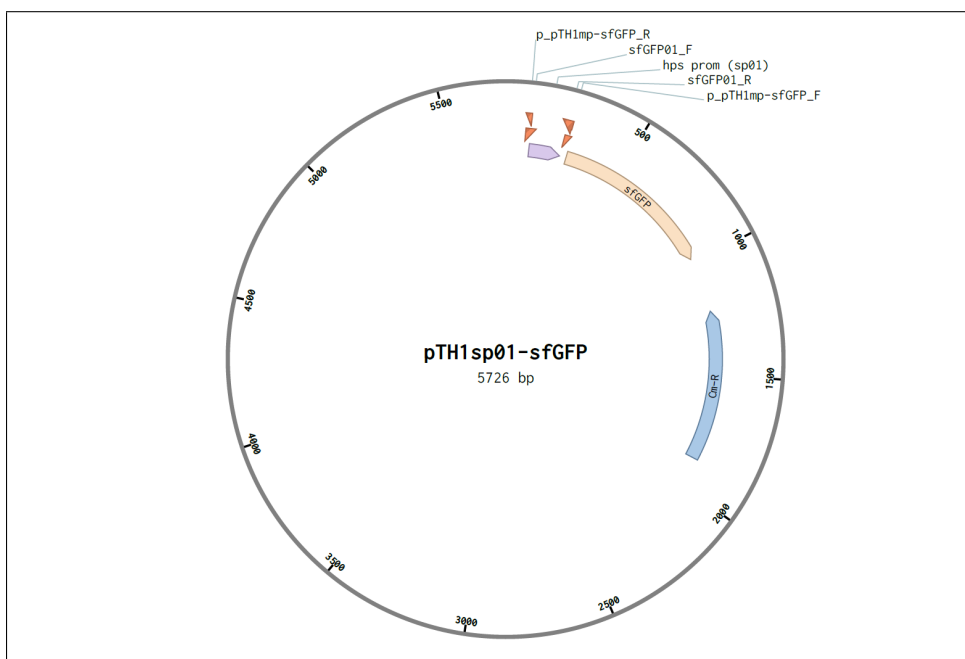


Figure 2.1: Example of the pTH1sp01-sfGFP plasmid with primers used for backbone and insert amplification. The primers used include p_pTH1mp-sfGFP_R and p_pTH1mp-sfGFP_F for amplification of the backbone, together with sfGFP01_F and sfGFP01_R for the amplification of the insert. The putative promoter 1 (sp01), *sfGFP*-gene and the gene encoding chloramphenicol resistance are annotated. Complete primer and promoter sequences are added in Appendix A.1

Part 2 included recombinant plasmids from part 1 as the template for the ~900 bp insert consisting of an *sfgfp* gene in control of the putative promoters. The backbone was amplified from a previously constructed pBV2-plasmid with *mdh*-promoter upstream a *cadA* gene (pBV2mp-CadA).

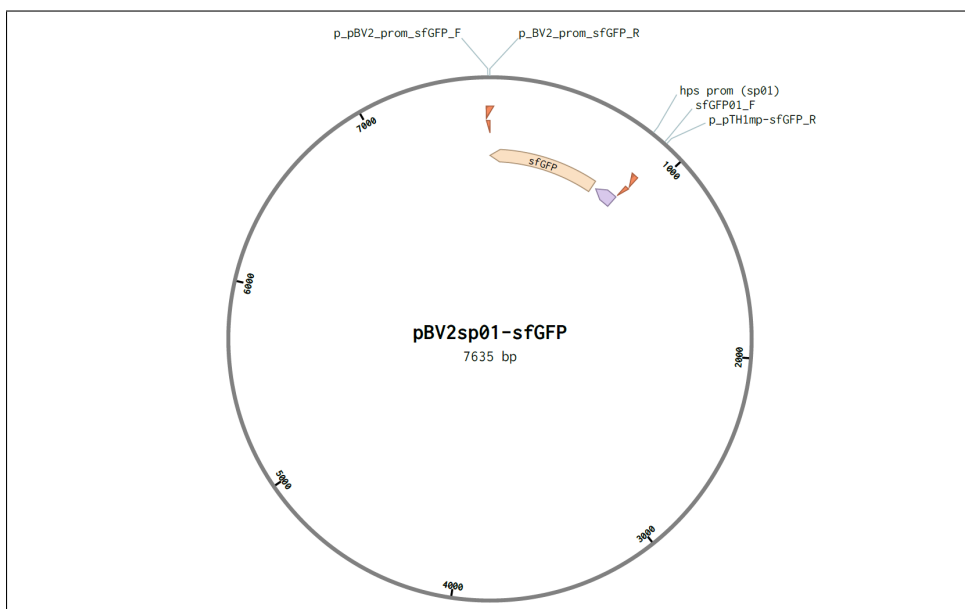


Figure 2.2: Example of the pBV2sp01-sfGFP plasmid with primers used for backbone and insert amplification. The primers used are p_pBV2_prom-sfGFP_F and p_pTH1mp-sfGFP_R for amplification of the backbone, and sfGFP01_F together with p_pBV2_prom-sfGFP_R for the amplification of the insert. The putative promoter 1 (sp01) and the *sfgfp*-gene are annotated. Complete primer and promoter sequences are added in Appendix A.1

Inserts for part 3 were amplified from genomic DNA from *B. methanolicus* MGA3. Plasmid from previously constructed MGA3 containing pBV2sp05-ribBI was purified and used as the template for the vector, creating a backbone with the riboflavin producing operon as the reporter genes.

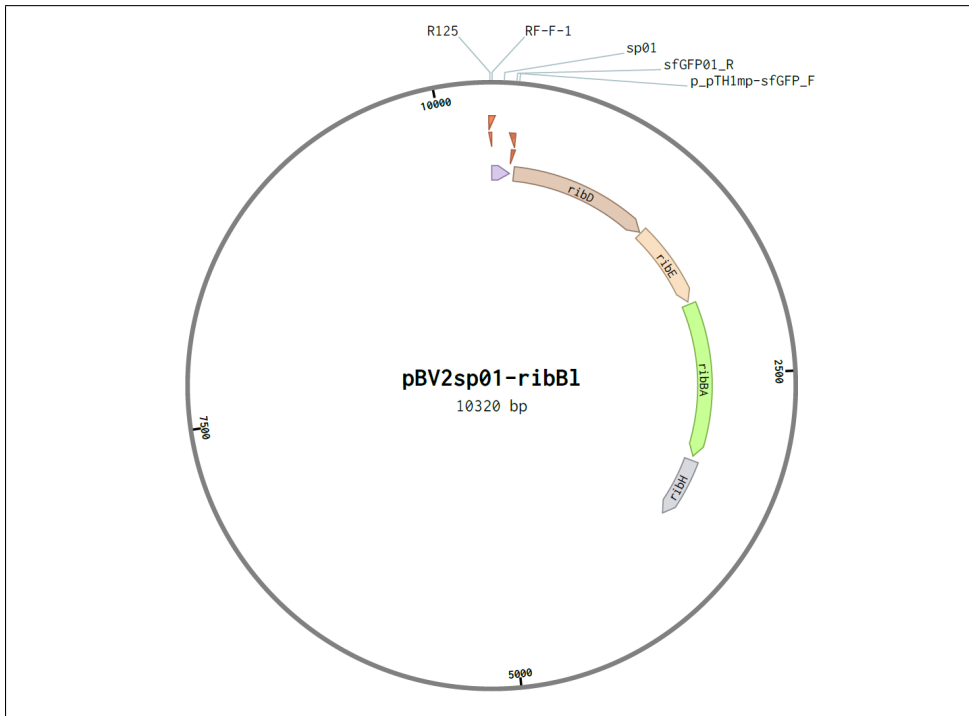


Figure 2.3: Example of the pBV2sp01-ribB1 plasmid with primers used for backbone- and insert amplification. The primers used are p_pTH1mp-sfGFP.F and R125 for amplification of the backbone, and sfGFP01_R together with RF-F-1 for the amplification of the insert. The putative promoter 1 (sp01) and the riboflavin pathway operon (*ribDEAH*-genes) are annotated. Complete primer and promoter sequences are added in Appendix A.1

The PCR-product of the promoters were verified by DNA electrophoresis according to the protocol (Appendix F.2) with GelGreen or GelRed agar, TAE-buffer and GeneRuler 1kb Plus (Appendix C.1) as the ladder. The gel was analyzed by Bio-Rad ChemiDoc™ XRS+ with Image Lab™ software.

The amplified vector was digested with DpnI overnight and separated by DNA gel electrophoresis (GelGreen). Desired DNA-fragments were cut out from the gel and recovered with Zymoclean™ Gel DNA recovery kit (Zymo research, Catalog no. D4002) and cleaned using DNA clean & concentrator™-5 (Zymo research, Catalog no: D4004).

The concentration of both promoters and cleaned vector backbone was determined using NanoDrop™ One (Thermo Scientific™), and stored in the freezer (-20 °C).

2.2.2 Assembly of backbone and inserts

Promoters and plasmid were assembled with Gibson Assembly by following protocol (Appendix F.3). The amount of insert was calculated based on 100 ng backbone, with recommended 3-5 times excess of insert (mole basis). The volume of backbone and insert was calculated by equation 2.1 and 2.2. Recombinant plasmids were named according to plas-

mid used as a vector, putative promoter sequence inserted and the reporter gene used, e. g. pBV2sp01-ribBI for pBV2 with a riboflavin operon in control of putative promoter 1.

$$m_{insert} = \frac{Y * X_1 * Mm_{insert}}{X_2 * Mm_{backbone}} * m_{backbone} \quad (2.1)$$

Where Y is the excess factor of insert, m_{insert} is the mass of insert, Mm_{insert} is the molar mass of the insert, $Mm_{backbone}$ is the molar mass of the backbone, $m_{backbone}$ is the mass of the backbone, X_1 is the size of insert (bp) and X_2 is the size of backbone (bp).

$$V_{insert} = \frac{m_{insert}}{c_{insert}} \quad (2.2)$$

Where V_{insert} is the volume of insert and c_{insert} is the concentration of insert.

2.3 Cloning, sequencing of recombinant plasmids

As a cloning host, chemically competent *E. coli* cells from strain DH5 α was made as described in Appendix F.4. The cells were transformed with assembled vector by mixing chemically competent *E. coli* with vector and utilizing heat-shock to destabilize the cell wall, allowing plasmid penetration. The vials were then suspended in LB (1000 μ L) and incubated at either 37 $^{\circ}$ C (225 rpm) for 1 hour or 25 $^{\circ}$ C (225 rpm) for 3 hours. The cells were spun down (4000 rcp, 2 min), re-suspended (100 μ L), and plated out on selective LB plates. The cells were cultivated on selective agar-plates at 37 $^{\circ}$ C or 25 $^{\circ}$ C until colonies were visible (16-48 hours). A detailed description is added in the protocol for transforming chemically competent *E. coli* (Appendix F.6).

Colony-PCR was used in order to further assess the transformants by using colonies as the template in the PCR amplification program described in section 2.1.1. Colony-PCR results were analyzed by DNA electrophoresis. Colonies that depicted an amplified putative promoter sequence were picked from LB-plates and transferred into 10 ml tubes containing LB medium (5 ml) supplemented with antibiotics. The cells were incubated at 37 $^{\circ}$ C overnight or three days at 25 $^{\circ}$ C before a freeze-culture was made. The remaining cells were treated with ZR-plasmid miniprepTM (Zymo research, Cat. No. D4016) to ligate the cell and for extraction of the recombinant plasmid. NanoDropTM One determined the concentration of plasmid DNA.

Plasmid DNA (400-500 ng) and promoter primers (25 pmol) were mixed in a micro-centrifuge tube (total volume of 10 μ L) and sent into sequencing in order to confirm correct promoter sequence. Sequencing of each transformant were performed with two parallels in order to increase sequencing credibility.

2.3.1 Transforming *B. methanolicus* with recombinant plasmids

Plasmids verified by sequencing were transformed into electrocompetent *B. methanolicus* by electroporation (GenePulser XcellTM, Bio-Rad), according to the protocol (Appendix F.7). The electrocompetent *B. methanolicus* was made according to the protocol presented

in Appendix F.5. Transformed *B. methanolicus* were plated on SOBsuc-plates supplemented with chloramphenicol (5 $\mu\text{g/ml}$) or kanamycin (50 $\mu\text{g/ml}$). Plates were inoculated overnight, and colonies were transferred into MvCM-media and incubated for 16 hours. Cultures in the exponential growth phase (OD_{600} between 1.0 and 1.5) were harvested, and freeze-cultures were made.

2.4 Detection of fluorescent intensity with Tecan Infinite[®] plate reader

A calibration curve for optical density and fluorescence was made by harvesting a cell-culture (pTH1sp05-sfGFP) and washing with phosphate buffered saline (PBS). The cells were diluted to obtain samples with a calculated $\text{OD}_{600}=0.2, 0.4, 0.6, 0.8,$ and 1.0. The exact OD_{600} after dilution was measured, and the cells were aliquoted in triplicates to Falcon 96-well plate (200 μL) and Nunclon transparent 96-well plate (100 μL). Tecan infinite[®] plate reader was used to measuring both fluorescence and optical density of the Falcon plate samples, and the optical density of the Nunclon-plate samples. A calibration curve was made in Excel for the relation of optical density signal from the plate reader to the OD measured in cuvette spectrophotometer, and a linear trend line was estimated.

Production cultures of recombinant strains were made as described in section 2.1. Following the cultivation step, 100 μL of cell culture was transferred to a transparent Nunclon 96-well plate, and the optical density was measured in Tecan infinite[®] plate reader. Simultaneously, the plate cultivations were spun down and washed twice with phosphate buffered saline (PBS) before they were re-suspended in PBS (700 μL). Further, the cells (200 μL) were transferred to a Falcon 96 well plate for fluorescence analysis by Tecan Infinite[®] plate reader following instrument settings given in Appendix A.3.

Optical density was related to the OD obtained in cuvette spectrophotometer by the use of the linear regression function obtained from the calibration series. The fluorescence results were then normalized by dividing detected fluorescence with OD_{600} .

2.5 Cultivation in BioLector[®] Pro and riboflavin quantification with HPLC

A calibration curve was made in order to assess riboflavin production in cultivations. Riboflavin was diluted in water (100, 80, 60, 40, and 20 $\mu\text{g/mL}$), and transferred to a 48-well FlowerPlate without optodes (MTP-48-B) for detection. The trend estimation was calculated using a polynomial function with 4 degrees.

Cultivations in BioLector[®] was performed in order to monitor growth characteristics and production of riboflavin. The production cultures were prepared by having pre-cultures transferred to pre-warmed media in the FlowerPlate, to a total volume of 1 mL ($\text{OD}_{600}=0.1$). The FlowerPlate were then inserted into the pre warmed BioLector[®] for cultivation (50 °C, 85% humidity, 1200 rpm). Both biomass and riboflavin were detected with an internal gain set to 6. For the detection of riboflavin, a fluorescence detector with an excitation wavelength of 436 nm and an emission wavelength of 540 nm was adopted.

The cultivations were terminated when all the cell cultures seemed to have reached their stationary phase, i. e. no more gain in biomass. After inoculation, the cells were pelletized, and the supernatant was stored dark in the freezer (-20 °C) before HPLC controlled final riboflavin concentration.

The HPLC sample preparation was based on Petteys et al. (2011) [41]. Firstly, the samples that were to be quantified were thawed and aliquoted (500 μ L) into sterile Eppendorf tubes (1,5 mL). Trichloroacetic acid (1 mL, 15 % (w/v)) were added to the sample for protein precipitation. The samples were then gently agitated for one minute and incubated at 25 °C for 20 minutes, away from light. Following the incubation, the samples were centrifuged (4 °C, 20 min, 8000 rcp) and the supernatant (100 μ L) was transferred to HPLC insert tubes. The pH was adjusted to 2.5-3.5 by addition of K_3PO_4 (2 M, 15 μ L) and mixed thoroughly. Further, the HPLC vials with inserts were placed in the HPLC rack for quantification.

For the quantification of riboflavin, a reversed-phase high- performance liquid chromatography (HPLC) with a Symmetry[®] C18, 3.5 m column and a fluorescence detector (λ_{Ex} =370 nm, λ_{Em} =520 nm) were adopted. Ammonium acetate (0.05 M) was prepared and adjusted to pH=6 by addition of acetic acid. A mixture of ammonium acetate and methanol (73:27) was used as an isocratic mobile phase with a flow rate of 0.8 ml/min. The column temperature was 25 °C with a sample run time of 8 minutes.

The concentration of riboflavin in the samples were calculated by making a calibration curve with five samples of known riboflavin concentrations and relating the area under the curve to each concentration.

Chapter 3

Results

Eleven putative promoter sequences given by the comprehensive transcriptome sequencing of *B. methanolicus* by Irla et al. [8] were studied and compared to the widely applied, constitutive *mdh*-promoter. The nucleotide sequences of the promoters studied can be found in Appendix A.1. Further, the associated protein for each putative promoter is presented in Table 3.1. The associated protein-encoding genes were found by a blastx query of the putative promoter sequences and examining the first gene located downstream the putative promoter sequence in the *B. methanolicus* MGA3 genome (GenBank: CP007739.1).

Table 3.1: Putative promoters with associated downstream protein located in *Bacillus methanolicus* MGA3 (GenBank: CP007739.1)

Putative promoter abbr.	Associated protein
sp01	3-hexulose-6-phosphate synthase, <i>hps</i>
sp02	30S ribosomal protein S10
sp03	BMMGA3_00355, hypothetical protein
sp04	Putative sugar phosphate isomerase <i>rpiB</i>
sp05	Glutamate syntase, large subunit, GltA, small subunit, <i>gltB</i>
sp06	Argininosuccinate synthase, <i>argG</i>
sp07	Thioredoxin-like protein, <i>ykuU</i>
sp08	Superoxide dismutase [Mn]
sp09	N-acetyl-gamma-glutamyl-phosphate reductase, <i>argC</i>
sp10	co-chaperonin <i>groES</i>
sp11	NH(3)-dependent NAD(+) synthetase, <i>nadE</i>
sp12	Dihydroxy-acid dehydratase, <i>ilvD</i>
sp13	BMMGA3_00260, hypothetical protein
sp14	Putative protein, <i>yjjA</i>
sp15	Pyridoxine kinase, <i>pdxK</i>
sp16	Transcriptional regulator

Table 3.1: Putative promoters with associated downstream protein located in *Bacillus methanolicus* MGA3 (GenBank: CP007739.1)

Putative promoter abbr.	Associated protein
sp17	BMMGA3_11740, hypothetical protein
sp18	D-isomer specific 2-hydroxyacid dehydrogenase NAD-binding protein
sp19	Putative membrane protein
sp20	BMMGA3_09845, hypothetical protein

3.1 Amplification, optimizing PCR-conditions and the sequencing of transformed plasmids from *E. coli*

Figure 3.1 and 3.2 shows how the annealing temperature depicts the PCR efficiency of the amplified pBV2-backbones containing sfGFP and the riboflavin operon, respectively. For pBV2-sfGFP, the optimal annealing temperature was found to be around 69,3 °C, whereas, for the pBV2-ribB1 vector, annealing temperatures between 58,0 °C and 63,5 °C was found to give the highest yield in the PCR reaction with the primers and template specified in Table 2.3.

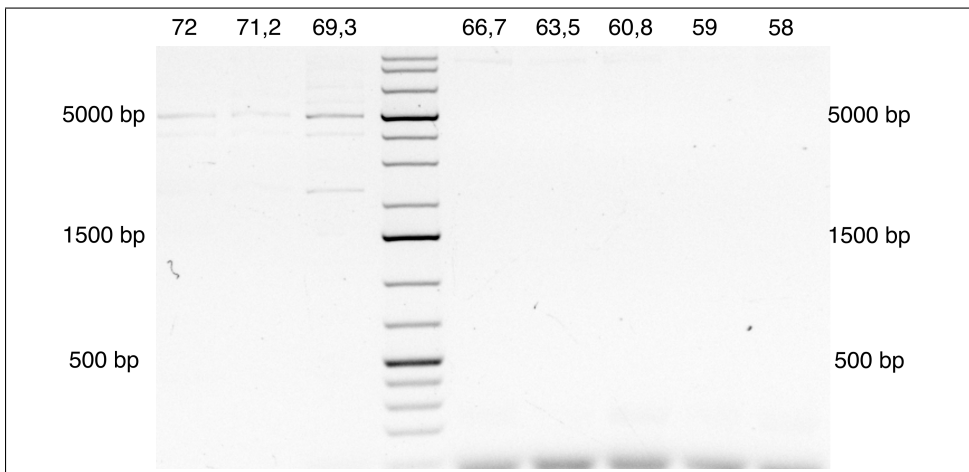


Figure 3.1: Electrophoresis results from PCR-amplified pBV2-sfGFP backbone by Q5 DNA polymerase kit with a temperature gradient in the annealing step of the PCR-program. Temperatures used are 58, 59, 60.8, 63.5, 66.7, 69.3, 71,2 and 72 °C, which is depicted above the gel image. Generuler 1 kb Plus C was used as the ladder, with 5000, 1500 and 500 base pairs (bp) being extra prominent.

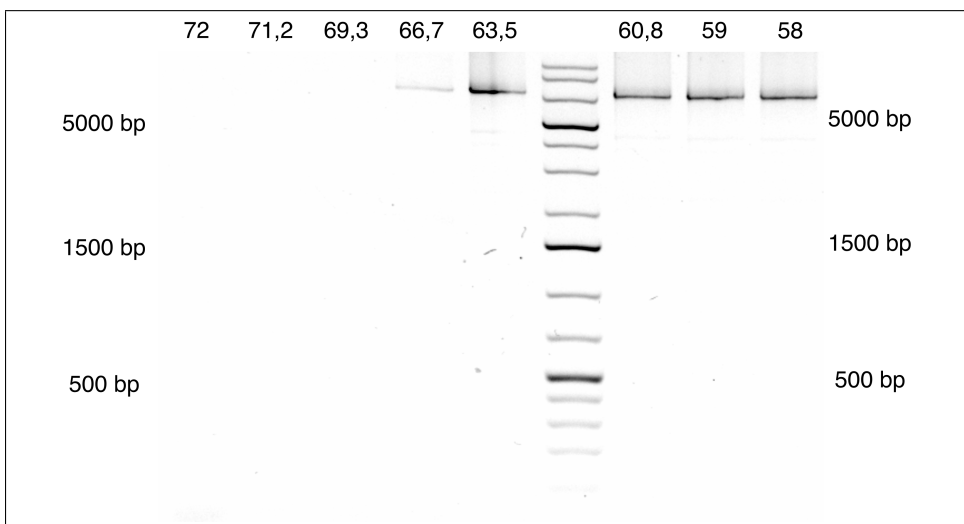


Figure 3.2: Electrophoresis results from PCR-amplified pBV2-ribB1 backbone by Q5 DNA polymerase kit with a temperature gradient in the annealing step of the PCR-program. Temperatures used are 58, 59, 60.8, 63.5, 66.7, 69.3, 71,2 and 72 °C, which is depicted above the gel image. Generuler 1 kb Plus C was used as the ladder, with 5000, 1500 and 500 base pairs (bp) being extra prominent.

Electrophoresis results from the amplified putative promoter sequences, as well as colony PCR-results are added in Appendix F.2.

3.1.1 Transformation of recombinant plasmids to *E. coli* and *B. methanolicus*

From the sequencing of transformed *E. coli* colonies, five new correct pTH1-constructs and seven new pBV2-constructs were attained in *E. coli*. The final overview of sequenced and approved constructs can be seen in Table 3.2. Putative promoter sequence 2, 7, 9 and 16 were inserted in pTH1-sfGFP and transformed to *E. coli*, but the sequencing of these plasmids revealed mutations. The sequencing results from putative promoter 9 revealed the same deletion of adenine in three of the six colonies that were sequenced (Appendix D). Mutations were also encountered when sequencing putative promoter 2 and 4 inserted in pBV2-sfGFP and putative promoter 2 and mp inserted in pBV2-ribB1 (not shown).

Putative promoter sequence	1	2	3	4	5	6	7	8	9	10	11	12	13	14	15	16	17	18	19	20	mp
pTH1-sfGFP	X*	-	X*	X*	X*	X	-	X	-	X	X*	X	X	X*	X*	-	X*	X*	X*	X*	X*
pBV2-sfGFP	X	-	X	-	X																X
pBV2-ribB1	X	-	X	X	X*																-

Table 3.2: Table of the confirmed sequenced putative promoters inserted in pTH1-sfGFP, pBV2-sfGFP, and pBV2-ribB1 plasmids after transformation into *E. coli* DH5. X marks constructs that have been validated during this research whereas X* represent validated plasmids from preliminary studies made by Jelstad (not published). Mutated sequences are denoted as a hyphen. Plasmids that have not been transformed to *E. coli* are left blank

Table 3.3 shows the putative promoters that were successfully transferred to *B. methanolicus*. Four new putative promoter sequences inserted in either pTH1-sfGFP, pBV2-sfGFP or pBV2-ribB1, were transformed to *B. methanolicus* MGA3.

Putative promoter sequence	1	3	4	5	11	12	15	17	18	19	20	mp
pTH1-sfGFP	–	–	X*	X*	X*	X	X*	X*	X*	X*	X*	X*
pBV2-sfGFP	–	X		–								X
pBV2-ribB1	X	–	–	X*								

Table 3.3: Table of the transformed putative promoters into *Bacillus methanolicus* MGA3 with the use of pTH1-sfGFP, pBV2-sfGFP, and pBV2-ribB1 as shuttle vectors. X marks constructs that have been transformed during this study, whereas X* represent transformed strains from previous work by Jelstad (not published). Failed transformations to *B. methanolicus* denoted as a hyphen. Plasmids that have not been validated by sequencing are left blank

3.2 Growth characteristics in different carbon sources and cultivation conditions

Growth curved obtained from BioLector in different cultivation conditions are added in Appendix B. Generally, a long lag-phase was observed in cultivation with methanol or mannitol as carbon source. Cultivation in glucose depicts a slow initial linear growth phase, followed by a short exponential growth phase before the stationary phase is reached.

3.3 Relating fluorescence to OD and calibrating riboflavin signal to concentration

The calibration curve for optical density at a wavelength of 600 nm (Appendix E) was performed in order to relate OD measured in Tecan plate reader to the OD measured in cuvette spectrophotometer. The calibration curve depicts a near linear relation of OD₆₀₀ measured in plate and cuvette, with a linear regression function depicted in Equation 3.1 and 3.2 for measurements in the Falcon (200 μ L) and Nunclon (100 μ L) plate respectively.

$$y = 2,669 * x - 0,129 \quad (3.1)$$

$$y = 4,7777x - 0,1755 \quad (3.2)$$

Where y is the optical density measured in the cuvette, and x is the optical density measured by Tecan Infinite Plate Reader.

The relation of detected riboflavin signal in BioLector ($\lambda_{Ex}=436$ nm, $\lambda_{Em}=540$ nm) is represented as a polynomial function of four degrees in Equation 3.3. Calibration curve of BioLector signal versus concentration is added in Appendix E.

$$y = -4 * 10^{-6}x^4 + 0,0011x^3 - 0,115x^2 + 5,8194x + 0,3803 \quad (3.3)$$

Where y is the riboflavin signal (gain=6), and x is the riboflavin concentration in mg/L

Furthermore, the calibration series performed for the HPLC quantification is added in Appendix E. A linear relation of the signal peak and the concentration of riboflavin was observed, and the linear regression function is presented in Equation 3.4. The retention time of riboflavin were measured to be 5.75 ± 0.01 min.

$$y = 4 * 10^{-10} * x - 1 * 10^{-4} \quad (3.4)$$

Where y is the riboflavin concentration in g/L, and x is the area of signal peak at $t_R = 5,75$ minutes.

3.4 Estimating promoter strength based on detected fluorescence intensity

3.4.1 Comparing protein expression from cells cultivated in flasks and deep well plates

Figure 3.3 shows the mean fluorescence intensity obtained from strains cultivated in flasks (preliminary research by Jelstad (not published)) or plate (this study). The studied strains contain eight of the putative promoters, as well as the *mdh* promoter inserted upstream an sfGFP encoding gene in the pTH1-plasmid. The fluorescence intensity from plate cultivations shows similar protein expression rate as cultivations performed in flasks. Furthermore, the putative promoter sequence 5 (glutamate synthase promoter) was found to have the highest expression of fluorescent protein in both cultivation conditions.

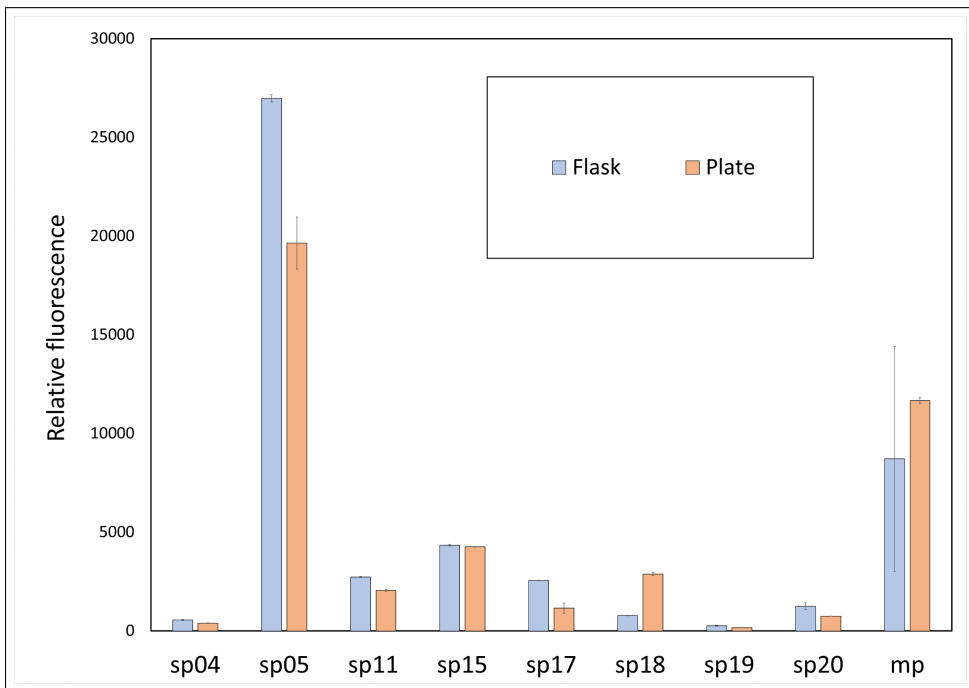


Figure 3.3: Comparison of relative fluorescence from strains cultivated in flask and 96-well plate with methanol as the carbon source. Presented strains contain pTH1-sfGFP vector with putative promoter 4, 5, 11, 15, 17, 18, 19, 20, and mp inserted upstream a green fluorescent protein-encoding gene (*sfGFP*). Results from flask cultivations are collected from preliminary research, whereas plate cultivations were performed as a part of the presented research (see text).

3.4.2 Comparing promoter strengths in different cultivation conditions

Figure 3.4 shows the mean relative fluorescent intensity in control of *mdh* promoter, putative promoter 4, 5, 11, 12, 15, 17, 18, 19, or 20. The strains were cultivated in minimal MVcM media with methanol, mannitol, or glucose as the carbon source. Protein expression did not vary based on carbon source for putative promoter 4, 12, 15, 17, 19 and 20, whereas a reduction in fluorescence are detected for sp05 and mp with mannitol as carbon source. Further, strains with the fluorescent protein in control of putative promoter 11 and 18 depicted a noticeably higher expression in cultivation with glucose as carbon source.

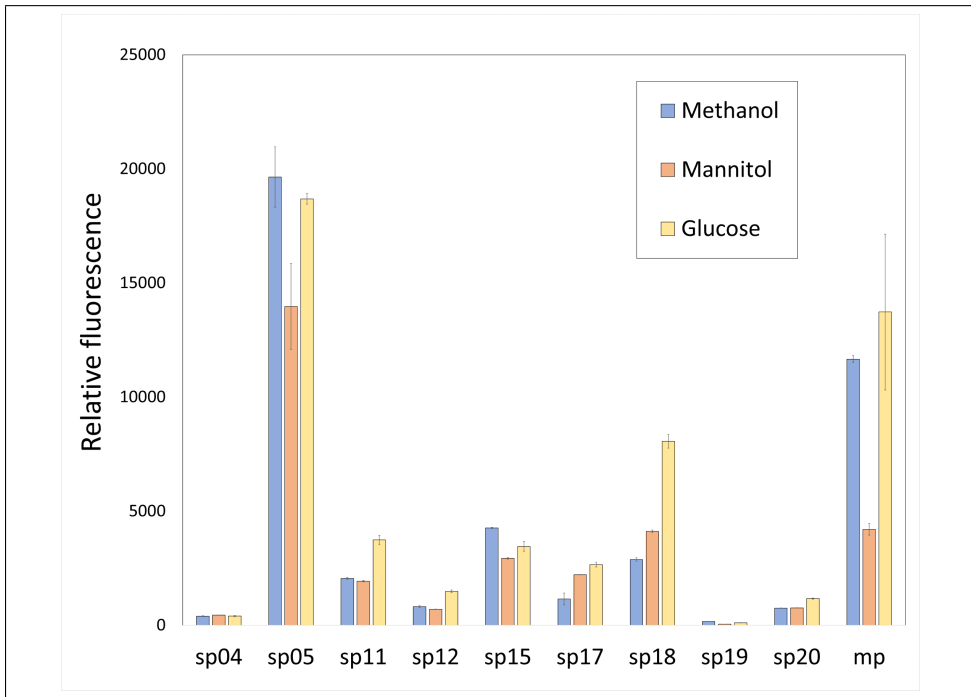


Figure 3.4: Comparison of relative fluorescence from the different pTH1-sfGFP containing strains with mp, sp04, sp05, sp11, sp12, sp15, sp17, sp18, sp19, and sp20 as fluorescent reporter promoter. Cultures were grown in MVcM-media with methanol (MeOH), mannitol (Man) or glucose (Glu) as carbon source.

Figure 3.5 compares the mean fluorescent intensity of strains with the putative promoters inserted in pTH1-sfGFP and cultivated in MVcM with methanol as the carbon source, with and without induced osmotic stress. Strains with the fluorescent protein in control of sp17 depict an increase in protein expression when cultivated with induced osmotic stress. No substantial variation in fluorescent intensity are detected for the other strains.

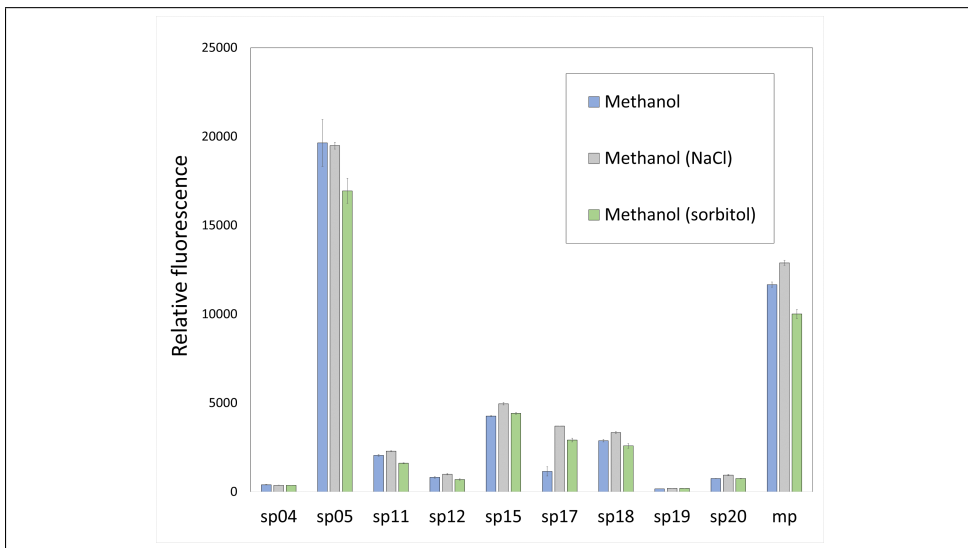


Figure 3.5: Comparison of relative fluorescence obtained from strains with sfGFP in control of *mdh*-promoter, putative promoter sequence 4, 5, 11, 12, 15, 17, 18, 19 or 20 in cultivation with induced osmotic stress. Osmotic stress was induced by addition of NaCl (160 mM) or sorbitol (Sorb, 300 mM) in MVcM-media with methanol as carbon source and pTH1 was used as the vector.

Figure 3.6 shows the expression of sfGFP controlled by putative promoter 4, 5, 11 and 15 in cultivations with different pH and with methanol as the carbon source. Similar expression rates of the fluorescent protein are observed for putative promoter sequence 4, 11 and 15, whereas sp05 depicts an increase in expression in basic conditions (pH=7.5).

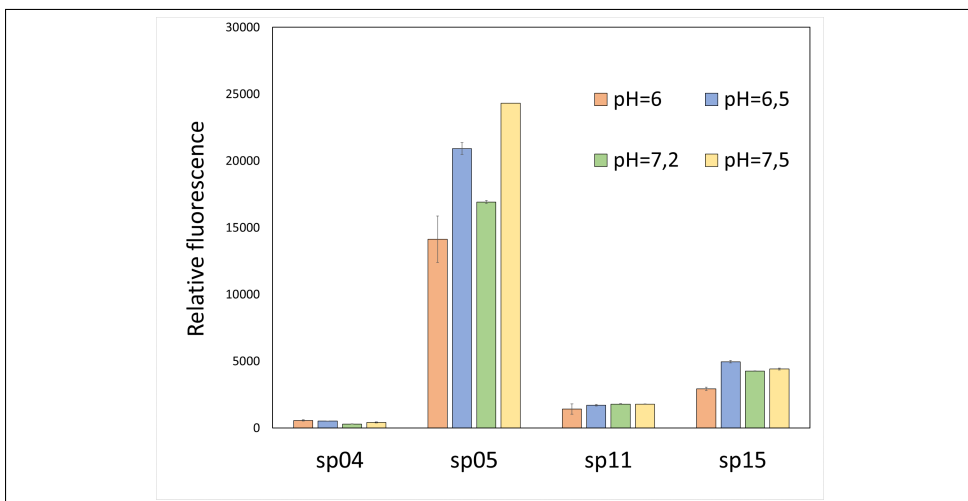


Figure 3.6: Relative fluorescence from putative promoter 4, 5, 11 and 15 inserted in pTH1-sfGFP and cultivated in different pH (pH=6, 6.5, 7.2 and 7.5)

3.4.3 Difference in expression rates for pTH1 plasmids and pBV2 plasmids

Figure 3.7 compares the fluorescent protein expression of pTH1 vector plasmid and pBV2 vector plasmid. The *mdh* promoter was used to relate the expression rates obtained in pBV2 to pTH1, whereas pBV2sp03-sfGFP represent fluorescent protein expression in control of putative promoter 3. Mean fluorescent intensity in control of *mdh* promoter are shown to increase by a factor of 1.9, 13.2, and 7.6 when cultivated in methanol, mannitol, and glucose, respectively (Appendix A.3, Table A.15). Further, sp03 shows similar expression rates as the *mdh* promoter in methylotrophic growth, but lower expression with mannitol or glucose as carbon source (72 % and 55 % respectively).

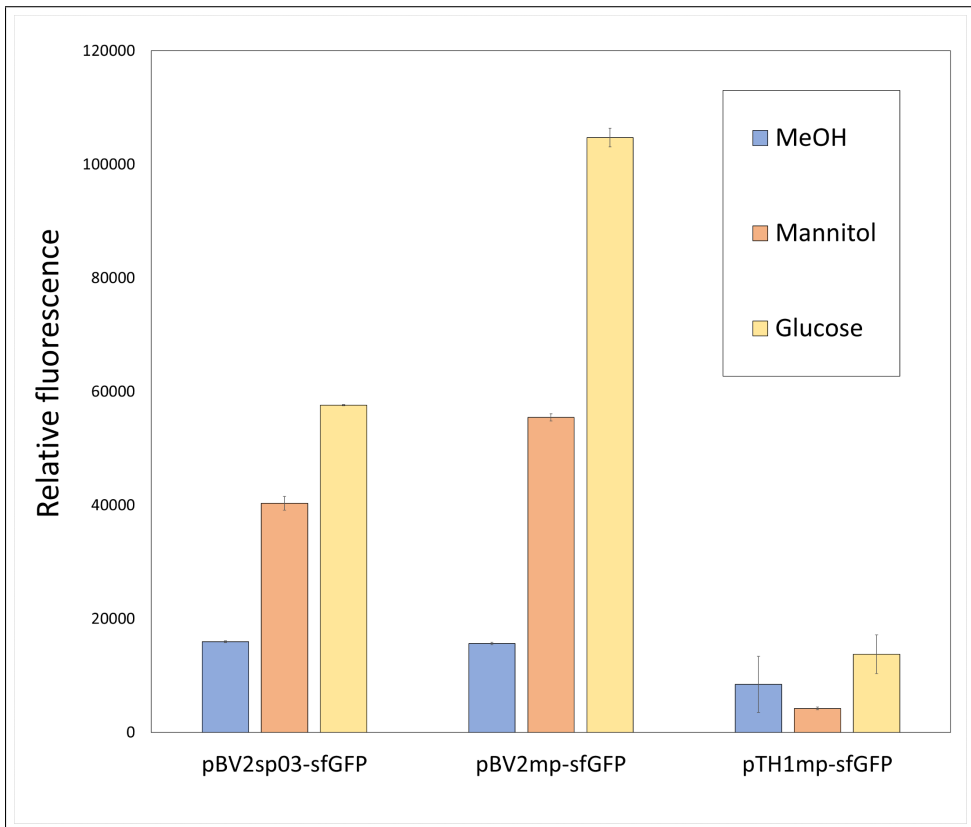


Figure 3.7: Fluorescent protein expression in pBV2 in control of sp03 and mp with methanol, mannitol and glucose as carbon source. pBV2mp-sfGFP are compared to pTH1mp-sfGFP

3.5 Predicting promoter strength of putative promoter 1 based on riboflavin production

Figure (3.8) represents the highest obtained riboflavin signal for pBV2sp01-ribB1 and pBV2sp05-ribB1 plasmids in the BioLector cultivation. Putative promoter 1 depicts a similar peak riboflavin concentration regardless of the carbon source utilized. However, the highest riboflavin concentration obtained for sp01 are increased under osmotic stress. The highest measured riboflavin signal was 12.4 (pBV2sp01-ribB1 (NaCl)), which correspond to a concentration of 2.2 mg/L riboflavin calculated from Equation 3.3 (Appendix A, Table A.16). This is a 15-fold increase to the sp05-strain in similar conditions (NaCl), based on the calculated concentration. The putative sp05-promoter showed a higher production of riboflavin when cultivated in mannitol rather than methanol, which contradicts the fluorescent protein expression using pTH1-sfGFP as vector.

HPLC was used in order to relate the calculated riboflavin concentration obtained in the BioLector (Appendix A, Figure A.17). The quantification of riboflavin in the supernatant measured by HPLC was found to be approximately 70 % of the riboflavin concentration calculated from the BioLector signal (Appendix A, Table A.17).

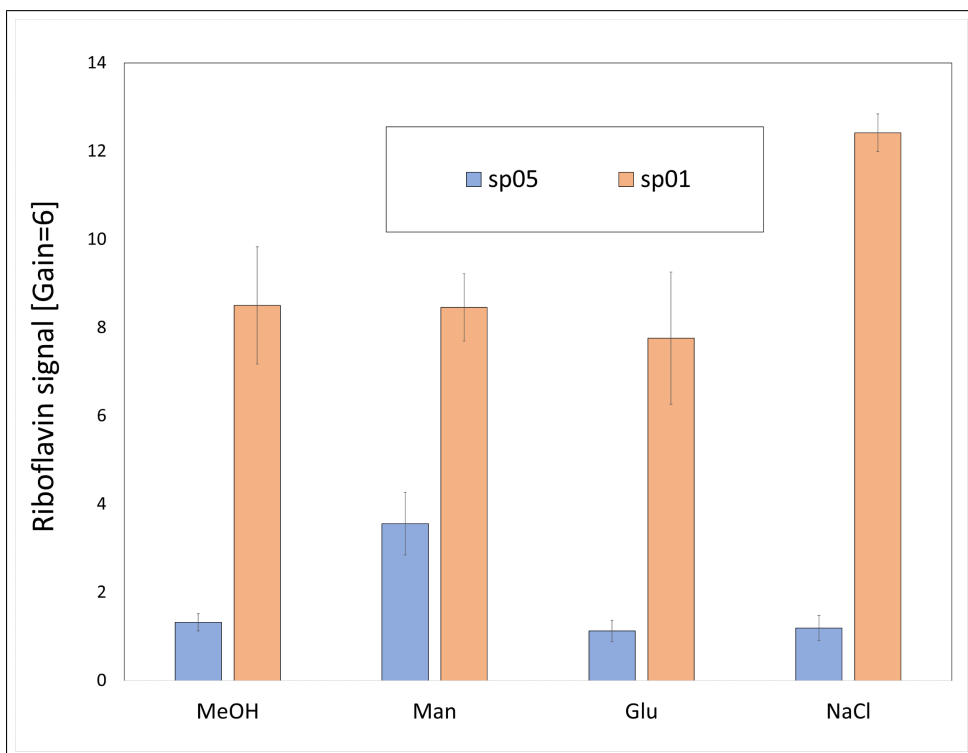


Figure 3.8: Maximum detected riboflavin signal from microbioreactor cultivations of pBV2sp01-ribB1 and pBV2sp05-ribB1 in MVcM minimal media containing methanol (MeOH), mannitol (Man) or glucose (Glu) as carbon source. Osmotic stress was induced by the addition of sodium chloride (160 mM) media with methanol as the carbon source.

Discussion

4.1 Amplification, optimizing PCR-conditions and sequencing transformed plasmids from *E. coli*

The two plasmids, pBV2 and pTH1, were chosen based on their low copy number which limits the added metabolic burden on the cell, thereby making transformation viable. Furthermore, knowing the promoter properties in multiple shuttle vectors (both theta- and rolling circle-replicating plasmids) expands the applicability of the studied putative promoters. Super-folded green fluorescence protein (sfGFP) was primarily used based on the thermostable folding feature of the protein, ease of detection, and not being a part of the cell's metabolism [21]. Having a protein that is not degraded by the cells leads to a more reproducible reporter signal that accumulates during cultivation. Conversely, the riboflavin operon produces metabolically active riboflavin, which is further consumed by the cells. What is more, the riboflavin, which is produced by the enzymes residing in the operon, are prone to additional translational regulation. The added enzymatic pathway in riboflavin production could make quantification of promoter strength less accurate. Nevertheless, the riboflavin operon was inserted as an example of the practical applications the putative promoter sequences could serve but were also used as a reporter to estimate the strength of putative promoter 1.

The Takara CloneAmp Hi-Fi DNA polymerase kit was the preferred PCR amplification kit based on the robustness, performance, and high fidelity of the polymerase. However, some problems regarding product yield when amplifying the pBV2 vector backbone were encountered. Therefore, Q5 High-Fidelity DNA polymerase was used as an alternative. The annealing temperature gradient was introduced in order to optimize Q5 polymerase performance. Standard taq-polymerase was used for the bulk colony-PCR amplifications due to the small required volume of the enzyme in each reaction.

4.1.1 Sequencing the promoter sequence and screening for mutations

Prolonged DpnI-digestion and lower cultivation temperature allowed 12 putative promoter sequences to be transformed successfully to *E. coli*

The amplified vectors were digested for one hour with DpnI, a restriction endonuclease that cuts between A and T in 5'-GATC-3' when the recognition site is methylated. This was done in order to remove template residues that have been methylated by *dam* or *dcm* in *E. coli* during the cloning of template plasmid [42, 43, 44]). Nonetheless, high transformation frequency when transforming competent *E. coli* with Gibson mix without the insert indicated a noticeable rest of template DNA in the backbone PCR-product (not shown). The digestion duration was therefore prolonged from one hour to 16-20 hours to ensure proper digestion of the methylated DNA, which reduced the frequency of the template residues being transformed.

The different vectors gave variable transformation frequencies in *E. coli*, with pBV2-*ribBI* generally giving fewest transformants. Although the pBV2 plasmid has a lower copy number than pTH1 (three and five respectively), the large riboflavin operon could contribute with an increased metabolic burden, thus exhausting the cells and reduce the growth rate of transformants.

Furthermore, the transformed *E. coli* DH5 α colonies were yellow for the sfGFP-containing strains, making screening for sfGFP producing strains easier. Contrarily, riboflavin producing strains colored the agar orange without any noticeable staining of the cultures, making differentiation of the recombinant colonies more difficult.

Colonies with putative promoter sequences that were successfully amplified in colony-PCR were sent to sequencing for further validation of the inserted sequence. The sequencing was performed in duplicates, preferably sequencing both directions of the promoter sequence in order to proof-read the initial sequence of each strain. However, due to elusive primer binding, the pBV2-constructs were only validated in one direction, which could present uncertainties in the sequencing results.

Random mutations were repeatedly encountered for a multiple of the recombinant strains. In order to limit the mutations, a reduced incubation temperature of 25 °C was applied, as the mutation rate is known to decrease with temperature [45]. However, mutants were still experienced for some strains, preventing further exploration of sp02, 07, 09 and 16. Interestingly, the same deletion mutation of adenine was observed for sp09 in three of six sequenced colonies (Appendix A.1). The deletion was found inside the -10 element (TATAT), and presumably detrimental for promoter function.

After reducing cultivation temperature and prolonging the DpnI digestion, a total of twelve new putative promoter sequences, either in pTH1 or pBV2, were attained in *E. coli*, and validated by sequencing (Table 3.2).

4.2 Transformation of *Bacillus methanolicus* MGA3

Transformation is often regarded as one of the main factors that hinder the genetic study of Gram-positive bacteria, which also was found to be the case for this study. The applied transformation method, i.e. electroporation, is the most widely used transformation method for Gram-positive bacteria and is the preferred transformation method for

B. methanolicus [21]. Alternatively, a protoplast transformation performed by enzymatic removal of the peptidoglycan cell wall to create a protoplast could be used [46, 21]. However, the latter method is time-consuming and labor-intensive with variable efficiency and was therefore not applied.

Electroporation enabled three new putative promoter sequences to be transformed to *B. methanolicus*

Transformation by electroporation gave low transformation frequency, and often no transformants at all. The transformation efficiency varied based on the plasmids used as shuttle vector, the inserted putative promoter sequence, and the chosen reporter gene. Multiple efforts were carried out for the validated pTH1-sfGFP plasmids with the putative promoters inserted. Still, no transformants were observed for the plasmids containing putative promoter sequence 1, 3, 6, 8, 10, 13 and 14. The transformation attempts varied in which plasmid prep that was used, concentration and volume of purified plasmid added to the competent cells. Different batches of competent cells were also explored in order to enhance transformation efficiency.

The electroporation protocol has previously been optimized for *B. methanolicus* and was not further investigated. However, many factors such as growth medium, growth phase, electric field, weakening agent, plasmid quantity, plasmid desalting, electroporation buffer, and heat treatment, all influence the electroporation efficiency [47, 46]. These factors have been thoroughly investigated for other bacilli [46, 47, 48, 49], where the main improvements have been made by cell weakening agents such as the addition of glycine to the competent cells. The improvement of electroporation protocols for other bacilli implies that further electroporation optimization could also be beneficial for *B. methanolicus*. However, this was not further studied in this project.

Multiple plasmid purification kits were explored to ensure a high plasmid concentration before the transformation. The obtained plasmid concentration ranged between 100 ng and 350 ng which required a volume of up to 20 μL in order to add 2 μg of plasmids as recommended in the protocol. An arc was observed in the electroporation cuvette if the volume of purified plasmid exceeded 10 μL . The formation of an arc is presumably caused by a too high electroporation voltage or a high salt concentration in plasmid solution. Initially, the plasmids were eluted from the purification column with an elution buffer. The elution buffer was replaced with DNase free water in order to reduce the salt content, thus allowing a higher plasmid volume in the electroporation cuvette before the arc appeared.

This enabled four new strains containing putative promoter sequence 1, 3, 12 and *mdh* promoter to be successfully transformed into *B. methanolicus* with the use of pTH1 and pBV2 as shuttle vectors, as presented in Table 3.3.

Strong putative promoter sequences are speculated to be the reason for transformation difficulties

As of why the transformation failed for some of the recombinant plasmids is speculated to be due to promoter strength. Transformation problems generally occurred for the putative promoters estimated to be the strongest, which induces a higher metabolic burden to the cells. The exhaustion of cells would explain lower transformation efficiency, but the failure

to obtain any viable transformants is believed to require a more complex explanation. A strong promoter could also lead to a higher expression of potentially toxic compounds residing inside the plasmid. Being unable to have a comprehensive understanding as to what functional genetic materials the plasmid is composed of, the pBV2 plasmid was used as an alternate shuttle vector with both lower copy number and a riboflavin operon as the alternative feature genes.

Interestingly, putative promoter sequence 1 was only successfully transformed with pBV2-ribB1 as the vector. The riboflavin operon used as the reporter contains four genes (*ribDEAH*) in an almost 3500 nucleotide long operon. Inserting sp01, which is expected to be the strongest promoter in front of this operon would introduce a high metabolic burden to the cells, which was one of the main hypothesis as of why there were no viable transformants of the pTH1sp01-sfGFP strain. It is possible that the riboflavin production is regulated at a translational level, thus reducing the metabolic burden caused by protein synthesis. Additionally, riboflavin is also metabolized by the cell, which could make up for the high energy demands.

What is more, *B. methanolicus* MGA3 has a native restriction endonuclease enzyme, *Bme*TI, which recognizes the sequence 5' TGATCA 3' [50]. This restriction site is found in the sp01-sequence and could be the reason for the initial transformation problems. The restriction enzyme *Bme*TI do not cleave when restriction site is methylated (TGm⁶ATCA). *B. methanolicus* holds a methylase partner gene to *Bme*TI (*m-Bme*TI) that copies the native methylation patterns during replication, thus preventing cleavage of the native DNA. Further, when introducing DNA from *dam*⁺ *E. coli*, the DNA gets methylated in a similar pattern, also inhibiting *Bme*TI cleavage [50]. It is possible that *dam*-methylated DNA, while being resistant to cleavage, is also a poor substrate for methylation by *m-Bme*TI, thus leaving the restriction sequence readily cleaved by *Bme*TI after a number of replications. If this is a problem or not for the perceived transformation problems require further research, but the fact that pBV2sp01-ribB1 eventually was transformed, indicates that the transformation of DNA containing the restriction site is possible.

4.3 Growth conditions and characteristics

Cultivation of *B. methanolicus* is challenging as the growth rate is highly susceptible to temperature changes [16]. *B. methanolicus* MGA3 is known to sporulate when growth temperature rapidly decreases from 50 °C to 37 °C [21]. Hence, handling of the bacteria outside incubator was done swiftly to limit the formation of inhibitory products and to limit the lag-phase when re-inoculating. The use of a heating block limited the heat dispersion, and all equipment and media were pre-warmed to 50 °C. Still, the re-inoculation to well plates was followed by an extended lag-phase and occasionally cell death. A fresh pre-culture in exponential growth phase was found to be crucial in order to have a consistently healthy production culture.

The aeration in square plate well cultivation is presumed to be sufficient

Cells that metabolize methanol has a higher metabolic demand for dissolved oxygen compared to cells growing on glucose or other sugar substrates due to methanol being more

reduced [17]. Consequently, aeration of cultivations is an important factor to consider. This was maintained by having a high shaking frequency (900 rpm) in the plate incubator, and by incubating in a plate with square wells. The increased oxygen demand of methylo-trophy could explain the variable growth rates observed in the cultivations. However, the cultivations with sugar substrate were not unambiguously thriving better than cultivations with methanol as the substrate. This indicates that the aeration was sufficient in plate cultivations for the cells to thrive. The metabolism is therefore regarded as the main reason for the variable growth characteristics.

Cultivation in BioLector showed distinct growth curves for the different cultivation conditions

When looking at the biomass accumulation of cultivations performed in the BioLector, the different carbon substrates gave rise to categorically characteristic growth curves (Appendix B). Cultivation with methanol and mannitol as carbon source was found to have a long lag phase, followed by a rapid exponential growth phase before the stationary phase was reached. Cultivation with glucose as substrate was however distinguished from methanol and mannitol cultivations by having a longer initial linear growth curve with a constant slow growth rate. The induction of osmotic stress by addition of sodium chloride seemed to slow down the exponential growth phase, and linear growth characteristics were observed before the stationary phase was reached. Interestingly, the strains cultivated with methanol as carbon source showed stagnation in the exponential growth. This could be due to formaldehyde accumulation caused by methanol dehydrogenase, which is toxic to the cells. However, stagnation of exponential growth is also somewhat present in pBV2sp05-ribB1 with mannitol as the carbon source, making the explanation questionable.

This data was obtained from cultures with pBV2sp01-ribB1 and pBV2sp05-ribB1 inserted. The addition of a riboflavin producing operon would presumably alter the growth characteristics, but the general trend for each cultivation is regarded to be representative for the different carbon sources.

4.4 Detection of fluorescence and riboflavin production

Furthermore, a relation of OD_{600} and fluorescence was measured in order to establish a linear detection area for fluorescence. Figure E.2 (Appendix E) depicts a linear relation for the OD_{600} and fluorescence when the OD is below 0.6 (measured in cuvette). When the OD_{600} surpasses 0.6, the relative fluorescence signal seems to drop off. This suggests that future measurements should be taken with an OD_{600} below 0,6 in order to produce reliable data. Interestingly, when plotting OD_{600} measured in the plate reader against fluorescence, the relation is linear throughout the measurement series (not shown). This indicates that the error is residing in OD measurement inaccuracy, and not a saturation of the fluorescent detector.

Figure E.3 (Appendix E) shows the relation of riboflavin signal measured in the BioLector with gain=6 compared to the concentration of riboflavin. The riboflavin signal is not proportional to the concentration, which could indicate that the detector is being saturated. However, an estimated polynomial function with four degrees (equation 3.3) fits

the data points with an R^2 value of 0.99995. Concentrations of riboflavin up to 100 mg/L was used based on previous cultivations of riboflavin producing MGA3-strains which produced up to 67 mg/L riboflavin in flask cultivations (not shown). Furthermore, the gain of 6 amplified the signal strength to be between 0 and 200, which is recommended by BioLector distributor.

4.5 Estimating promoter strength based on detected fluorescence and riboflavin production

The occasional large standard deviation (e. g. pTH1mp-sfGFP (flask) in figure 3.3) depicts a large variation of fluorescent protein expression in isogenic cultures under the same cultivation condition. Protein expression is dependent on many systemic and protein-specific factors that are susceptible to either intrinsic or extrinsic factors [51]. However, the phenotypic "noise" was not evident within the parallels of each cultivation, and the large variation of fluorescence was only noticeable when comparing production cultivations prepared on separate occasions. The state of the pre-cultures is therefore presumed to be decisive for protein expression. However, when comparing the two cultivation methods, it is clear that the obtained fluorescent signal from plate cultivation provides a qualitative indication of promoter strength, even if the exact quantitative values are variable.

Putative promoter sequence 5 (glutamate synthase promoter) was found to have the highest expression of fluorescent protein

From the preliminary research, it was found that putative promoter sequence 5 exhibits the strongest promoter strength in cultivations with methanol as carbon source, compared to putative promoter 4, 11, 17, 18, 19, 20 and mp. In the preliminary research, the promoter strength of putative promoter 5 depicts a three-fold increase compared to the commonly used methanol dehydrogenase promoter (mp). Contrarily, the other studied putative promoter sequences displayed a low expression of the fluorescent protein when cultivated in methanol as c-source. The same trend is continued in this research where the cultivations have been performed in well plates (Figure 3.3). Similar results imply that the presented promoter strengths are comparable and reproducible.

Promoter 5 is located upstream of a glutamate synthase gene cluster in the *B. methanolicus* MGA3 genome (Table 3.1). Wild type *B. methanolicus* is known to have a high production of glutamate, which is likely due to the low native activity of 2-oxoglutarate dehydrogenase (ODHC) preventing oxidation of 2-oxoglutarate from the citric acid cycle [17]. Glutamate synthase (GOGAT) is responsible for the transamination of glutamine and 2-oxoglutarate into glutamate. Alternatively, glutamate is synthesized by amination of 2-oxoglutarate by glutamate dehydrogenase (GDH1) if there is an excess of nitrogen [52]. Which of the two alternative mechanisms that are dominant for the high glutamate production of *B. methanolicus* is not known [17].

The strong promoter properties of sp05 would suggest a high transcriptional rate of *gltAB* if the genes are transcribed under the control of the same promoter, thus making the glutamate synthase enzymes abundant and thereby available for transamination of 2-oxoglutarate. If the elevated *gltAB* transcription leads to highly expressed enzymes, and if

the available enzymes are a decisive factor for which of the pathways *B. methanolicus* are utilizing for glutamate production require further research.

Elevated expression in cultivations using glucose as the carbon source for putative promoter 11 and 18

The different cultivation conditions did not seem to present any substantial variance in fluorescence for most of the strains, except down-regulation of sp05 and *mdh*-promoter cultivated with mannitol and possibly an up-regulated sp18 and sp11 in glucose cultivation (Figure 3.4).

Methanol dehydrogenase expression has previously been shown by Heggeset et al. (2012) to decrease in cultivation with mannitol as the carbon source [18]. The down-regulated *mdh* expression was presumed to be due to non-methylotrophic growth. However, the increased expression observed in glucose cultivations suggests a more complex regulatory system. What is more, cultivations with glucose as carbon source shows the highest reporter protein expression in 5 out of 10 strains. Protein expression is known to be growth-dependent [53, 51], which is presumably the main cause of the increased expression, rather than promoter regulation.

A substantial increase in fluorescent protein expression was observed for strains containing sp11 and sp18 (1.8 fold and 2.8-fold increase, respectively, compared to methylotrophic growth). Promoter sp11 and 18 are found upstream the genes encoding NH(3)-dependent NAD(+) synthetase and 2-hydroxyacid dehydrogenase (NAD-binding protein) respectively (Table 3.1). Both of which are required in biological processes and metabolic function regardless of carbon source. It is difficult to hypothesize if the increased expression rates are due to the glucose directly influencing promoter properties or another indirect factor. The final obtained cell density of cultures cultivated on glucose as c-source were comparable to the other cultivations. Further, with fluorescence related to OD, the final cell density is therefore not regarded as a contributing factor for the increased expression as long as the cells were in exponential phase during harvesting.

Unexpected low fluorescence from putative promoter 4

One of the peculiar findings was that putative promoter 4, which is located upstream a putative sugar phosphate isomerase (*rpiB*) gene in the MGA3 genome (Table 3.1), depicted very low fluorescence in all of the studied cultivation conditions. RpiB is active in the RuMP pathway regeneration phase by converting ribose-5-phosphate to ribulose-5-phosphate. This implies that RpiB is most active in methylotrophic cultivation. As of why putative promoter 4 depicts similar and low expression rates regardless of cultivation condition are therefore bizarre. Low expression of *rpiB* would benefit the cells if the general need of the enzyme were low, but the RNA-sequencing performed by Irla et al. (2015) [8] revealed a high abundance of transcript downstream putative promoter 4, indicating a strong promoter. It is therefore suspected that a mutation in either the putative promoter sequence or the reporter gene causing a loss of function is the reason for the unexpectedly low expression. Mutations in transformed plasmids could be investigated further by sequencing.

Because of the relatively small variances in fluorescence of the different studied promoter sequences, it is assumed that they are all constitutive. Finding either inducible or constitutive promoters of variable strength is highly valuable for *B. methanolicus* since the genetic toolbox is poorly developed with limited research regarding promoter function and performance. Furthermore, promoters with different strengths are often used as a regulation mechanism of specific pathway genes to further understand the contribution of each enzyme. Enabling scientists with a wider promoter library are highly valuable for the future endeavour of relevant genetic material residing in *B. methanolicus*.

Expression of sfGFP increased in pBV2 compared to pTH1

Figure 3.7 shows an increase in fluorescence for strains with pBV2mp-sfGFP plasmids compared to strains with pTH1mp plasmids. Fluorescence from pBV2 also depicts a larger variability depending on the carbon source. The expression of the reporter gene is reduced in methylotrophic growth but are highly up-regulated in both mannitol and glucose cultivation. Furthermore, the fluorescence is similar for sp03 and the *mdh* promoter when the strains are cultivated with methanol as the carbon source but differ greatly when the carbon source is replaced with mannitol or glucose. Nevertheless, the same trend in increased fluorescence is observed for sp03 and mp in the different carbon sources. With previous data suggesting a down-regulated *mdh*-promoter activity in mannitol, the variation in expression is thought to be due to an increased copy number, growth rate, or a combination of the two.

Irla et al. (2016) [19] reported a 4.5-fold increase in reporter gene expression in pTH1mp-*gfpuv* strains compared to pBV2mp-*gfpuv* in methylotrophic growth. This was in agreement with the higher copy number of pTH1-plasmid compared to pBV2 (5 ± 1 and 3 ± 1 , respectively [19]). Contradicting this data, Figure 3.7 depicts an increase in expression for the pBV2-vector in both methylotrophic and non-methylotrophic growth. What is more, the ribosomal binding site (RBS) was the same for the two plasmids, indicating that the translation rate is not the limiting factor. The pBV2 strains were observed to have a slower growth rate, compared to strains with pTH1. Also, pBV2sp03-sfGFP grew slower than pBV2mp-sfGFP (not shown), possibly indicating a higher metabolic burden with the fluorescent protein in control by sp03. However, a higher metabolic burden would also indicate a higher fluorescent protein production for pBV2sp03-sfGFP, which is not observed.

4.5.1 Putative promoter sequence 1 revealed 15 times higher production of riboflavin than glutamate synthase promoter (sp05) in microbioreactor cultivation

Riboflavin is produced in the riboflavin pathway (RBP) catalyzed by the *ribADEH* genes in the *ribBl* operon [54]. A strong expression of the *ribBl* operon would presumably be followed by higher riboflavin production, but the relation of operon expression and riboflavin production are difficult to predict.

The riboflavin signal obtained from pBV2sp01-*ribBl* suggests a 15-fold increase in riboflavin production when the riboflavin operon is in control by the putative promoter

1 compared to sp05, and cultivated in high osmotic stress (Figure 3.7 and Table A.16). This would make sp01 the strongest of the studied promoters. Interestingly, the highest obtained riboflavin concentration in cultivation using mannitol as the carbon source only depicts the sp01 promoter to be 2.6 times as strong as the putative sp05 promoter. The upregulation of riboflavin production for the sp05 in cultivations with mannitol as the carbon source is contradicting the fluorescent intensity obtained from pTH1sp05-sfGFP cultivated in mannitol. The conflicting results could be due to the chosen reporter genes, but also as a function of the chosen vector.

Further, a pBV2xp-ribB1 MGA3-strain containing a xylose-inducible promoter (xp) shown riboflavin signals 8-folds higher than that observed in this experiment (not shown). Thus, implying that higher riboflavin production is possible in a strain where the promoter is the only genetic material that differs, suggesting the promoter strength to be the limiting factor in the riboflavin production.

The most riboflavin was produced in cultivations with induced osmotic stress. Whether the osmotic stress improved promoter function or altered feedback mechanisms is difficult to hypothesize. The riboflavin derivatives are metabolically active in bacteria in a variety of physiological processes [54]. This is depicted in the measurement series by an accumulation of riboflavin in lag-phase and peaking in exponential growth before the riboflavin concentration diminishes as the growth rate decreases as the stationary phase is reached. Further attempts in transforming sp01 in front of sfGFP should therefore be performed in order to accurately assess the promoter characteristics and reliably compare it to the other putative promoters presented in this study.

It is not observed any significant differences in riboflavin production on methanol, mannitol, or glucose as carbon source. This suggests that sp01 is equally active in cultivations regardless of carbon sources used. The sp01 putative promoter is located upstream a 3-hexulose-6-phosphate synthase (*hps*)-gene, which condensates formaldehyde and ribulose 5-phosphate in methylotrophic growth. The condensation prevents the accumulation of formaldehyde and is crucial for the high methanol tolerance shown in *B. methanolicus*. Previously published transcriptome data by Heggeset et al. (2012) [18] has reported an up-regulated transcription of *hps*-gene in cultivations with methanol as the carbon source. Müller et al. (2015)[29] found proteomic expression in agreement with transcriptome data, thus indicating a promoter induced in methylotrophic growth. The *hps* gene is one of the two genes encoded on the chromosome that is associated with methanol metabolization. It is therefore speculated if the location on the chromosome regulates the *hps* gene expression and not promoter sequence.

When comparing calculated riboflavin concentration from the BioLector signal and HPLC, the concentration obtained in the BioLector is higher. It is not known whether the loss of riboflavin is due to the unstable nature of the molecule, or measurement error. The riboflavin signals from the BioLector were lower than expected when making the calibration series, making the calibration curve inaccurate for the measured signals. However, even if the quantitative value is inaccurate, the relation of expressed riboflavin is still sufficient in order to differentiate the promoter strengths of putative promoter 1 and 5.

4.6 Future work

The studied putative promoter sequences provide a much-needed expansion to the limited promoter library available for *B. methanolicus*. Having a diverse pool of promoters with different strengths and properties provides researchers a valuable molecular tool in studying gene function as it can be used to fine-tune the expression of specific genes [55, 56]. However, the findings presented in this study also depicts conflicting results for protein expression in control of homologous promoters in two of the applied shuttle vectors (pTH1 and pBV2). The contradictory results urge further studies in transcriptional regulation to and protein expression to be performed on these shuttle vectors. The promoter strength of putative promoter sequence 1 also needs further evaluation using a different reporter gene. More effort can also be made in order to properly appraise the promoter strength of the remaining putative promoter sequences.

Conclusion

This research aimed to identify the promoter strength in different cultivation conditions for putative promoter sequences residing in *Bacillus methanolicus*. Based on a quantitative analysis of fluorescent protein expression and production of riboflavin, the strength of eleven novel putative promoter sequences were studied with methanol, mannitol and glucose as the carbon source, in varying osmotic stress, and in different pH. Two putative promoters (*hps*-promoter and *gltAB*-promoter) revealed higher expression rates than the commonly used, constitutive *mdh* promoter in *Bacillus methanolicus* MGA3. The *gltAB* promoter showed higher fluorescent intensity than *mdh* promoter regardless of carbon source, pH and osmotic stress when inserted in the pTH1 plasmid. What is more, putative *hps* promoter depicted a 15-fold increase in riboflavin production when compared to the putative *gltAB* promoter in cultivations with high osmotic stress and in methylotrophic growth. However, the increased production in riboflavin is suspected to not be proportional to the promoter strength, thus requiring further research with a more suitable reporter in order to properly assess the promoter strength of the putative *hps* promoter. Furthermore, increased protein expression was observed for pBV2-plasmids with highly variable expression when cultivated with different carbon sources. The increased expression rates in pBV2 contradict previously published data and suggest a more complex regulatory system.

Available promoters are limited for *Bacillus methanolicus*, making any progress in the expansion of possible promoter sequences attractive. The study of promoter strengths under different cultivation conditions has provided the much-needed augmentation of the usable molecular toolbox, thus facilitating future molecular genetic research in *B. methanolicus*. This research has suggested eleven constitutive promoters with varying strength, but the need for good alternatives for inducible promoters are still desirable and require further exploration.

Bibliography

- [1] Michael D Engstrom and Brian F Pflieger. Transcription control engineering and applications in synthetic biology. *Synthetic and systems biotechnology*, 2(3):176–191, 2017.
- [2] Heladia Salgado, Gabriel Moreno-Hagelsieb, Temple F Smith, and Julio Collado-Vides. Operons in escherichia coli: genomic analyses and predictions. *Proceedings of the National Academy of Sciences*, 97(12):6652–6657, 2000.
- [3] W Terrance Godbey. *An Introduction to Biotechnology: The Science, Technology and Medical Applications*. Elsevier, 2014.
- [4] David L Nelson, Albert L Lehninger, and Michael M Cox. *Lehninger principles of biochemistry*. Macmillan, 2008.
- [5] Douglas F Browning and Stephen JW Busby. The regulation of bacterial transcription initiation. *Nature Reviews Microbiology*, 2(1):57, 2004.
- [6] CA Gross, C Chan, A Dombroski, T Gruber, M Sharp, J Tupy, and B Young. The functional and regulatory roles of sigma factors in transcription. In *Cold Spring Harbor symposia on quantitative biology*, volume 63, pages 141–156. Cold Spring Harbor Laboratory Press, 1998.
- [7] Elizabeth A Campbell, Oriana Muzzin, Mark Chlenov, Jing L Sun, C Anders Olson, Oren Weinman, Michelle L Trester-Zedlitz, and Seth A Darst. Structure of the bacterial rna polymerase promoter specificity σ subunit. *Molecular cell*, 9(3):527–539, 2002.
- [8] Marta Irla, Armin Neshat, Trygve Brautaset, Christian Rückert, Jörn Kalinowski, and Volker F Wendisch. Transcriptome analysis of thermophilic methylotrophic bacillus methanolicus mga3 using rna-sequencing provides detailed insights into its previously uncharted transcriptional landscape. *BMC genomics*, 16(1):73, 2015.
- [9] Akira Ishihama. Functional modulation of escherichia coli rna polymerase. *Annual Reviews in Microbiology*, 54(1):499–518, 2000.

-
- [10] Melanie M Barker, Tamas Gaal, Cathleen A Josaitis, and Richard L Gourse. Mechanism of regulation of transcription initiation by ppgpp. i. effects of ppgpp on transcription initiation in vivo and in vitro. *Journal of molecular biology*, 305(4):673–688, 2001.
- [11] Ernesto Pérez-Rueda and Julio Collado-Vides. The repertoire of dna-binding transcriptional regulators in escherichia coli k-12. *Nucleic acids research*, 28(8):1838–1847, 2000.
- [12] Karin Schnetz. Silencing of escherichia coli bgl promoter by flanking sequence elements. *The EMBO journal*, 14(11):2545–2550, 1995.
- [13] Bart JAM Jordi and Christopher F Higgins. The downstream regulatory element of the prou operon of salmonella typhimurium inhibits open complex formation by rna polymerase at a distance. *Journal of Biological Chemistry*, 275(16):12123–12128, 2000.
- [14] Sarah M McLeod and Reid C Johnson. Control of transcription by nucleoid proteins. *Current opinion in microbiology*, 4(2):152–159, 2001.
- [15] Zafar Alam Mahmood. Microbial amino acids production. In *Microbial Biotechnology*, pages 202–227. CRC Press, 2014.
- [16] Nader Al-Awadhi, Thomas Egli, and Geoffrey Hamer. Growth characteristics of a thermotolerant methylotrophic bacillus sp.(ncib 12522) in batch culture. *Applied microbiology and biotechnology*, 29(5):485–493, 1988.
- [17] Trygve Brautaset, Øyvind M Jakobsen, Kjell D Josefsen, Michael C Flickinger, and Trond E Ellingsen. Bacillus methanolicus: a candidate for industrial production of amino acids from methanol at 50 c. *Applied microbiology and biotechnology*, 74(1):22–34, 2007.
- [18] Tonje MB Heggeset, Anne Krog, Simone Balzer, Alexander Wentzel, Trond E Ellingsen, and Trygve Brautaset. Genome sequence of thermotolerant bacillus methanolicus: features and regulation related to methylotrophy and production of l-lysine and l-glutamate from methanol. *Applied and environmental microbiology*, pages AEM-00703, 2012.
- [19] Marta Irla, Tonje M. B. Heggeset, Ingemar Nrdal, Lidia Paul, Tone Haugen, Simone B. Le, Trygve Brautaset, and Volker F. Wendisch. Genome-based genetic tool development for bacillus methanolicus: Theta- and rolling circle-replicating plasmids for inducible gene expression and application to methanol-based cadaverine production. *Frontiers in Microbiology*, 7:1481, 2016.
- [20] Marc Carnicer, Gilles Vieira, Trygve Brautaset, Jean-Charles Portais, and Stephanie Heux. Quantitative metabolomics of the thermophilic methylotroph bacillus methanolicus. *Microbial cell factories*, 15(1):92, 2016.

-
- [21] Eivind Drejer, Sigrid Hakvåg, Marta Irla, and Trygve Brautaset. Genetic tools and techniques for recombinant expression in thermophilic bacillaceae. *Microorganisms*, 6(2):42, 2018.
- [22] Dewi Nilasari, Nir Dover, Sabine Rech, and Claire Komives. Expression of recombinant green fluorescent protein in bacillus methanolicus. *Biotechnology progress*, 28(3):662–668, 2012.
- [23] Claire F Komives, Louis Yip-Yan Cheung, Stefanie B Pluschkell, and Michael C Flickinger. Growth of bacillus methanolicus in seawater-based media. *Journal of Industrial Microbiology and Biotechnology*, 32(2):61–66, 2005.
- [24] Elrike Frenzel, Jelmer Legebeke, Atze Van Stralen, Richard Van Kranenburg, and Oscar P Kuipers. In vivo selection of sfgfp variants with improved and reliable functionality in industrially important thermophilic bacteria. *Biotechnology for biofuels*, 11(1):8, 2018.
- [25] Zehra Kazmi, Iffat Fatima, Shaghuftha Perveen, and Saima Shakil Malik. Monosodium glutamate: Review on clinical reports. *International Journal of Food Properties*, 20(sup2):1807–1815, 2017.
- [26] Igor Vassilev, Gideon Giebelmann, Susanne K Schwechheimer, Christoph Wittmann, Bernardino Viridis, and Jens O Krömer. Anodic electro-fermentation: Anaerobic production of l-lysine by recombinant corynebacterium glutamicum. *Biotechnology and bioengineering*, 115(6):1499–1508, 2018.
- [27] Patrick M Boyle and Pamela A Silver. Parts plus pipes: synthetic biology approaches to metabolic engineering. *Metabolic engineering*, 14(3):223–232, 2012.
- [28] Patrick Kiefer, Uwe Schmitt, Jonas EN Muller, Johannes Hartl, Fabian Meyer, Florian Ryffel, and Julia A Vorholt. Dynamet: a fully automated pipeline for dynamic lc–ms data. *Analytical chemistry*, 87(19):9679–9686, 2015.
- [29] Jonas EN Müller, Fabian Meyer, Boris Litsanov, Patrick Kiefer, and Julia A Vorholt. Core pathways operating during methylotrophy of bacillus methanolicus mga 3 and induction of a bacillithiol-dependent detoxification pathway upon formaldehyde stress. *Molecular microbiology*, 98(6):1089–1100, 2015.
- [30] Jiyeun Yi, Jinhyuk Lee, Bong Hyun Sung, Du-Kyeong Kang, GyuTae Lim, Jung-Hoon Bae, Seung-Goo Lee, Sun Chang Kim, and Jung-Hoon Sohn. Development of bacillus methanolicus methanol dehydrogenase with improved formaldehyde reduction activity. *Scientific reports*, 8(1):12483, 2018.
- [31] Stefanie B Pluschkell and Michael C Flickinger. Dissimilation of [13c] methanol by continuous cultures of bacillus methanolicus mga3 at 50 c studied by 13c nmr and isotope-ratio mass spectrometry. *Microbiology*, 148(10):3223–3233, 2002.
- [32] Thomas Rygus and Wolfgang Hillen. Inducible high-level expression of heterologous genes in bacillus megaterium using the regulatory elements of the xylose-utilization operon. *Applied microbiology and biotechnology*, 35(5):594–599, 1991.

-
- [33] Øyvind M Jakobsen, Trygve Brautaset, Kristin F Degnes, Tonje MB Heggeset, Simone Balzer, Michael C Flickinger, Svein Valla, and Trond E Ellingsen. Overexpression of wild-type aspartokinase increases l-lysine production in the thermotolerant methylotrophic bacterium *Bacillus methanolicus*. *Appl. Environ. Microbiol.*, 75(3):652–661, 2009.
- [34] Ingemar Nærdal, Johannes Pfeifenschneider, Trygve Brautaset, and Volker F Wendisch. Methanol-based cadaverine production by genetically engineered *Bacillus methanolicus* strains. *Microbial biotechnology*, 8(2):342–350, 2015.
- [35] Marta Irla, Ingemar Nærdal, Trygve Brautaset, and Volker F Wendisch. Methanol-based γ -aminobutyric acid (gaba) production by genetically engineered *Bacillus methanolicus* strains. *Industrial crops and products*, 106:12–20, 2017.
- [36] Jonas EN Müller, Boris Litsanov, Miriam Bortfeld-Miller, Christian Trachsel, Jonas Grossmann, Trygve Brautaset, and Julia A Vorholt. Proteomic analysis of the thermophilic methylotroph *Bacillus methanolicus* mga 3. *Proteomics*, 14(6):725–737, 2014.
- [37] Biology software. Tm-calculator nebul tools™. <https://www.benchling.com>. Accessed: 2019-03-01.
- [38] New England Biolabs Inc. Protocol for q5 high-fidelity 2x master mix. <https://www.neb.com/protocols/2012/12/07/protocol-for-q5-high-fidelity-2x-master-mix-m0492>. Accessed: 2019-03-01.
- [39] New England Biolabs Inc. Pcr protocol for taq dna polymerase with standard taq buffer (m0273). <https://www.neb.com/protocols/0001/01/01/taq-dna-polymerase-with-standard-taq-buffer-m0273>. Accessed: 2019-03-01.
- [40] New England Biolabs Inc. Tm-calculator nebul tools™. <http://tmcalculator.neb.com/#!/main>. Accessed: 2019-03-03.
- [41] Brian J Petteys and Elizabeth L Frank. Rapid determination of vitamin b2 (riboflavin) in plasma by hplc. *Clinica Chimica Acta*, 412(1-2):38–43, 2011.
- [42] Michael P Weiner, Gina L Costa, Warren Schoettlin, Janice Cline, Eric Mathur, and John C Bauer. Site-directed mutagenesis of double-stranded dna by the polymerase chain reaction. *Gene*, 151(1):119–123, 1994.
- [43] Douglas W Smith, Adella M Garland, Gary Herman, Robert E Enns, Tania A Baker, and Judith W Zyskind. Importance of state of methylation of oric gatc sites in initiation of dna replication in *Escherichia coli*. *The EMBO journal*, 4(5):1319–1326, 1985.
- [44] A. Bart, A. van der Ende, K. van Amsterdam, and M. W. J. van Passel. Direct detection of methylation in genomic DNA. *Nucleic Acids Research*, 33(14):e124–e124, 01 2005.

-
- [45] Xiao-Lin Chu, Bo-Wen Zhang, Quan-Guo Zhang, Bi-Ru Zhu, Kui Lin, and Da-Yong Zhang. Temperature responses of mutation rate and mutational spectrum in an escherichia coli strain and the correlation with metabolic rate. *BMC evolutionary biology*, 18(1):126, 2018.
- [46] Pongsak Rattanachaikunsopon and Parichat Phumkhachorn. Glass bead transformation method for gram-positive bacteria. *Brazilian Journal of Microbiology*, 40(4):923–926, 2009.
- [47] Zhi Zhang, Zhong-Tao Ding, Dan Shu, Di Luo, and Hong Tan. Development of an efficient electroporation method for iturin a-producing bacillus subtilis zk. *International journal of molecular sciences*, 16(4):7334–7351, 2015.
- [48] Masahiro Ito and Makoto Nagane. Improvement of the electro-transformation efficiency of facultatively alkaliphilic bacillus pseudofirmus of4 by high osmolarity and glycine treatment. *Bioscience, biotechnology, and biochemistry*, 65(12):2773–2775, 2001.
- [49] D Peng, Y Luo, S Guo, H Zeng, S Ju, Z Yu, and M Sun. Elaboration of an electroporation protocol for large plasmids and wild-type strains of bacillus thuringiensis. *Journal of applied microbiology*, 106(6):1849–1858, 2009.
- [50] David Cue, Hong Lam, Richard S Hanson, and Michael C Flickinger. Characterization of a restriction-modification system of the thermotolerant methylotroph bacillus methanolicus. *Appl. Environ. Microbiol.*, 62(3):1107–1111, 1996.
- [51] Niclas Nordholt, Johan Van Heerden, Remco Kort, and Frank J Bruggeman. Effects of growth rate and promoter activity on single-cell protein expression. *Scientific reports*, 7(1):6299, 2017.
- [52] Catriona J Harper, Don Hayward, Martin Kidd, Ian Wiid, and Paul Van Helden. Glutamate dehydrogenase and glutamine synthetase are regulated in response to nitrogen availability in mycobacterium smegmatis. *BMC microbiology*, 10(1):138, 2010.
- [53] Stefan Klumpp, Zhongge Zhang, and Terence Hwa. Growth rate-dependent global effects on gene expression in bacteria. *Cell*, 139(7):1366–1375, 2009.
- [54] Víctor Antonio García-Angulo. Overlapping riboflavin supply pathways in bacteria. *Critical reviews in microbiology*, 43(2):196–209, 2017.
- [55] Karin Hammer, Ivan Mijakovic, and Peter Ruhdal Jensen. Synthetic promoter libraries—tuning of gene expression. *Trends in biotechnology*, 24(2):53–55, 2006.
- [56] Marjan De Mey, Jo Maertens, Gaspard J Lequeux, Wim K Soetaert, and Erick J Vandamme. Construction and model-based analysis of a promoter library for e. coli: an indispensable tool for metabolic engineering. *BMC biotechnology*, 7(1):34, 2007.
- [57] Inc. A Takara Bio Company Clontech Laboratories. Cloneamp hifi pcr pre-mix protocol-at-a-glance. https://www.takarabio.com/assets/documents/User%20Manual/CloneAmp%20HiFi%20PCR%20Premix%20Protocol-At-A-Glance_092612.pdf. Accessed: 2018-09-01.
-

-
- [58] New England Biolabs Inc. Gibson assembly protocol (e5510). <https://international.neb.com/protocols/2012/12/11/gibson-assembly-protocol-e5510>. Accessed: 2018-09-01.
- [59] Rachel Green and Elizabeth J Rogers. Chemical transformation of e. coli. *Methods in enzymology*, 529:329, 2013.

Appendix **A**

Supplementary tables

The primer and promoter sequences are presented in Appendix A.1 along with a short description of

A.1 Primer and promoter sequences

Table A.1: Primer sequences used in this study. Bases in lower case denote overlapping regions.

Primer	Primer sequence 5'→3'	Purpose
sfGFP01_F	tcgcttattttcaaaagattTATTCTTT CCCTTTAAACTT	Amplification of putative promoter 1 for pTH1-sfGFP and pBV2-sfGFP
sfGFP01_R	ctattatgtaattgtttacACTGTTAAT ATACTATCTATCA	Amplification of putative promoter 1 for pTH1-sfGFP and pBV2-ribB1
RF-F-01	aagcccctcattagcgtTATTCTTT CCCTTTAAACTT	Amplification of putative promoter 1 for pBV2-ribB1
sfGFP02_F	tcgcttattttcaaaagattAAAAGTTCC TGTTGAAAATGGTA	Amplification of putative promoter 2 for pTH1-sfGFP and pBV2-sfGFP
sfGFP02_R	ctattatgtaattgtttacGTTGTCTATTA TACAGAAAACATAAAGT	Amplification of putative promoter 2 for pTH1-sfGFP and pBV2-ribB1
RF-F-02	aagcccctcattagcgtAAAAGTTCC TGTTGAAAATGGTA	Amplification of putative promoter 2 for pBV2-ribB1
sfGFP03_F	tcgcttattttcaaaagattATAATGAAATT ATCTTTAATTTGCCAAAAGAGAAA	Amplification of putative promoter 3 for pTH1-sfGFP and pBV2-sfGFP
sfGFP03_R	ctattatgtaattgtttacATTACATATTATAC AAAATTAAGAAAAGAGTGTC AAT	Amplification of putative promoter 3 for pTH1-sfGFP and pBV2-ribB1
RF-F-03	aagcccctcattagcgtATAATGAAATTA TCTTTAATTTGCCAAAAGAGAAA	Amplification of putative promoter 3 for pBV2-ribB1
sfGFP04_F	tcgcttattttcaaaagattTTTAAGCTATAAG CTCTTT	Amplification of putative promoter 4 for pTH1-sfGFP and pBV2-sfGFP
sfGFP04_R	ctattatgtaattgtttacATATTATTCATAA AATG	Amplification of putative promoter 4 for pTH1-sfGFP and pBV2-ribB1
RF-F-04	aagcccctcattagcgtTTAAGCTATAAG CTCTTT	Amplification of putative promoter 4 for pBV2-ribB1
sfGFP05_F	tcgcttattttcaaaagattTAAAAATATTGAA GTTGTCTTA	Amplification of putative promoter 5 for pTH1-sfGFP
sfGFP05_R	ctattatgtaattgtttacAACTATTATTTTAGTT TTCAAAAAT	Amplification of putative promoter 5 for pTH1-sfGFP
sfGFP06_F	tcgcttattttcaaaagattATTTATCTTTTTCAG CCATTTTCCTTTATT	Amplification of putative promoter 6 for pTH1-sfGFP

Table A.1: Primer sequences used in this study. Bases in lower case denote overlapping regions.

Primer	Primer sequence 5'→3'	Purpose
sfGFP06_R	ctattatgtaattgtttacGGTATTAACCTTAACA ACTTTTACGAAAAATTCA	Amplification of putative promoter 6 for pTH1-sfGFP
sfGFP07_F	tcgcttattttcaaaagattAAACAATTAATGGCA TTTTCTTAG	Amplification of putative promoter 7 for pTH1-sfGFP
sfGFP07_R	ctattatgtaattgtttacGAATATCATTATAGTAC AAGGCTTATTT	Amplification of putative promoter 7 for pTH1-sfGFP
sfGFP08_F	tcgcttattttcaaaagattAGGGAATTGTATATTT GTCTTCGTTT	Amplification of putative promoter 8 for pTH1-sfGFP
sfGFP08_R	ctattatgtaattgtttacAAGTTAAGATTACCAA AGTTGGAGAA	Amplification of putative promoter 8 for pTH1-sfGFP
sfGFP09_F	tcgcttattttcaaaagattATTATTTGAAATCCCG CATAATTG	Amplification of putative promoter 8 for pTH1-sfGFP
sfGFP09_R	ctattatgtaattgtttacCTCTTATTATAAAAAGT TAGGAAACTAAAATC	Amplification of putative promoter 9 for pTH1-sfGFP
sfGFP10_F	tcgcttattttcaaaagattAAAATCTTTGGACATA AAGGAATAAATTA	Amplification of putative promoter 9 for pTH1-sfGFP
sfGFP10_R	ctattatgtaattgtttacAATTATTATATTAATAAA ATCGAATCTCTTTTG	Amplification of putative promoter 10 for pTH1-sfGFP
sfGFP11_F	tcgcttattttcaaaagattAAAATTTGAAATGGCA GCCACATTTT	Amplification of putative promoter 10 for pTH1-sfGFP
sfGFP11_R	ctattatgtaattgtttacATTATCATTATATCCTT TCTTAACCTTTCT	Amplification of putative promoter 11 for pTH1-sfGFP
RF-F-11	aagcccgcctaggcgtAAAATTTGAAATGGC AGCCACATTTT	Amplification of putative promoter 11 for pBV2-ribB1
sfGFP12_F	tcgcttattttcaaaagattAATCGCATTTTCTTCC ATTA	Amplification of putative promoter 12 for pTH1-sfGFP
sfGFP12_R	ctattatgtaattgtttacCTTCAAATATAGACCT TTTCAC	Amplification of putative promoter 12 for pTH1-sfGFP
sfGFP13_F	tcgcttattttcaaaagattAATAATGTTGAAATT TGGAGGAAAA	Amplification of putative promoter 13 for pTH1-sfGFP
sfGFP13_R	ctattatgtaattgtttacATGTAAAGTATAACACA CAAACATATTTGA	Amplification of putative promoter 13 for pTH1-sfGFP
sfGFP14_F	tcgcttattttcaaaagattAATAATTATGCTGCTTT GATTCATTTT	Amplification of putative promoter 14 for pTH1-sfGFP
sfGFP14_R	ctattatgtaattgtttacATATTCATTTTAATAAAA AAGTATTCGATTTA	Amplification of putative promoter 14 for pTH1-sfGFP
sfGFP15_F	tcgcttattttcaaaagattATACTATCATAAAATTTT GGTTTTTCAT	Amplification of putative promoter 15 for pTH1-sfGFP
sfGFP15_R	ctattatgtaattgtttacTTTAAATTATATCACTA CAAAAAGAGAGTACAA	Amplification of putative promoter 15 for pTH1-sfGFP
sfGFP16_F	tcgcttattttcaaaagattTTATTCATTC AATTGGA AATAATAAAA	Amplification of putative promoter 16 for pTH1-sfGFP
sfGFP16_R	ctattatgtaattgtttacATAATAAGCTATCATA TTTAATTTAGGA	Amplification of putative promoter 16 for pTH1-sfGFP
sfGFP17_F	tcgcttattttcaaaagattGGAAGTTTTATCTAT CTACAACCTTGAA	Amplification of putative promoter 17 for pTH1-sfGFP
sfGFP17_R	ctattatgtaattgtttacAATCATTTATTGTATATAA ATTAAAAGTATTTTCTAATTAC	Amplification of putative promoter 17 for pTH1-sfGFP
sfGFP18_F	tcgcttattttcaaaagattGTAAACCTTCAACTG AATAAGTTCGGTTATATCC	Amplification of putative promoter 18 for pTH1-sfGFP
sfGFP18_R	ctattatgtaattgtttacTGTATTATTTTAACATA TTGATGGGAAGCTGGCCTGA	Amplification of putative promoter 18 for pTH1-sfGFP
RF-F-18	aagcccgcctaggcgtGTAAACCTTCAACT GAATAAGTTCGGTTATATCC	Amplification of putative promoter 18 for pBV2-ribB1
sfGFP19_F	tcgcttattttcaaaagattAAAAGTTCTAGTTAAT AAATGAGTTTTAAT	Amplification of putative promoter 19 for pTH1-sfGFP
sfGFP19_R	ctattatgtaattgtttacACTATAAAATATGTTTC TAAAAAGAAATC	Amplification of putative promoter 19 for pTH1-sfGFP
sfGFP20_F	tcgcttattttcaaaagattAATAGATTACGGGAA CCGTCAT	Amplification of putative promoter 20 for pTH1-sfGFP
sfGFP20_R	ctattatgtaattgtttacCGTCTAATATTTTCGA CAAAAGGAG	Amplification of putative promoter 20 for pTH1-sfGFP
sfGFP-F-mp	tcgcttattttcaaaagattGTTCATTAAGAGC AGCTGA	Insert for empty vector pBV2-sfGFP

Table A.1: Primer sequences used in this study. Bases in lower case denote overlapping regions.

Primer	Primer sequence 5'→3'	Purpose
RF-F-mp	aagcccgcctaggcgtGTTTCATTAAGAG CAGCTGA	Insert for empty vector pBV2-ribB1
RF-R-mp	ctatttatgtaattgtttacAAAAGCTAGTTTAA ATGCTAA	Insert for empty vector pBV2-ribB1
R125	cgccctaatgagcgggcttT	Vector amplification for pBV2-ribB1
p_pTH1mp-sfGFP_F	gtaacaattacataaatagGAGGTAGT	Vector amplification for pTH1-sfGFP and pBV2-ribB1
p_pTH1mp-sfGFP_R	aatcttttgaaaaaagcgaGAGAA	Vector amplification for pTH1-sfGFP and pBV2-sfGFP
p_pBV2_prom_sfGFP_F	ctagagcttgaattcactgg	Vector amplification for pBV2-sfGFP
p_pBV2_prom_sfGFP_R	ccagtgaattcaagetctagTCATTTGTACAG TTCATCCA	Amplification of inserts for pBV2-sfGFP
p_seq_prom_For	GAGCAGCTGATGATGACTTT	Primer for sequencing of promoter inserted in pTH1-sfGFP
p_seq_prom_Rev	CACCATCCAGTTCACCAGA	Reverse sequencing for promoter in pTH1-sfGFP and pBV2-sfGFP
RBS_ATG-F2	GTAACAATTACATAAATAGGAGG TAGTAAGAATG	Sequencing of RBS
Seq_prom	TTGCAGACAAAGATCTCCAT	Sequencing of promoter inserted in pBV2-sfGFP and pBV2-ribB1
seq_p_sfGFP-R	ACGACGTTGTAAAACGACGG	Sequencing of sfGFP

Table A.2: Promoter sequences used in this study

Promoter	Sequence 5' → 3'
1	TTCCGGCTCAITTTTATTTCCCTTTAAACTTTCCAGTTTTTGATCACAITTCCCATAGATAAATTTTCTTATA GTATACITTTTATACTATGTGTTAATAAAGTGGTACTTTTTTAAAAAATGATAGATAGTATATTAACAGT
2	TGATAATCCATCTGCTTTTTTAATTTTAAATAAAAAGTTCCTGTGAAAATGGTATATAGGGCCGTATAATTGA AAAGGTGTGAAACATAAGATTTTTCAAGAATCTTGCCTCACITTTATGTCTGTATAATAGACAAC
3	GACGACTATATAGCAAACTTTGCCAGGAGAGAITTTCCTATCTGAGAATAATGAAATTAICTTTAATTTGCCAA AAGAGAAAAGGAAAAAACAACCGTAAAGTAGTATTAATGACACTCTTTTTCTTAAATTTGTATAAATATGTAAT
4	GGCTGAAAAACTAAAAGCACCAATACAAGTTTAAAGCTATAAGCTCTTTCCCTGTTGGAGGGAGCTTTTAT ATCCCTGCACATATGAATGGAATCTTTGTGAATAAGAAAATCTTATAATTTTTTCATTTTATGCAATAATAT
5	GAAACGTGTTCCCGTTGGCCACCTCAAAAATAATGAAAGTGTGCTTAGTCCAITTTCTCCCTCTCTGCTAIT TATCTCAAAATGAGATTAATTTAATCTAAAATTAATATGTTTATATTTTGTGAAAACATAAAATAATAGTT
6	CTTTCCGGATGCCAGCGATTCCCATTATCTTTTTTCAGCCATTTCCCTTATTTTTTATTTGCAAAATGCCCTGTAT ATAAATAAATCTATACATTTTTAGATAACTATGAAAATTTTCGTAAAAGTTGTTAAAGTTAATACC
7	CAGATCCAGTACAATTAATAAGGAATAAATAATGTGTGATAAGGGAAAAACAATTAATGGCAITTTCTTAGAATA ATAATTAATCTTTATTTAATAAATTATAATTTAATAATGACTAAATAAAGCCTTGTACTATAATGATATTC
8	AACATTTGAAAAAACGATTAGTCTGTATAATTTTAAAAACGGAGGGAATGTATATTTGTCTTCGTTTCATTTTGTCA GGAAACTAAAACATGCTCTTGTAAGCATTTCAITTTGAAAACGATTTCTCCAACITTTGGTAATCTAACTT
9	ATTAATTTGAAAATCCCGCATAAATGAAAACAGGAATFCAAGTGAATAATAAAAATAAAGTTGGATTAATCTGCAGGCAG ACTTTCAAAATTTAATAAATAATATAAATTTCAAAAATAATGATTAATTTAGTTTCCTAACITTTTATAATAAGAG
10	TCAAAATCTTTGGACATAAGGAATAAATAGGGTTATTGAAGCATACTTTATATGCAGAAAAAACGGTGAAGAAA ATCGGGTTATTAATTTCAAATTTTTCTTTATGCTTGCAAAAGAGATTCGATTTAATATAATAAT
11	CAAACGATGATTAATAAAGTATCGGGCATAACCGGCAAAAATTTGAAATGGCAGCCACATTTCAACAAAAGGCACCTT TTTATCTCTTTTATACGAAGATCGTTTACACCCATAITTTTCAGAAAAAGTTAAGAAAAGGATATAATGATAAAT

Table A.2: Promoter sequences used in this study

Promoter	Sequence 5' -> 3'
12	TAGATAATCGCATTCTTCCATTACCGAGAAATACCGAATTTCCCACTTTGTGCGTTATTTCTTTTTTCGAAAACGATT TCATATAATTGAAAACATTAATAATTTTGCAAATTATTGAAAATATTTGTGAAAAGGTCTATATTTGAAAG
13	ATACATAATCTTTGTGCGAAAAAGGTCAACCTAATAATGTTGAAATTTGGAGGAAAAATAAAAGAAAAATTATTGAC AATCATTTCAAATGACTGTTATAATTTATATTTTTTATTTGACTCAAATATGTTTGTGTGTTATACTTTACAT
14	CGAATAATTATGCTGCTTTGATTCATTTTTCTAAAAAAGGCGCCAGGCACCTATCAGAGGCTAATGTTTATTGATAGT GCATCTCCTTTTTTTGACCCTTTTTGATGCTAACCTTTAAATCGAAATACTTTTTTATTAAAATGAATAT
15	TAAAACTCATGCACAATTTCTGATGATTTTGCATACTATCATAAAATTTCGGTTTTTTCATTCAATAACCTTCATTTCCG CGTTACTTATTCCAAAGCCCTTTTCGTTTCTAAAATTTGTACTCTCTTTTTGTAGTGATATAATTTAAAA
16	AGCGCGGTTTACGGCTTGAACAGAGCCAATTTTTTATTCAATTCAATTGGAAATAATAAAATATGAAAGATATCATTATA GTAAAATAAATAATTAATAAAATTTTCAGAAAAGTAATTGAATTCCTAAATTAATATGATAGCTTTATTAT
17	TAAGACCTCGGCAGGGGAAGTTTTTATCTATCTACAACCTTGAACGGGAGTATCCTTTTCTCCCGTTTTTTTTCCGTTCAA TAATTATTAAGCCAGATTGTGAAAAATTTCCGTAATAGAAAAATACTTTTAATTTATATACAATAATGATT
18	TGGAACACAGTATTTATTGGAGCAAAAAGAGTTTTTCGATCAAATGTAAACCTTCAACTGAATAAGTTCGGTTATATCC CTTACACTGTTTACTACCAAGAGTCTTGCGCAAATTCAGGCCAGCTTCCCATCAATATGTTAAAATAATACA
19	TATTTTAAAAAAGTTCTAGTTAATAAATGAGTTTTAATTTTTTACAAGATTTTTTATGTAAACAATGCGATAAATTCAGG CAAAAGTGAATTTCTTTAATCTTCGTGGCCTTTGTCCAATCGATTTCTTTTTTAGAAACATATTTTATAGT
20	GCGATAAATGAATTAGTTGAACAAAACAACAAAAAATGAATAGATTACGGGAACCGTCATGAAATATCTCATTAGGA TACTTAATTATATGGCGAGCAGGAGAAAGTAATTTGCAGGAGATTATCTCCTTTTGTGCGAAATATTAGGACG

A.2 Plasmids used in this study

Table A.3: Plasmids used and constructed in this study. Plasmids with sfGFP or riboflavin expression under control of the sequence promoters (spXX) or *mdh*-promoter. pTH1spXX-plasmids were further derived from pTH1mp-sfGFP, whereas pBV2-sfGFP plasmids were derived from pBV2mp-cadA

Plasmid	Relevant characteristics	Reference
pTH1mp	Cm ^R ; <i>E. coli</i> and <i>B. methanolicus</i> spp. shuttle vector	Irla et al. [19]
pTH1mp-sfGFP	Cm ^R ; pHP13 derivative for sfGFP expression	Irla et al. [19]
pBV2mp-cadA	Kan ^R ; pBV2mp derivative for cadA expression	Irla et al. [19]
pBV2xp-ribB1	Kan ^R ; pBV2mp derivative for riboflavin expression in control by xylose inducible promoter	Irla et al. [19]
pTH1sp01-sfGFP	Cm ^R ;	Preliminary research
pTH1sp02-sfGFP	Cm ^R ;	Preliminary research
pTH1sp03-sfGFP	Cm ^R ;	Preliminary research
pTH1sp04-sfGFP	Cm ^R ;	Preliminary research
pTH1sp05-sfGFP	Cm ^R ;	Preliminary research
pTH1sp06-sfGFP	Cm ^R ;	Preliminary research
pTH1sp07-sfGFP	Cm ^R ;	Preliminary research
pTH1sp08-sfGFP	Cm ^R ;	Preliminary research
pTH1sp09-sfGFP	Cm ^R ;	Preliminary research
pTH1sp10-sfGFP	Cm ^R ;	Preliminary research
pTH1sp11-sfGFP	Cm ^R ;	Preliminary research
pTH1sp12-sfGFP	Cm ^R ;	Preliminary research
pTH1sp13-sfGFP	Cm ^R ;	This study
pTH1sp14-sfGFP	Cm ^R ;	Preliminary research
pTH1sp15-sfGFP	Cm ^R ;	Preliminary research
pTH1sp16-sfGFP	Cm ^R ;	Preliminary research
pTH1sp17-sfGFP	Cm ^R ;	Preliminary research
pTH1sp18-sfGFP	Cm ^R ;	Preliminary research
pTH1sp19-sfGFP	Cm ^R ;	Preliminary research
pTH1sp20-sfGFP	Cm ^R ;	Preliminary research
pBV2mp-sfGFP	Kan ^R ;	This study
pBV2sp03-sfGFP	Kan ^R ;	This study
pBV2sp01-ribB1	Kan ^R ;	This study
pBV2sp05-ribB1	Kan ^R ;	This study

A.3 Fluorescence results data sheets

Table A.4 present the applied settings for the fluorescence analysis in Tecan Infinite plate reader. Table A.5 to A.14 shows the fluorescence results from 11 strains of *B. methanolicus* with inserted pTH1-sfGFP plasmid containing the fluorescent protein (sfGFP) in control of putative promoters, cultivated in methanol, mannitol glucose or induced osmotic stress by NaCl or sorbitol. The measurements were performed in triplicates in all the cultivation conditions, and the the mean value and standard deviation are presented. "OD cultivation" is the OD₆₀₀ measured by Tecan plate reader after six hours of inoculation. "OD wash" is the obtained OD₆₀₀ after washing with phosphate buffered saline (PBS). Fluorescence is the measured signal from Tecan plate reader, whereas "Relative Fluorescence" is the measured fluorescence divided by "OD wash".

Table A.4: Settings for the fluorescent measurements in Tecan Infinite Plate Reader.

Fluorescence Top Reading	
Excitation Wavelength	485 nm
Emission Wavelength	535 nm
Excitation Bandwidth	9 nm
Emission Bandwidth	20 nm
Gain	90
Number of Flashes	25
Integration Time	20 μ s
Lag Time	0 μ s
Settle Time	0 μ s
Z-Position (Manual)	20000 μ m

Table A.5: Cultivation datasheet for **pTH1sp04-sfGFP** in different cultivation conditions (see text).

Cultivation Condition	OD cultivation	OD wash	Fluorescence	Relative Fluorescence
Methanol	0.526 ±0.09	0.392 ±0.09	252 ±29	398 ±15
Mannitol	1.041 ±0,16	0.329 ±0.00	243 ±2	442 ±9
Glucose	0.733 ±0,04	0.488 ±0,11	293 ±47	401 ±34
Osmotic stress (NaCl)	0.634 ±0.00	0.576 ±0,01	314 ±5	377 ±11
Osmotic stress (Sorbitol)	0.564 ±0.01	0.455 ±0.03	262 ±9	364 ±2

Table A.6: Cultivation datasheet for **pTH1sp05-sfGFP** in different cultivation conditions (see text).

Cultivation Condition	OD cultivation	OD wash	Fluorescence	Relative Fluorescence
Methanol	0.547 ±0,01	0.445 ±0.02	8 254 ±324	19 642 ±1 320
Mannitol	0,45 ±0,01	0.27 ±0.01	4 414 ±117	13 973 ±1 879
Glucose	0,44 ±0,00	0.18 ±0.02	3 385 ±339	18 687 ±239
Osmotic stress (NaCl)	0,62 ±0,02	0.50 ±0.02	9 801 ±403	19 484 ±189
Osmotic stress (Sorbitol)	0,45 ±0,10	0.35 ±0.12	6 052 ±2 190	16 943 ±708

Table A.7: Cultivation datasheet for **pTH1sp11-sfGFP** in different cultivation conditions (see text).

Cultivation Condition	OD cultivation	OD wash	Fluorescence	Relative Fluorescence
Methanol	0.367 ±0.05	0.242 ±0.07	590 ±128	2 054 ±1 47
Mannitol	0.44 ±0.02	0.40 ±0.01	874 ±15	1 932 ±31
Glucose	0.42 ±0.02	0.66 ±0.08	16 842 ±2 397	3 742 ±202
Osmotic stress (NaCl)	0.42 ±0.01	0.37 ±0.00	941 ±6	2 290 ±19
Osmotic stress (Sorbitol)	0.36 ±0.00	0.29 ±0.02	564 ±22	1 614 ±21

Table A.8: Cultivation datasheet for **pTH1sp12-sfGFP** in different cultivation conditions (see text).

Cultivation Condition	OD cultivation	OD wash	Fluorescence	Relative Fluorescence
Methanol	0.53 ± 0.05	0.18 ± 0.04	244 ± 32	812 ± 39
Mannitol	0.85 ± 0.03	0.43 ± 0.06	400 ± 40	702 ± 10
Glucose	0.62 ± 0.02	0.23 ± 0.03	434 ± 46	$1\ 485 \pm 56$
Osmotic stress (NaCl)	± 0.01	0.07 ± 0.00	164 ± 2	993 ± 43
Osmotic stress (Sorbitol)	0.47 ± 0.01	0.31 ± 0.09	310 ± 52	690 ± 37

Table A.9: Cultivation datasheet for **pTH1sp15-sfGFP** in different cultivation conditions (see text).

Cultivation Condition	OD cultivation	OD wash	Fluorescence	Relative Fluorescence
Methanol	n.a.	0.509 ± 0.01	$2\ 269 \pm 14$	$4\ 265 \pm 16$
Mannitol	n.a.	0.19 ± 0.00	647 ± 13	$2\ 934 \pm 39$
Glucose	0.44 ± 0.01	0.16 ± 0.06	627 ± 155	$3\ 455 \pm 214$
Osmotic stress (NaCl)	n.a.	0.21 ± 0.01	$1\ 147 \pm 60$	$4\ 960 \pm 76$
Osmotic stress (Sorbitol)	n.a.	0.37 ± 0.02	$1\ 749 \pm 93$	$4\ 418 \pm 60$

Table A.10: Cultivation datasheet for **pTH1sp17-sfGFP** in different cultivation conditions (see text).

Cultivation Condition	OD cultivation	OD wash	Fluorescence	Relative Fluorescence
Methanol	0.558 ± 0.02	0.332 ± 0.08	$1\ 152 \pm 262$	$3\ 181 \pm 22$
Mannitol	0.38 ± 0.01	0.26 ± 0.02	682 ± 44	$2\ 213 \pm 11$
Glucose	0.60 ± 0.01	0.29 ± 0.07	855 ± 148	$2\ 658 \pm 105$
Osmotic stress (NaCl)	$0.46 (\pm 0.01)$	0.28 ± 0.01	$1\ 148 \pm 7$	$3\ 705 \pm 55$
Osmotic stress (Sorbitol)	0.42 ± 0.09	0.31 ± 0.11	996 ± 298	$2\ 914 \pm 108$

Table A.11: Cultivation datasheet for **pTH1sp18-sfGFP** in different cultivation conditions (see text).

Cultivation Condition	OD cultivation	OD wash	Fluorescence	Relative Fluorescence
Methanol	0.623 ±0.08	0.598 ±0.11	1 813 ±277	2 881±70
Mannitol	0.53 ±0.00	0.51 ±0.10	2 210 ±393	4 114 ±56
Glucose	0.75 ±0.07	0.61 ±0.13	5 036 ±1 096	8 061 ±297
Osmotic stress (NaCl)	0.55 ±0.06	0.50 ±0.14	1 759 ±452	3 337 ±58
Osmotic stress (Sorbitol)	0.56 ±0.04	0.31 ±0.10	881 ±217	2 586 ±131

Table A.12: Cultivation datasheet for **pTH1sp19-sfGFP** in different cultivation conditions (see text).

Cultivation Condition	OD cultivation	OD wash	Fluorescence	Relative Fluorescence
Methanol	0.623 ±0.01	0.542 ±0.09	189 ±13	170 ±8
Mannitol	0.49 ±0.01	0.48 ±0.07	121 ±5	49 ±3
Glucose	0.55 ±0.00	0.47 ±0.10	145 ±5	106 ±12
Osmotic stress (NaCl)	0.62 ±0.01	0.54 ±0.10	199 ±18	190 ±3
Osmotic stress (Sorbitol)	0.57 ±0.02	0.45 ±0.10	183 ±18	194 ±2

Table A.13: Cultivation datasheet for **pTH1sp20-sfGFP** in different cultivation conditions (see text).

Cultivation Condition	OD cultivation	OD wash	Fluorescence	Relative Fluorescence
Methanol	0.367 ±0.01	0.249 ±0.01	283 ±10	746 ±4
Mannitol	0.47 ±0.01	0.32 ±0.01	344 ±11	764 ±9
Glucose	0.38 ±0.01	0.23 ±0.00	363 ±6	1 167 ±26
Osmotic stress (NaCl)	0.39 ±0.01	0.30 ±0.01	380 ±24	941 ±41
Osmotic stress (Sorbitol)	0.32 ±0.05	0.16 ±0.04	220 ±33	746 ±15

Table A.14: Cultivation datasheet for **pTH1mp-sfGFP** in different cultivation conditions (see text).

Cultivation Condition	OD cultivation	OD wash	Fluorescence	Relative Fluorescence
Methanol	0.350 ±0.001	0.259 ±0.04	3 119 ±467	11 663 ±149
Mannitol	0.443 ±0.01	0.303 ±0.05	1 362 ±169	4 203 ±256
Glucose	0.654 ±0.16	0.355 ±0.14	5 149 ±2577	13 728 ±3417
Osmotic stress (NaCl)	0.423 ±0.01	0.325 ±0.02	4 277 ±211	12 884 ±143
Osmotic stress (Sorbitol)	0.303 ±0.01	0.264 ±0.04	2 729 ±384	10 013 ±252

Table A.15: Fluorescence from pBV2mp-sfGFP and pBV2sp03-sfGFP in different carbon sources. Mean values and standard deviation are presented.

Strain	Rel. Fluorescence (methanol)	Rel. Fluorescence (mannitol)	Rel. Fluorescence (glucose)
pBV2mp-sfGFP	15 621 ±192	55 453 ±622	104 687 ±1627
pBV2sp03-sfGFP	15 936 ±157	40 289 ±1 206	57 588 ±106

A.4 Riboflavin production

Table A.16: Highest obtained riboflavin signal obtained from BioLector cultivation of strains with pBV2sp05-ribB1 and pBV2sp01-ribB1 cultivated in different carbon sources. Mean values and standard deviation are presented. Calculated highest riboflavin concentration for each of the conditions are also shown.

Strain	Riboflavin signal (methanol)	Riboflavin signal (mannitol)	Riboflavin signal (glucose)	Riboflavin signal (NaCl)
pBV2sp05-ribB1	1.32 ±0.20	3.55 ±0.71	1.13 ±0.24	1.19 ±0.29
pBV2sp01-ribB1	8.51 ±1,33	8.46 ±0.76	7.76 ±1.50	12.42 ±0.43
Calculated riboflavin concentrations [mg/L]				
pBV2sp05-ribB1	0.16	0.55	0.13	0.14
pBV2sp01-ribB1	2.44	1.43	1.3	2.16

Table A.17: Calculated riboflavin concentration in supernatant from cultivations with pBV2xp-ribB1 and pBV2sp01-ribB1. Supernatant from strains cultivated in mannitol and induced osmotic stress (NaCl) was studied. The concentration was calculated based on the last obtained signal from the BioLector experiment and area under the curve of HPLC peak.

Strain	Concentration calculated from HPLC [mg/L]	Concentration calculated from BioLector [mg/L]	Change in calculated concentration
pBV2xp-ribB1 (mannitol)	7,13 ±3,02	9,23 ±3,67	77 %
pBV2sp01-ribB1 (mannitol)	0,91 ±0,11	1,43 ±0,08	64 %
pBV2sp01-ribB1 (mannitol)	1,16 ±0,02	1,70 ±0,03	68 %

Appendix B

BioLector growth curves and riboflavin production

B.1 Biomass and riboflavin signal plotted against time for pBV2sp01-ribB1

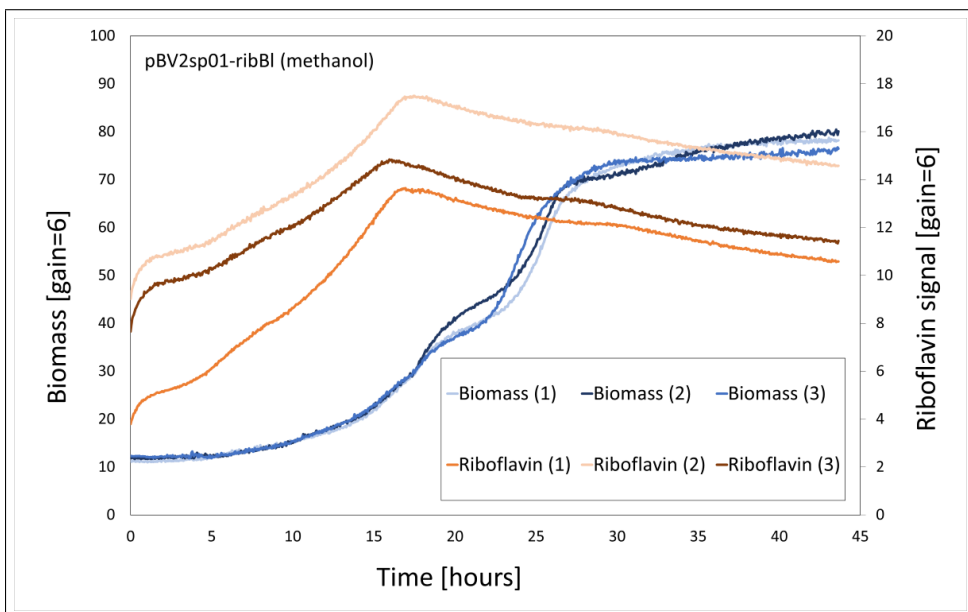


Figure B.1: Biomass and riboflavin signal plotted against time for pBV2sp01-ribB1 cultivated in methanol

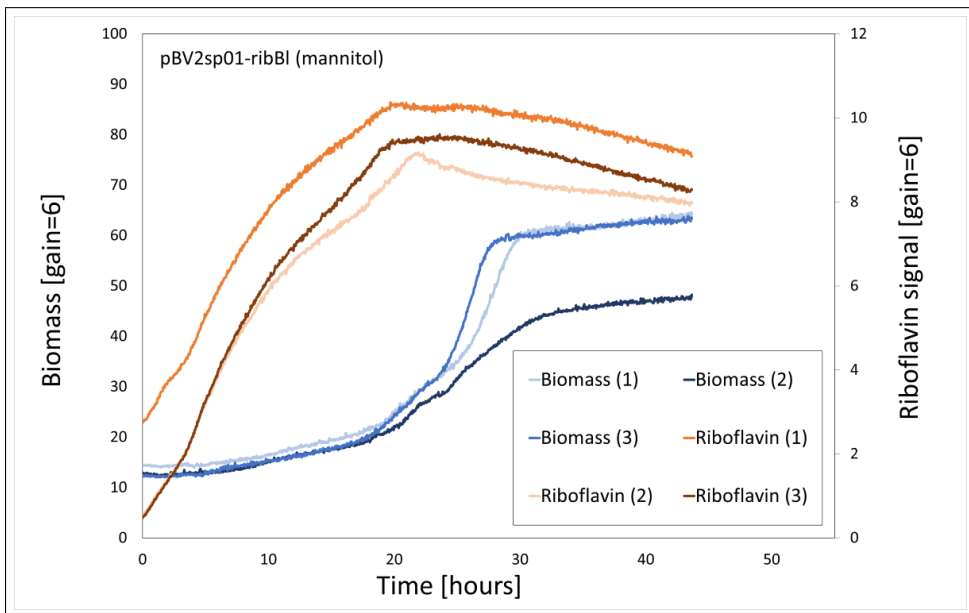


Figure B.2: Biomass and riboflavin signal plotted against time for pBV2sp01-ribBI cultivated in mannitol

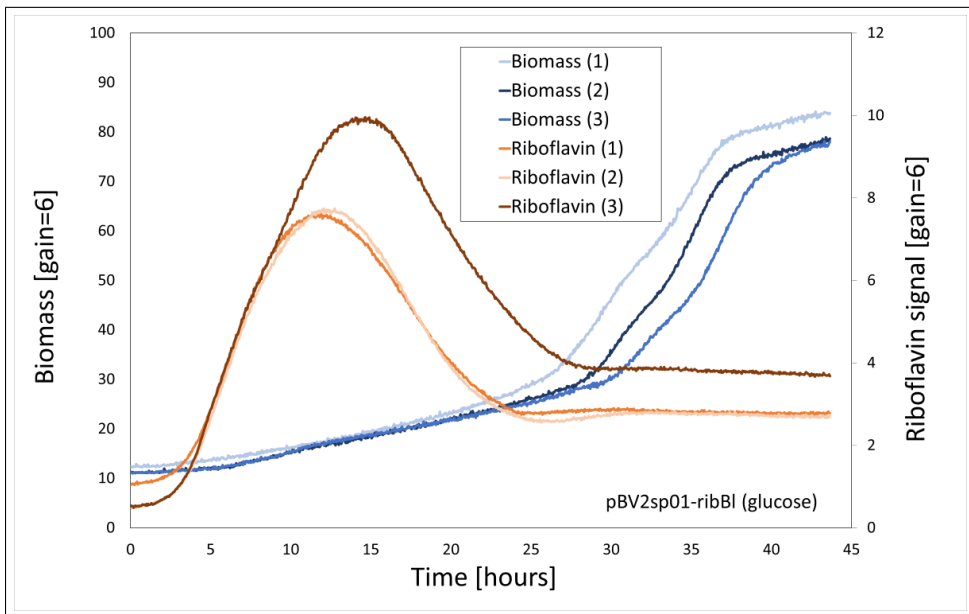


Figure B.3: Biomass and riboflavin signal plotted against time for pBV2sp01-ribBI cultivated in glucose

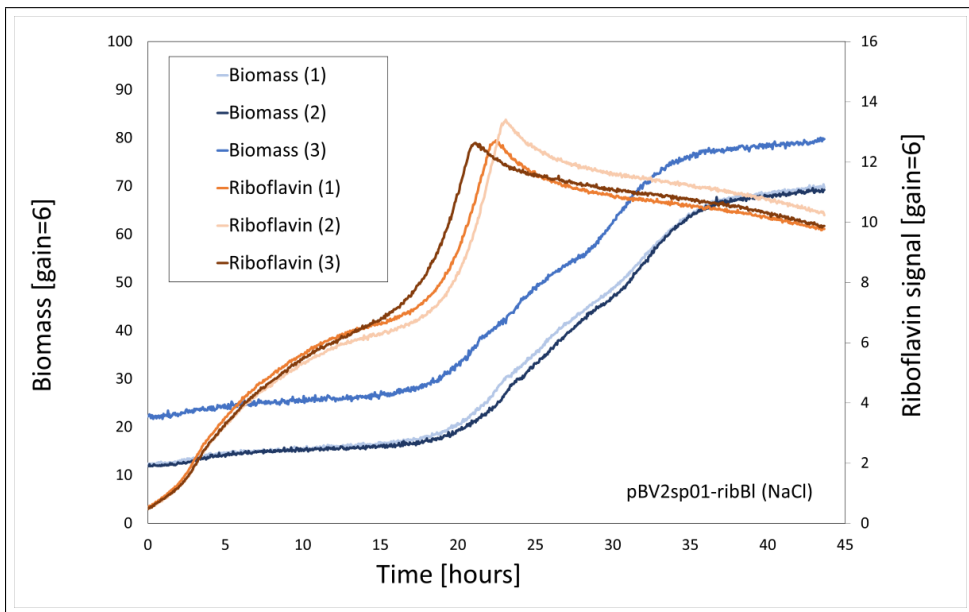


Figure B.4: Biomass and riboflavin signal plotted against time for pBV2sp01-ribBI cultivated in methanol with induced osmotic stress by added NaCl

B.2 Biomass and riboflavin signal plotted against time for pBV2sp05-ribBI

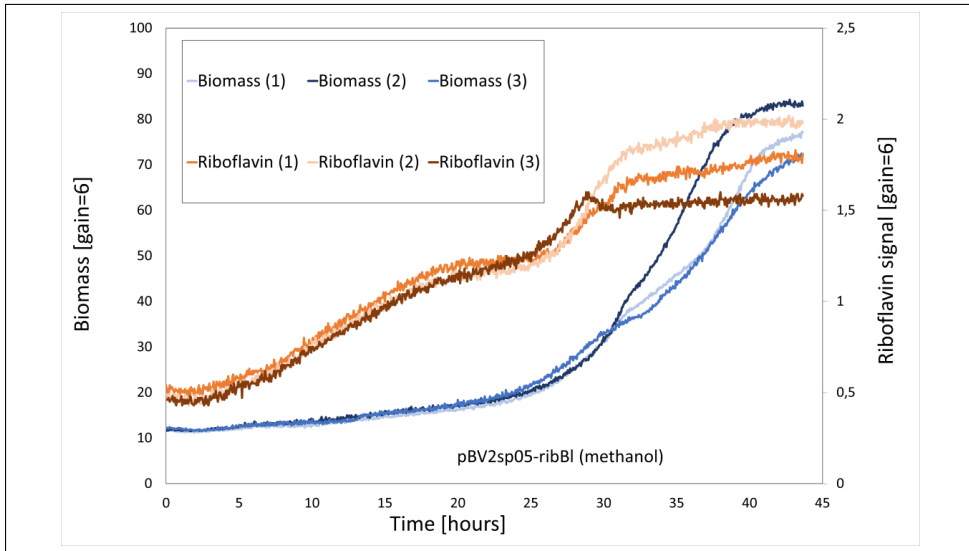


Figure B.5: Biomass and riboflavin signal plotted against time for pBV2sp05-ribBI cultivated in methanol

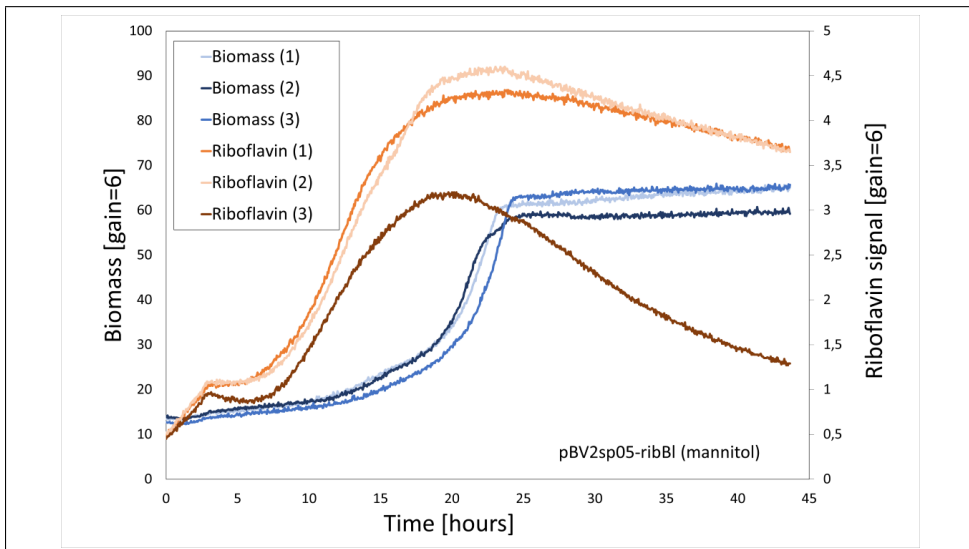


Figure B.6: Biomass and riboflavin signal plotted against time for pBV2sp05-ribBI cultivated in mannitol

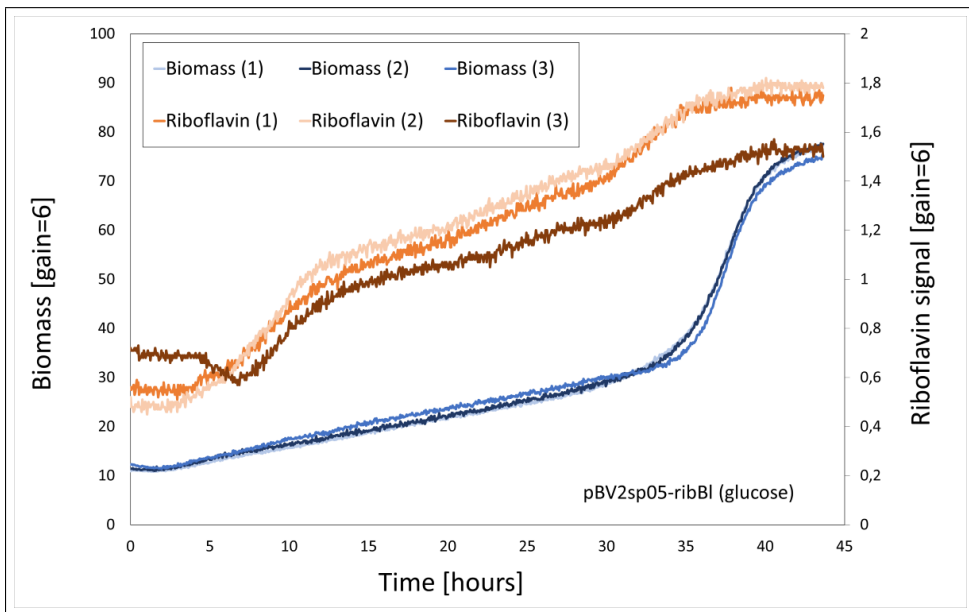


Figure B.7: Biomass and riboflavin signal plotted against time for pBV2sp05-ribBI cultivated in glucose

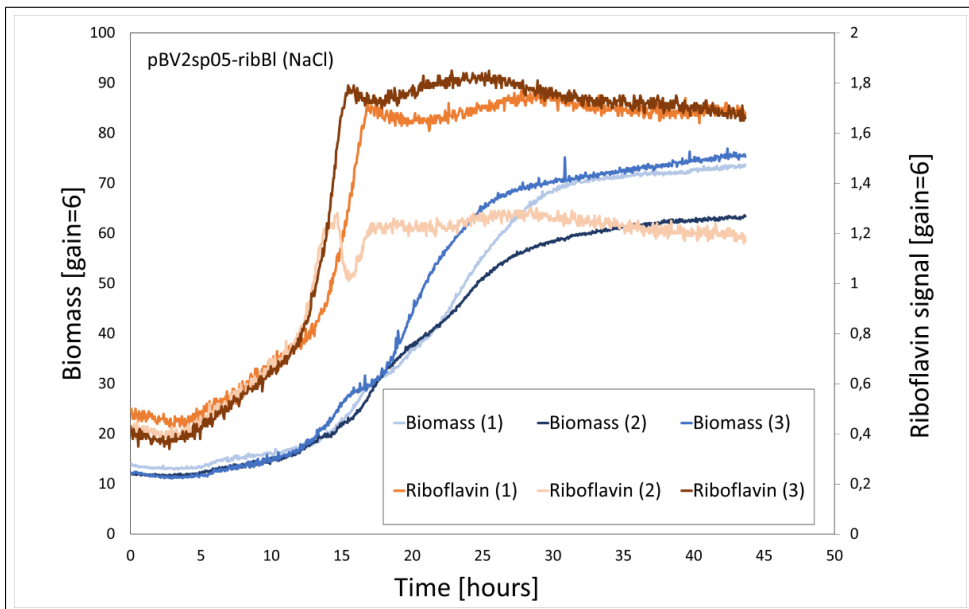


Figure B.8: Biomass and riboflavin signal plotted against time for pBV2sp05-ribBI cultivated in methanol with induced osmotic stress by added NaCl

Appendix C

Electrophoresis results

In Appendix C, the electrophoresis results from amplification of the pBV2-inserts, as well as the electrophoresis results from colony-PCR are presented.

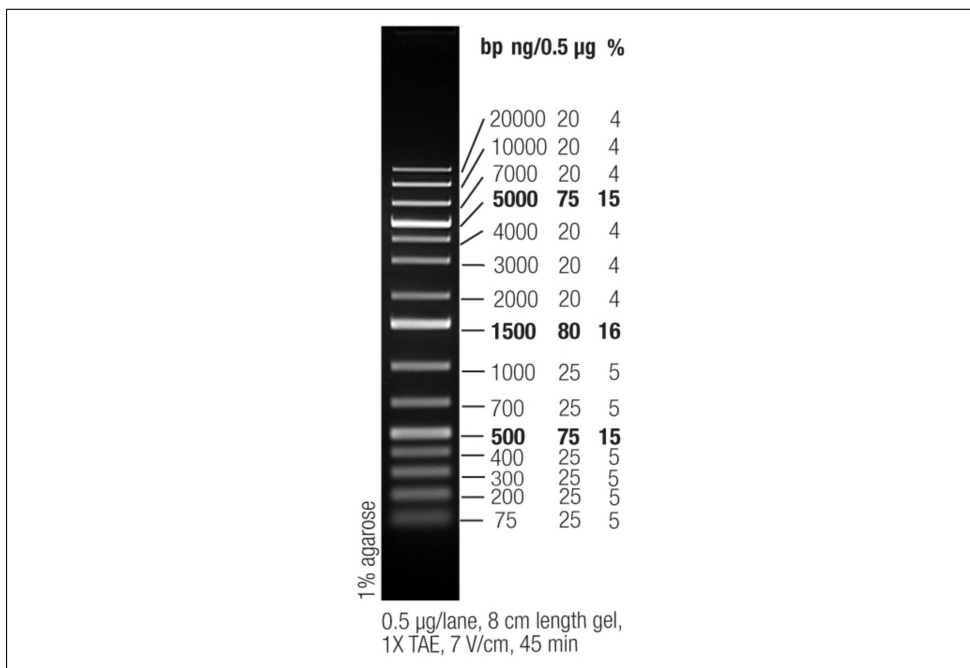


Figure C.1: Picture of electrophoresis bands with the use of GeneRuler 1kb plus DNA ladder. The fragment size ranges from 75 bp to 20 000 bp, with 500 bp, 1500 bp and 5000 bp giving the strongest bands.

Figure C.1 shows the ladder (GeneRuler 1 kb Plus) that was used for all of the elec-

trophoresis runs. The ladder shows extra strong bands at 5000, 1500 and 500 bp. All of the electrophoresis solutions were mixed with Gel Loading Dye (6X) from New England Biolabs (Catalog: B7021S). Unsuccessful electrophoresis runs are omitted from the thesis.

C.1 Amplification of inserts

The inserts were amplified by PCR using Takara CloneAmp HiFi PCR-mix, as described in text (section 2.1.1). Figure C.2 shows the separated DNA fragments after PCR amplification of mp, sp01, sp03, sp04 and sp05 upstream a *sfgfp* gene. Figure C.3 and C.4 shows the amplified mp, sp01, sp02, sp03, sp04, sp11 and sp18 with PCR primers designed to be ligated with pBV2-ribB1 backbone.

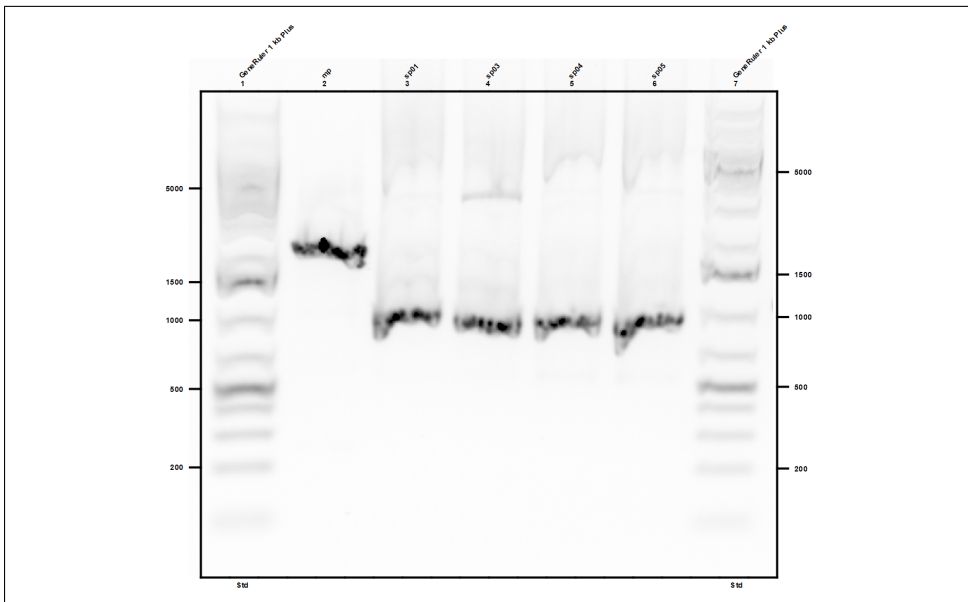


Figure C.2: Amplification of *mdh*-promoter with the *sfgfp*-gene (mp, 1798 bp) and putative promoter sequence 1, 2, 3, 11 and 18 with *sfgfp* (~ 900 bp) for insertion in pBV2 plasmid. GeneRuler 1kb Plus (Appendix C.1) was used as ladder.

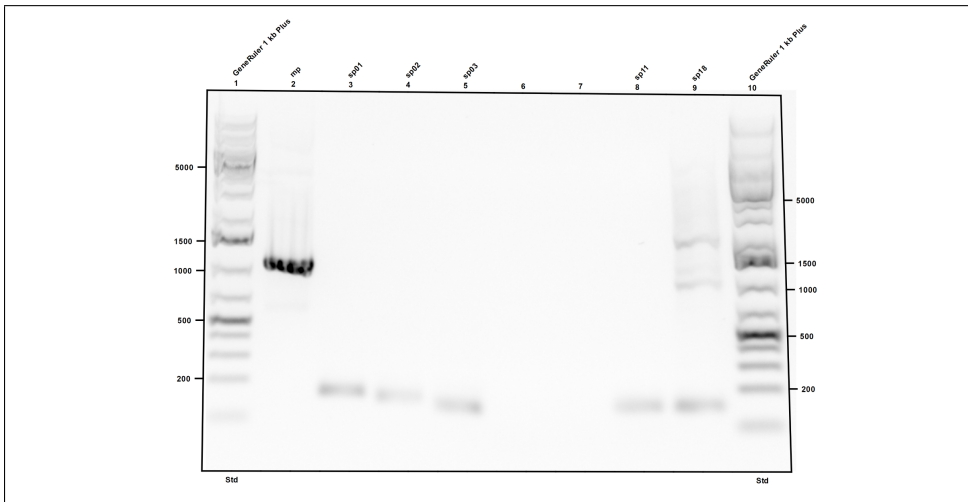


Figure C.3: Amplification of *mdh*-promoter (mp, 1079 bp) and putative promoter sequence 1, 2, 3, 11 and 18 (~ 150 bp) for insertion in pBV2-ribB1 plasmid. GeneRuler 1kb Plus (Appendix C.1) was used as ladder.

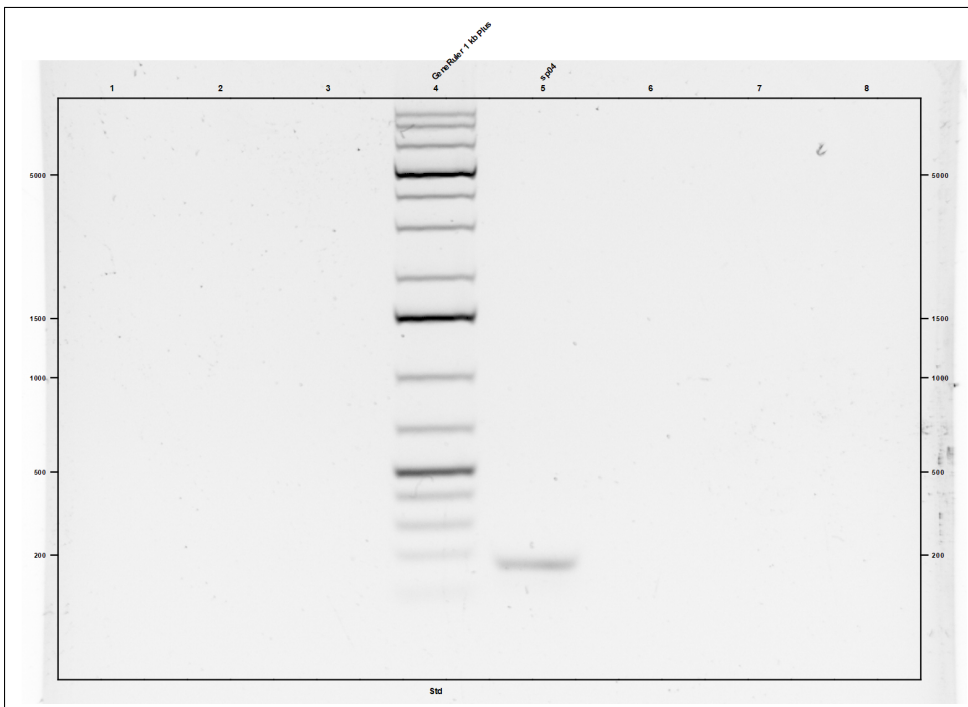


Figure C.4: Amplification of putative promoter 4 (150 bp) for insertion in pBV2-ribB1 plasmid. GeneRuler 1kb Plus (Appendix C.1) was used as ladder.

C.2 Colony-PCR product

Amplified putative promoter sequences in pTH1-sfGFP plasmids from *E. coli* colonies

Figure C.5, C.6 and C.7 shows the amplified promoter sequences from colonies with transformed pTH1-sfGFP into *E. coli*. Figure C.5 depicts an amplified sp10 (lane 6), Figure C.6 shows PCR-amplified sequences for sp06, sp07, sp08, sp09, sp12 and sp16, whereas Figure C.7 presents amplified promoter sequences matching sp02, sp06 and sp07.

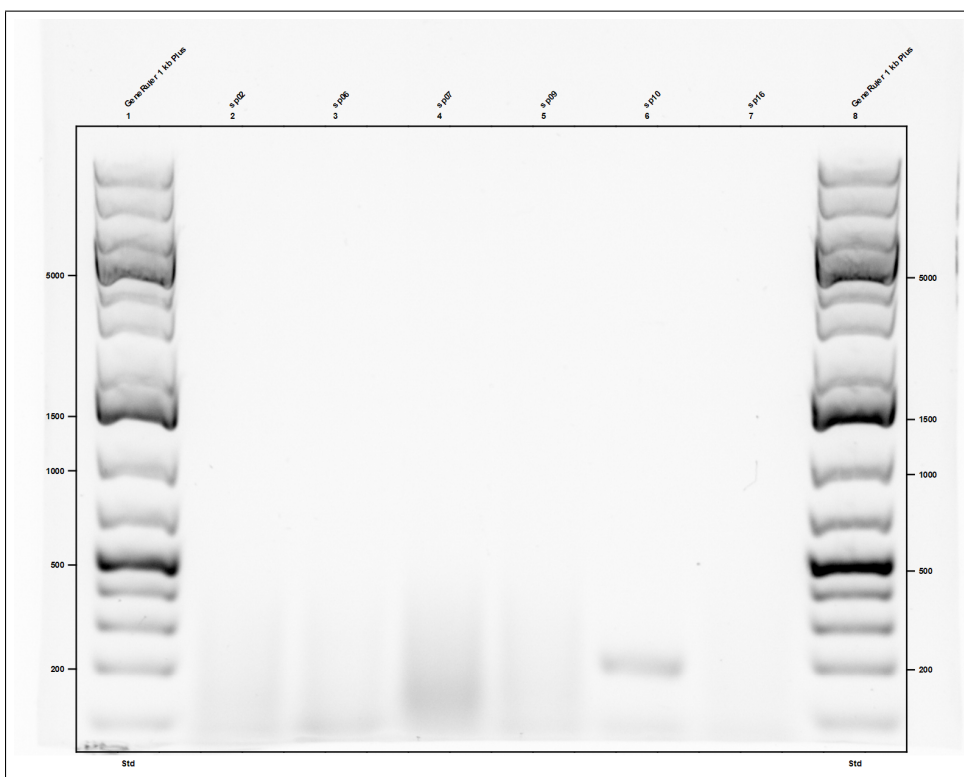


Figure C.5: Electrophoresis results after PCR-amplification of putative promoter 10 inserted upstream *sfGFP* gene in pTH1. Putative promoter 2, 6, 7, 8 and 16 are also attempted amplified, but without success. GeneRuler 1kb Plus (Appendix C.1) was used as ladder.

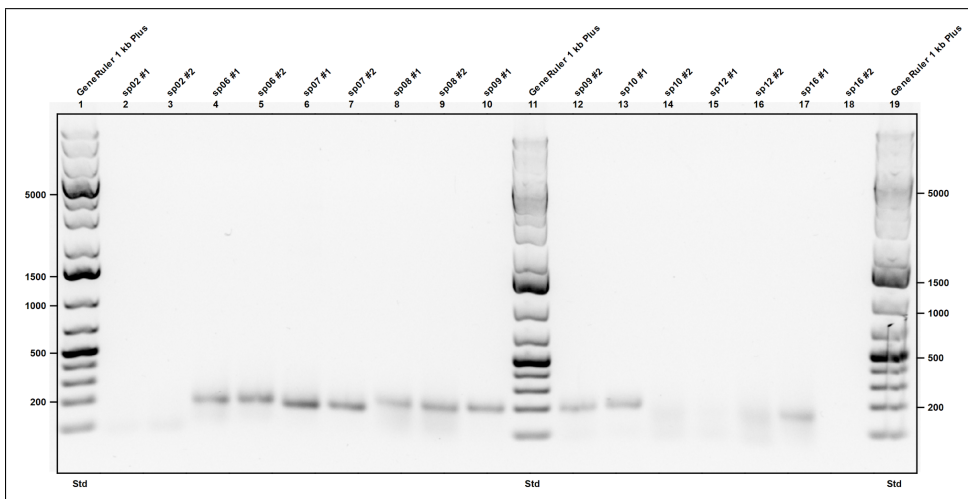


Figure C.6: Electrophoresis results from colony PCR amplification of putative promoter sequences 2, 6, 7, 8, 9, 10, 12 and 16 together with upstream *sfgfp* gene inside a pTH1 plasmid. Colonies with putative promoter 02 (sp02) did not show a visible PCR-result. Weak bands are detected for sp12 and sp16. GeneRuler (Appendix C.1) was used as ladder.

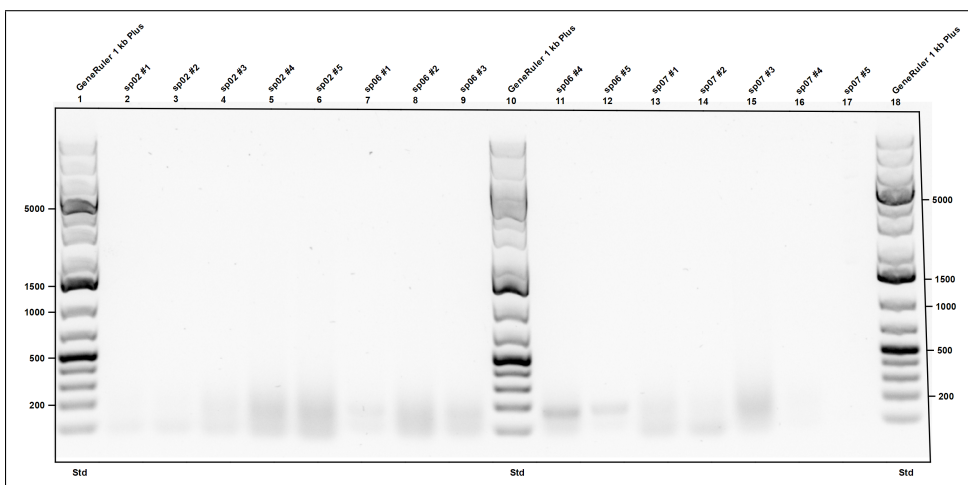


Figure C.7: Electrophoresis results from colony PCR amplification of putative promoter sequences 2, 6 and 7 together with upstream *sfgfp* gene inside a pTH1 plasmid. Weak bands are detected for sp02, sp06 and sp07 which were further studied by sequencing. GeneRuler 1kb Plus (Appendix C.1) was used as ladder.

Electrophoresis results from PCR-amplified promoters that are to be inserted in pBV2-plasmids

Figure C.8 shows the separated colony PCR-product for colonies, transformed with with pBV2mp-ribB1 and pBV2sp01-ribB1. A visible band were detected for colony 4 (lane 2) for the pBV2mp-ribB1-plasmid, as well as colony 4 (lane 4) for the pBV2sp01-ribB1 plasmid. Figure C.9 present separated colony PCR product for strains containing the pBV2-sfGFP plasmid and pBV2-ribB1 plasmid with inserted promoters upstream *sfGFP* or *ribBL*, respectively. Colonies containing mp, sp01 and sp03 were found for the pBV2-sfGFP plasmid, and colonies containing mp and sp02 were found for the pBV2-ribB1 plasmid. Furthermore, colonies with inserted putative promoter 1, 3, 4, 11 and 18 in the pBV2-ribB1 plasmid are presented in Figure C.10 and C.11.

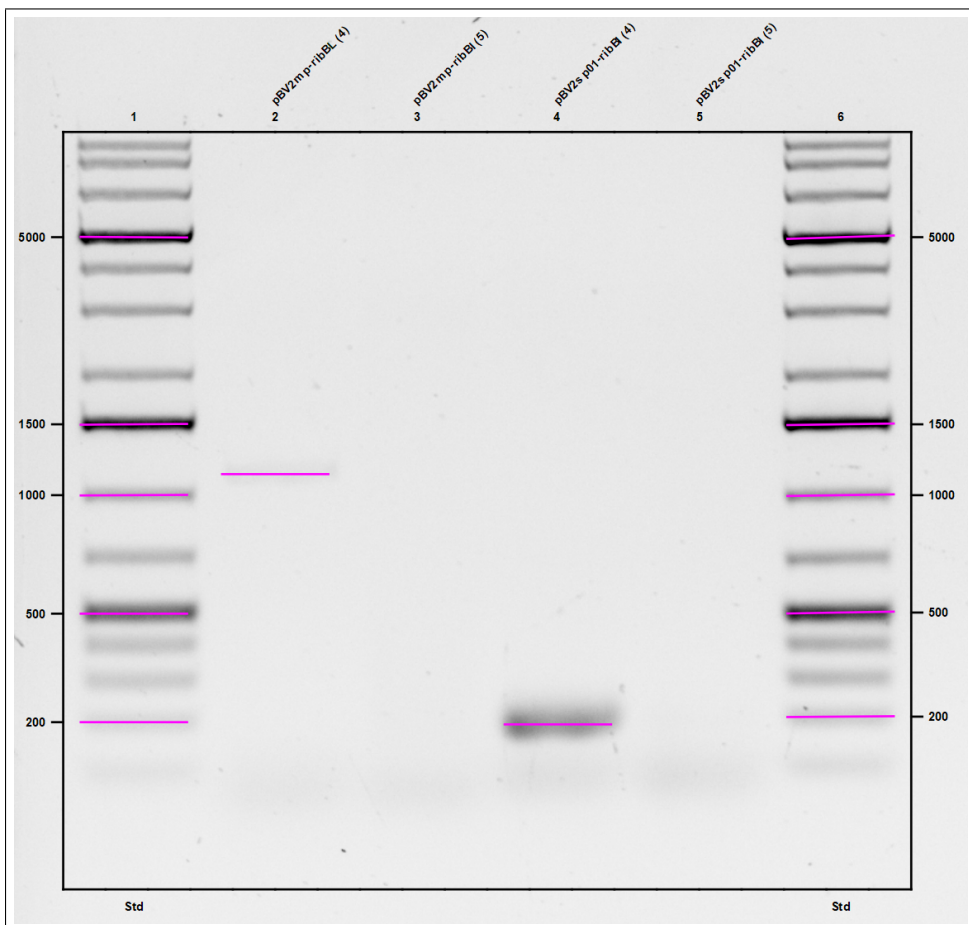


Figure C.8: Electrophoresis results from PCR-amplified putative promoter 1 and *mdh* promoter inserted in pBV2-ribB1 plasmid from *E. coli* DH5 α colonies. GeneRuler 1kb Plus (Appendix C.1) was used as ladder.

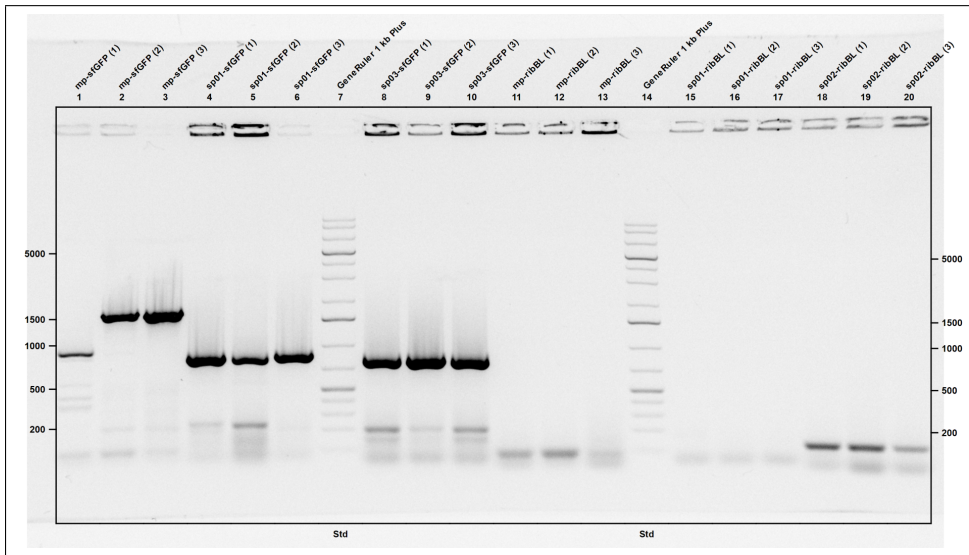


Figure C.9: Electrophoresis results from colony PCR amplification of *mdh* promoter and putative promoter sequences 1, 3, 4 and 5 together with upstream *sfGFP* gene from a pBV2-sfGFP plasmid. Promoter sequences from pBV2-ribB1 with riboflavin in control by *mdh* promoter or putative promoter 1, 2, 3, 4, 11 or 18 were also amplified. Visible bands were not detected for mp and sp01 from the pBV2-ribB1 plasmid. GeneRuler 1kb Plus (Appendix C.1) was used as ladder

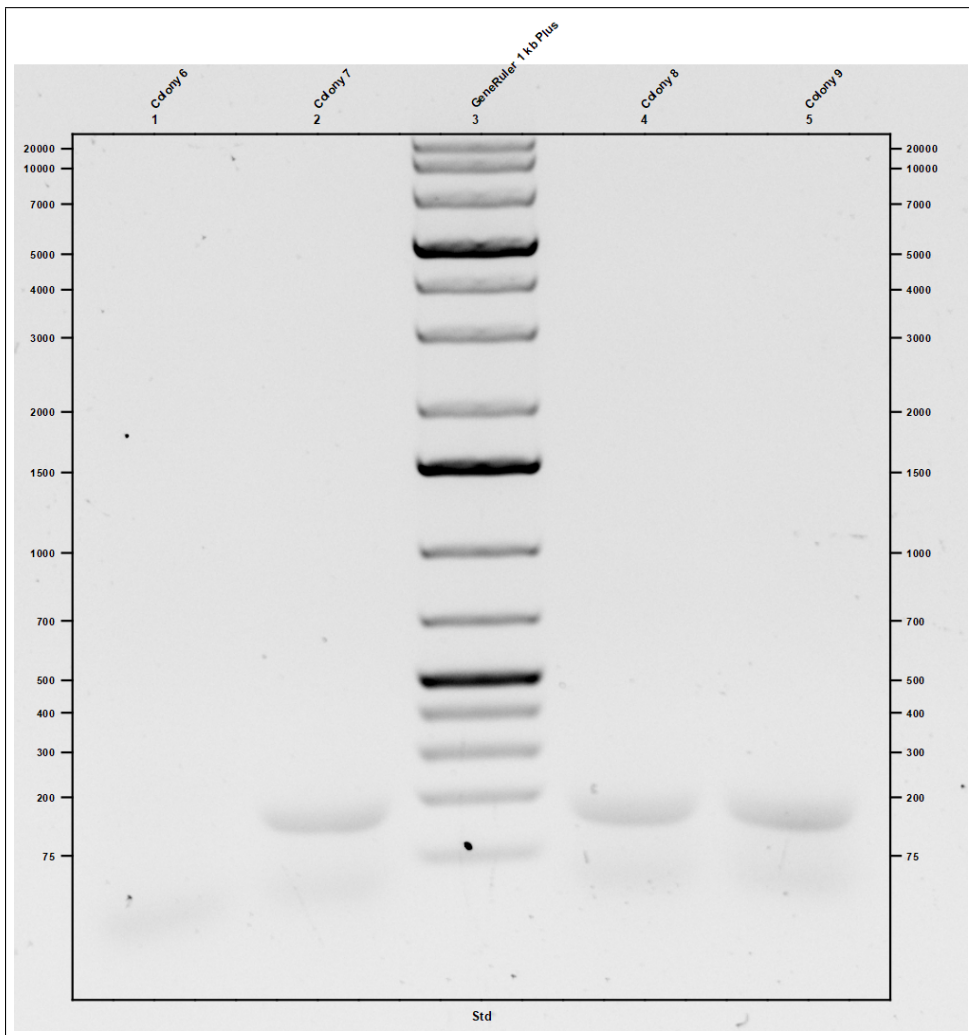


Figure C.10: Electrophoresis results from PCR-amplified putative promoter 1 inserted in pBV2-ribBI plasmid from *E. coli* DH5 α colonies. GeneRuler 1kb Plus (Appendix C.1) was used as ladder

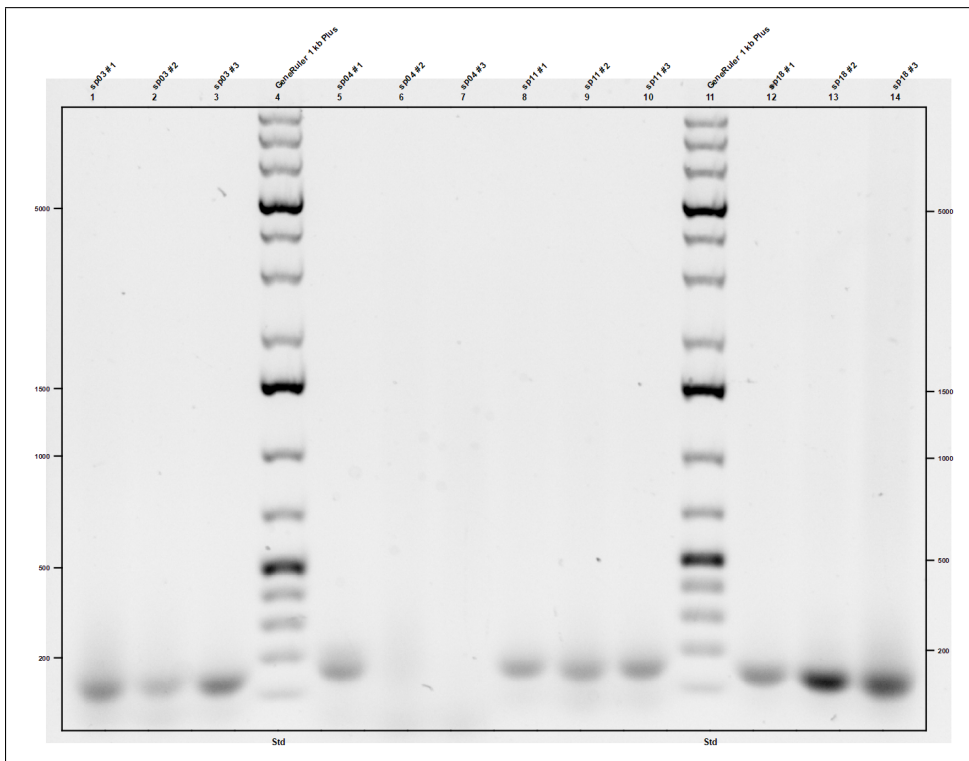


Figure C.11: Electrophoresis results from PCR-amplified putative promoter 3 (lane 1, 2, 3), 4 (lane 5, 6, 7), 11 (lane 8, 9, 10) and 18 (lane 12, 13, 14) inserted in pBV2-ribB1 plasmid from *E. coli* DH5 α colonies. GeneRuler 1kb Plus (Appendix C.1) was used as ladder

Appendix D

Alignments of sequencing results

The following figures in appendix D represents alignments of sequencing results with promoter primers and putative promoter sequence.

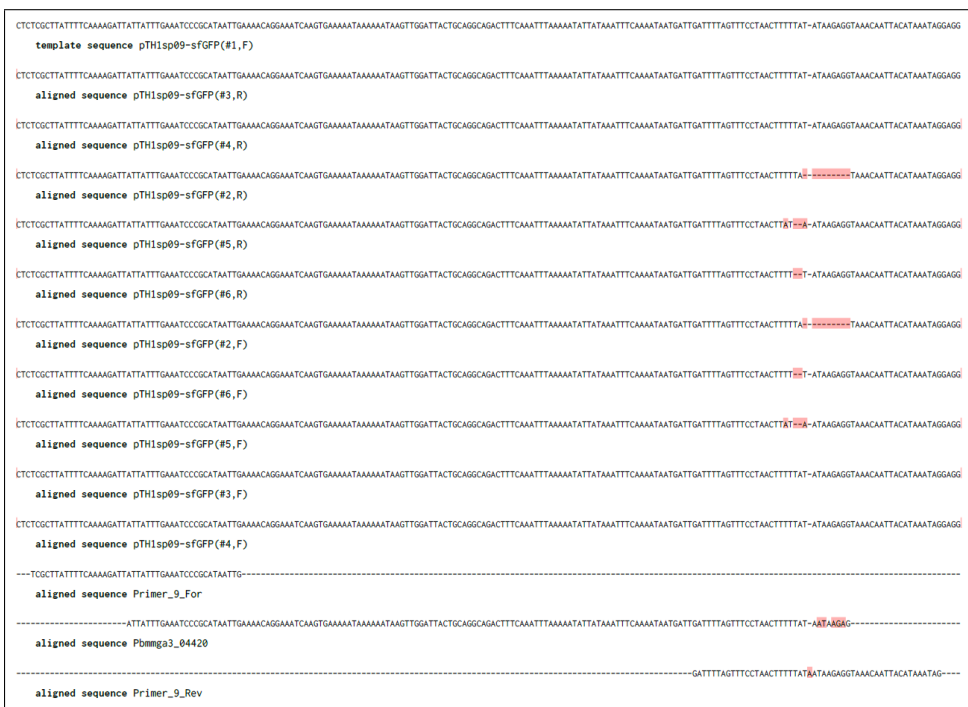


Figure D.1: Sequencing alignment from 6 colonies of *E. coli* with inserted pTH1sp09-sfGFP. The same deletion inside -10 element is present in sequencing attempt 1, 3 and 4. The sequenced promoters are aligned with putative promoter sequence, and primers (forward and reverse) for sp09. Mis-matches are marked in red, and gaps are filled with hyphen (-).

```

GCTCATT-----AGGCGTTATTCTTCCCTTAAACTTCCAGTTTTGATCACATTTCCCATAGATAAAATTTTCTTATAGTACTTTTTATACTATGTGTTAATAAAGTCCGTACTTTTTAAAAAATTTGATAGATATATTAACAGTGAACAATTACATAAATAGGAG
  template sequence pBV2sp01-ribB1(colony#7F)
TC&CGT-----CATTTTATTCTTCCCTTAAACTTCCAGTTTTGATCACATTTCCCATAGATAAAATTTTCTTATAGTACTTTTTATACTATGTGTTAATAAAGTCCGTACTTTTTAAAAAATTTGATAGATATATTAACAGT-----
  aligned sequence Phx1A
GCTTATTTCAAAAGATTATTCTTCCCTTAAACTT-----
  aligned sequence Primer_1_For
GCTCATT-----AGGCGTTATTCTTCCCTTAAACTTCCAGTTTTGATCACATTTCCCATAGATAAAATTTTCTTATAGTACTTTTTATACTATGTGTTAATAAAGTCCGTACTTTTTAAAAAATTTGATAGATATATTAACAGTGAACAATTACATAAATAGGAG
  aligned sequence pBV2sp01-ribB1(colony#7R)
-----TGATAGATAGTATATTAACAGTGAACAATTACATAAATAG---
  aligned sequence Primer_1_Rev

```

Figure D.2: Example of correctly aligned putative promoter sequence to sequencing query. pBV2sp01-ribB1 collected from *E. coli* was sequenced with primers flanking the putative promoter sequence. Mis-matches are marked in red, and gaps are filled with hyphen (-).

Appendix E

Calibration curves

Figure E.1 displays the relation of OD measured from cuvette and the OD measured in the Tecan Infinite plate reader for both Nunclon- (100 μL) and Falcon- (200 μL) plates. Figure E.2 compares the fluorescence intensity and OD to find a linear relation. Figure E.3 shows how the riboflavin concentration relates to the signal from the fluorescence detector in the BioLector, and Figure E.4 presents the relation of riboflavin concentration to the area under the HPLC curve peak, corresponding to riboflavin ($t_R=5.75$ sec).

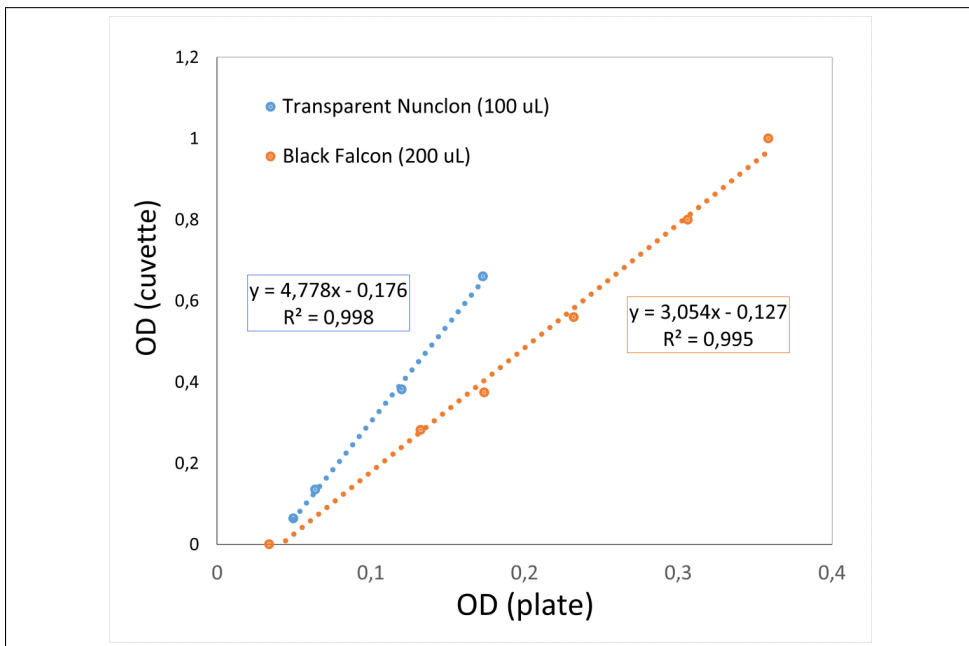


Figure E.1: Calibration measurements of the relation of optical density with the wavelength of 600 nm of sample measured in cuvette, black Falcon 96-well plate and transparent Nunclon 96-well plate. A volume of 200 μL was used for the Falcon plate, whereas 100 μL was used in the Nunclon plate. The linear regression function with R^2 -value is presented inside orange and blue box for the Falcon and Nunclon plate respectively

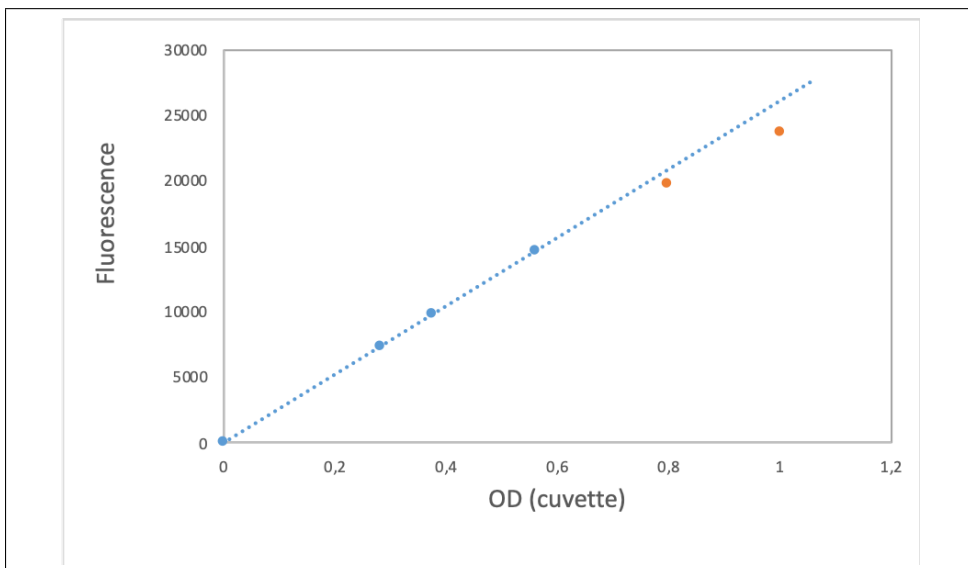


Figure E.2: Relation of fluorescence detected in Tecan infinite[®] plate reader and OD measured in cuvette spectrophotometer. The four lowest OD₆₀₀ measurements are included in the linear regression, whereas the two highest OD₆₀₀ measurements falls outside the linear region of detection.

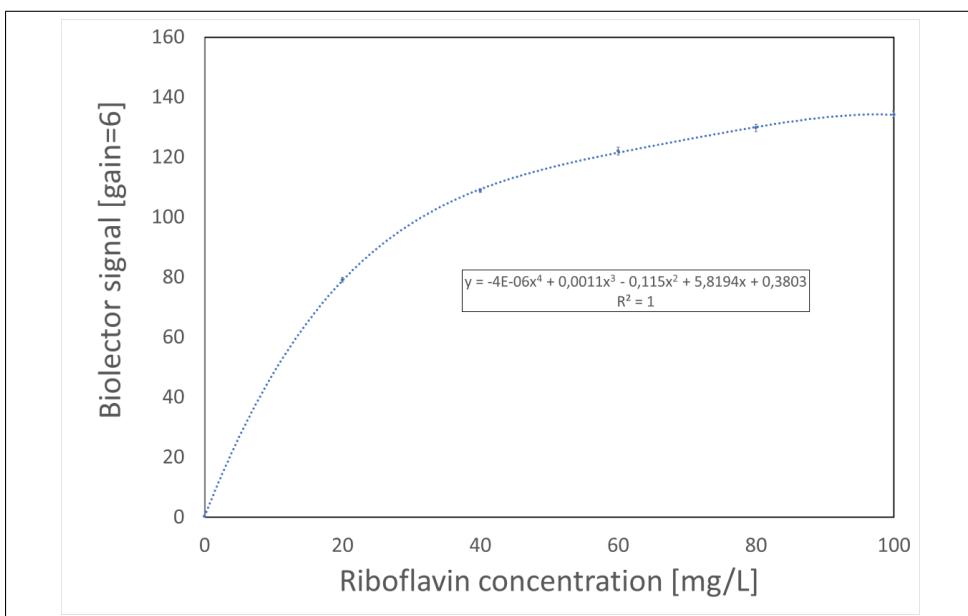


Figure E.3: Calibration curve for concentration and detected signal of riboflavin in the BioLector with gain=6. Regression function (inside box) was calculated in Excel using a polynomic function of 4 degrees.

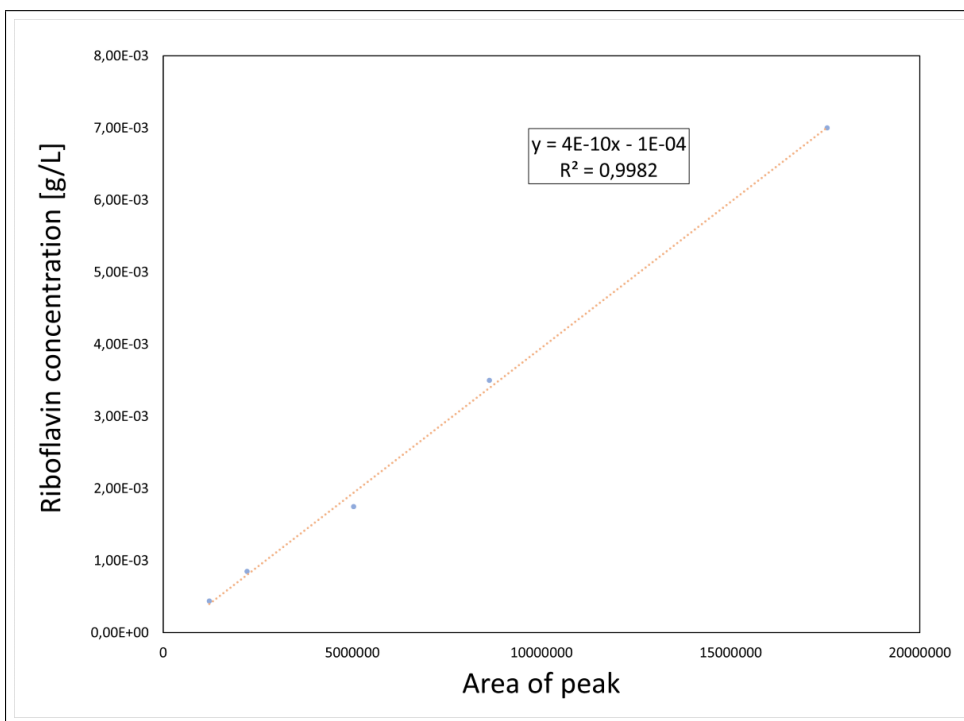


Figure E.4: Relation of area of riboflavin peak from HPLC and riboflavin concentration. Fluorescence detector ($\lambda_{Ex}=370$ nm, $\lambda_{Em}=520$ nm) detected riboflavin signal peak from HPLC with a C_{18} column.

Appendix F

Protocols

F.1 Takara Cloneamp HiFi polymerase

CloneAmp HiFi PCR Premix (Cat. No. 639298) is a convenient 2X master mix that provides exceptionally accurate and efficient DNA amplification, due to the high sensitivity, specificity, priming efficiency, and extension efficiency of CloneAMP HiFi Polymerase [57]

1. Prepare Master Mix according to table F.1

Reagent	Volume	Final Concentration
CloneAmp HiFi PCR Premix	12.5 μ L	1X
Primer 1	5-7.5 pmol	0.2-0.3 μ M
Primer 2	5-7.5 pmol	0.2-0.3 μ M
Template	<100 ng	
Sterilized distilled water	up to 25 μ L	
Total volume per reaction	25.0 μ L	

Table F.1: Master Mix as recommended by Clonotech Laboratories

2. Mix the Master Mix by tapping the bottom of the tube, then centrifuge briefly. Transfer 25 μ L of the Master Mix into individual PCR tubes. Centrifuge briefly.
3. Program your thermocycler with the cycling conditions indicated in table F.2

Step	Temperature	Time
	98 °C	10 seconds
30-35 Cycles	55 °C	5 or 15 seconds
	72 °C	5 seconds/kb
Final extension	72 °C	2 min
Hold	4 °C	Infinite

Table F.2: Thermocycler program as recommended by Clonotech Laboratories

F.2 DNA gel electrophoresis

Materials

- Agarose gel (0.8 % agarose, GelGreen)
- Gel electrophoresis running buffer

Procedure

1. Cast a gel of your choice. Liquid gels are stored in a heating cabinet to keep them from setting. Don't pour the gel too thick (5 mm is a good starting point). Remember to insert a comb to make wells for depositing DNA.
2. After letting the gel set for 20-30 minutes, transfer it from the casting tray to an empty gel electrophoresis chamber of appropriate size.
3. Add gel electrophoresis running buffer to the chamber until the gel is submerged in buffer.
4. Mix the DNA to be separated with loading dye.
5. Load the DNA/loading dye solution into a well. Use different wells for different DNA solutions.
6. Add a DNA ladder of your choice to one of the empty wells.
7. Run the gel by connecting the gel electrophoresis chamber to a power source.
8. Depending on which buffer system you chose, use the following voltages for running the gel:
 - (a) For TAE buffer use 8-10 volts per cm of distance between the electrodes of the chamber.
 - (b) For LAB buffer use 15-20 volts per cm of distance between the electrodes of the chamber.
9. For good separation, end the run when the indicator dye has travelled approximately $\frac{2}{3}$ down the length of the gel slab.
10. Visualize the gel in a UV chamber such as the BioRad GelDoc XR+.
11. Confirm that the bands on the gel correspond to the expected DNA sizes.

F.3 Gibson Assembly

The Gibson Assembly protocol are based on recommendations by New England BioLab [58]

Optimized cloning efficiency is 50100 ng of vectors with 23 fold of excess inserts. Use 5 times more of inserts if size is less than 200 bps. Total volume of unpurified PCR fragments in Gibson Assembly reaction should not exceed 20 %.

1. Set up the following reaction on ice:

Total Amount of Fragments	0.02-0.5 pmol (X μ L)
Gibson Assembly Master Mix (2X)	10 μ L
Deionized H ₂ O	10-X μ L
Total Volume	20 μ L

Table F.3: The recommended amount of fragments used for assembly

2. Incubate samples in a thermocycler at 50C for 15 minutes when 2 or 3 fragments are being assembled or 60 minutes when 4-6 fragments are being assembled. Following incubation, store samples on ice or at 20 °C for subsequent transformation. Note: Extended incubation up to 60 minutes may help to improve assembly efficiency in some cases
3. Transform Competent *E. coli* cells with 2 μ L of the assembly reaction, following the transformation protocol.

F.4 Making chemically competent *Escherichia coli*

This protocol describes how to make chemically competent *E. coli* cells. These cells can be transformed using heat shock transformation, which is the most popular method of introducing plasmid DNA into *E. coli* DH5alpha cells. This protocol is based on the following paper: Chemically competent E. coli cells.pdf [59]

Materials

Component	Amount
PSI medium	105 ml
TfbII	40 ml
TfbII	2 ml
Microcentrifuge tubes	20-40

Procedure

Day 1 (performed in afternoon)

1. Pick a single colony from a freshly streaked plate and inoculate a small culture (25 mL of Psi medium). Grow overnight at 37 °C, 225 RPM.

Day 2:

Tip: Cells and transformation buffers should be kept cold at all times. It is also preferable to use chilled pipets and do everything in the cold room if possible.

1. Inoculate 100 mls of Psi medium with 0.5 ml of overnight culture and incubate at 37 °C, 225 RPM.
2. When OD600 reaches 0.4–0.5 place culture on ice and chill 5–10 minutes
3. Transfer cells to 50 ml sterile, chilled centrifuge tubes. Pellet cells at 4 °C for 5 minutes at 5,000 * g.
4. Discard supernatant carefully and gently resuspend cell pellet in 0.4 volumes ice cold TfbI (20 mLs for each 50 mL tube). Do not vortex and keep on ice while resuspending.
5. Incubate cells on ice for 15 minutes. Tip: Some protocols incubate for only 5 minutes and cells can be left on ice for longer periods (i.e. 12 hrs) without any harm
6. Pellet cells at 4 °C for 10 minutes at 2,000 * g
7. Discard supernatant carefully and gently resuspend in 0.02 volumes (1 mL for 50 mL of culture) TfbII while keeping on ice.
8. Aliquot 50–100 microliters into 1.5 mL sterile microcentrifuge tubes with conical bottom.
9. Flash freeze in dry ice ethanol bath or liquid nitrogen and store at 80 °C

F.5 Making electrocompetent *Bacillus methanolicus*

This protocol details the production of electrocompetent *Bacillus methanolicus* cells. Electrocompetent cells can be transformed using electroporation. This protocol results in approximately 40 vials of electrocompetent cells.

Materials

1. SOBSuc medium
2. Baffled flasks, 500 mL
3. Electroporation buffer (EPB)
4. Work ampoule of *B. methanolicus*
5. Cryotubes
6. Falcon tubes, 50 mL

Procedure

1. Inoculate 200 μ L *B. methanolicus* from a work ampoule harvested at $OD_{600} = 1.0-1.5$ into 100 mL SOBSuc medium. Grow for about 16 hours at 50 °C, 200 RPM.
2. Reinoculate overnight culture into 4 x 100 mL pre-warmed SOBSuc medium baffled flasks (to $OD_{600} = 0.05$) and continue to grow at 50 °C, 200 RPM until $OD_{600} = 0.25$ (an interval of 0.18-0.30 is acceptable).
3. Transfer the cultures to 50 mL tubes (2 tubes per flask = 8 tubes). Centrifuge for 10 minutes at 5000 x g, 25 °C.
4. Pour off the supernatant and resuspend the cells in each tube with 4.5 mL room-temp EPB. Combine the cell suspension from two tubes (4 tubes total).
5. Centrifuge for 10 minutes, 5000 x g, 25 °C.
6. Pour off supernatant and resuspend cells in each tube with 9 mL EPM. Mix gently to resuspend, Centrifuge for 10 minutes, 5000 x g, 25 °C.
7. Pour off all supernatant. Resuspend the cells in each tube in 0.8 mL EPM. Collect all cell suspensions in one tube and aliquot into sterile cryotubes (100 μ L/tube). Freeze in liquid nitrogen or put directly into freezer and store at -80 °C.

F.6 Transformation of chemically competent *Escherichia coli*

Materials

Component	Amount/transformation
Chemically competent <i>E. coli</i> cells	1 vial
SOC medium	900 μ L
Plasmid	10 pg-100 ng
Selective agar plates	1

Procedure

1. Set water bath/heat block to 42 °C.
2. Thaw 1 vial of chemically competent *E. coli* cells for each plasmid to be transformed on ice for 10 minutes. Add one more vial as a negative control.
3. Once thawed, add 10 pg - 100 ng of plasmid DNA to chemically competent cells.
4. Incubate on ice for 20 minutes.
5. Heat shock the cells in water bath or heat block at 42 °C for 45 seconds.
6. Immediately place cells on ice. Incubate for 2 minutes.
7. Add 900 μ L SOC medium to each vial of heat shocked cells.
8. Incubate at 37 °C, 225 RPM for 1 hour. Tip: If transforming a plasmid which confers resistance to Ampicillin you can plate the cells directly out at this stage.
9. Plate out 100 μ L of cell culture on selective agar plates. Streak out culture thoroughly to avoid tight clustering of colonies.
10. Incubate at appropriate temperature overnight (most commonly at 37 °C).

F.7 Transformation of electrocompetent *Bacillus methanolicus*

This protocol transforms plasmid DNA into electrocompetent *B. methanolicus* cells by use of electroporation. It requires 3 days from start to finish (not including making electrocompetent cells).

Procedure

Day 1 (Performed in the morning)

1. Mix 100 μl electrocompetent cells with 2 μl of plasmid midi prep (0.5-1 $\mu\text{g}/\mu\text{l}$) in an eppendorf tube.
2. Incubate on ice for 15 min.
3. Transfer into cold electroporation cuvette (0.2 cm) and electroporate, 200 Ω , 25 μF and 12.5 kV/cm (2.5 kV). (time constant: 4.5 5.5)
4. Prewarm 5 ml SOBsuc medium in 50 ml Falcon tubes. One for each transformation.
5. Immediately add 1 ml SOBsuc medium (from the falcon tube) carefully into the electroporation cuvette and pipette up and down few times.
6. Transfer the cell suspension back into the 50 ml Falcon tube.
7. Incubate at 50 $^{\circ}\text{C}$, 200 rpm, for about 5-6 hours in a shaking incubator.
8. Spin down (4000 rpm, 5 min, 25 $^{\circ}\text{C}$), resuspend in 100 μl SOBsuc medium and plate out the up-concentrated cell suspension.
9. Incubate the plates at 50 $^{\circ}\text{C}$ over night.

Day 2

1. Inoculate fresh colonies from plates in 50 ml MVcM broth medium added:
 - (a) 0.05 ml 1M MgSO_4 stock solution
 - (b) 0.05 ml Trace metals stock solution
 - (c) 0.05 ml Complete vitamin stock solution
 - (d) 61 μl Methanol (30 mM)
 - (e) Antibiotic(s)
2. Pick three transformants of each strain.
3. Grow for 6-8 hours at 50 C, 200 rpm. Add another 345 l methanol to give a final concentration of 200 mM. Grow over night as above.

Day 3

-
1. Grow until OD₆₀₀=1.0 1.5. (you should reinoculate if OD₆₀₀ > 1.5)
 2. Mix 10 ml culture + 2 ml 87
 3. Aliquot 1 ml x 9 cryo tubes and store directly at -80C.

Appendix **G**

Medium and buffer compositions

G.1 LB medium

LB medium is one of the most widely used growth media for cultivating bacterial cells. It is a complex medium, and supports growth in organisms such as a *E. coli* well.

Component	ml/L	g/L
Bacto tryptone		10
Yeast extract		5
NaCl		10
Agar (if making plates)		15
Ion free water	up to 1000 ml	

G.2 SOC medium

SOC medium is a complex medium with additions to make it support high growth rates in bacterial cultures. It is commonly used to incubate cells after heat shock transformation.

Component	Final concentration	Stock	Amount/100 mL
Tryptone	2 %		0.5 g
Yeast extract	0.5 %		2.0 g
NaCl	10 mM	3 M	0.33 mL
KCl	2.5 mM	1 M	0.25 mL
MgCl ₂	10 mM	1 M	1 mL
MgSO ₄	10 mM	1 M	1 mL
Glucose	20 mM	1.1 M	1.82 mL
Ion free water			up to 100 mL

G.3 SOBsuc medium

SOBsuc medium contains sucrose and is a complex growth medium for *B. methanolicus*. It can also be made into agar plates by adding 15 g/L of agar before autoclaving.

Component	Concentration (g/L)
SOB medium	28
Sucrose	85
ion free water	Up to 1000
Agar (if making plates)	15

G.4 PSI medium

Psi medium is used when preparing chemically competent *E. coli* cells

Component	g/L	ml/L
Tryptone	20	
Yeast extract	5	
MgCl ₂	5	
Ion free water		up to 1000

G.5 TfbI buffer

TfbI is one of the cell wash buffers used for preparing chemically competent *E. coli* cells.

Component	Final concentration	Amount /400 mL
Potassium acetate	30 mM	1.18 g
RbCl ₂	100 mM	4.84 g
CaCl ₂ *2H ₂ O	10 mM	0.59 g
MnCl ₂	50 mM	3.96 g
Glycerol	15 % v/v	60 mL
Ion free water		up to 400 mL

G.6 TfbII buffer

TfbII (Transformation buffer II) is a cell wash buffer used for preparing chemically competent *E. coli* cells.

Component	Final concentration	Amount /100 mL
MOPS	10 mM	0.21 g
CaCl ₂ *2H ₂ O	75 mM	1.1 g
RbCl ₂	10 mM	0.12 g
Glycerol	15 % v/v	15 mL
Ion free water		up to 100 mL

G.7 MVcM minimal media

Component	g/L	ml/L
MVcM High Salt Buffer 10x	100	
Yeast extract		0.250
Ion free water	890*	

*Reduce water-content if other C-source than MeOH is going to be used

Nutrient additions (add to 100 mL media)

1. 0.1 mL MgSO₄ stock solution
2. 0.1 mL trace metals stock solution
3. 0.1 mL complete vitamin stock solution
4. 811 uL MeOH (200 mM final concentration)
5. Chloramphenicol if required, giving a final concentration of 5 ug/mL
6. If cultivating *B. methanolicus* M168-20 cells add 1000 uL methionine.

G.8 MVcM high salt buffer 10X

This salt buffer solution provides the necessary salts for the MVcM medium.

Component	Molarity	mL/L
K ₂ HPO ₄	0.1175	
NaH ₂ PO ₄	0.054	
(NH ₄) ₂ SO ₄	0.08	
Ion free water		up to 500 mL

G.9 MgSO₄ stock solution

Component	g/mol	M	ml/L	g/L
MgSO ₄ *7H ₂ O	246,47	1		246,47
Ion free water			up to 1000 mL	

G.10 Trace metals solution

The MVcM BPTI Trace Metals 1000x solution gives all necessary mineral additions to support growth in MVcM medium.

Component	g/mol	M	ml/L	g/L
H ₃ BO ₃	61.83	0.0005		0.031
FeSO ₄ *7H ₂ O	278.02	0.020		5.56
CuCl ₂ *2H ₂ O	170.49	0.00016		0.027
CaCl ₂ *2H ₂ O	147.02	0.050		7.35
CoCl ₂ *6H ₂ O	237.93	0.00017		0.040
MnCl ₂ *4H ₂ O	197.91	0.050		9.90
ZnSO ₄ *7H ₂ O	287.54	0.0010		0.288
Na ₂ MoO ₄ *2H ₂ O	241.98	0.0002		0.048
Ion free water			500	
Concentrated HCl	36.46	1.99	80	72.720
Ion free water			up to 1000	

G.11 Vitamin stock solution

MVcM complete vitamins 1000x is a necessary addition to MVcM medium for it to support growth.

Component	g/mol	M	ml/L	g/L
d-Biotin	244.31	0.00041		0.100
Ion free water			up to 800 mL	
Thiamine*HCl (Vitamin B1)	300.81	0.00033		0.100
Riboflavin (Vitamin B2)	376.37	0.00027		0.100
Pyridoxine*HCl	169.18	0.00059		0.100
Pantothenate	219.24	0.00046		0.100
Nicotinamide (Vitamin B3)	122.13	0.00082		0.100
p-Aminobenzoic acid (Vitamin L1)	137.14	0.00015		0.020
Folic acid (Vitamin B11)	441.4	0.00002		0.010
Alphamine (Vitamin B12)	1355.38	0.00001		0.010
Lipoic acid (Thioctic Acid)	206.32	0.00005		0.010
Ion free water			up to 1000	

G.12 Electroporation buffer (EPB)

Electroporation buffer is needed when preparing electrocompetent *B. methanolicus* cells.

Component	g/mol	M	ml/L	g/L
HEPES	560.3	560.3		0.240
PEG8000				250
Ion free water				750

